

[REDACTED]  
SAND78-8193  
[REDACTED]

# HELIOSTAT MATERIALS DEVELOPMENT AND EVALUATION

## FINAL TECHNICAL REPORT

February 5, 1979 - June 30, 1980

Work Performed under Sandia Contract  
No. 83-0024B

GENERAL ELECTRIC COMPANY  
ENERGY SYSTEMS PROGRAMS DEPARTMENT  
SCHENECTADY, NEW YORK

GENERAL  ELECTRIC

*When printing a copy of any digitized SAND  
Report, you are required to update the  
markings to current standards.*

Printed in the United States of America  
Available from  
National Technical Information Service  
U. S. Department of Commerce  
5285 Port Royal Road  
Springfield, VA 22161  
Price: Printed Copy \$6.50; Microfiche \$3.00

## FOREWORD

The Heliostat Materials Development and Evaluation Program was conducted for the Solar Projects Division of Sandia Corporation, Livermore, California, by the Energy Systems Programs Department, General Electric Company, Schenectady, New York, under Sandia Contract No. 83-0024B. This final report is submitted in fulfillment of the contract Work Statement Task 8 covering the period February 5, 1979 through June 30, 1980. The program was under the direction of Mr. Clayton Mavis, Sandia Program Manager and was managed for the General Electric Company by Dr. R.N. Griffin, Manager-Solar Energy Materials Programs. Other General Electric personnel contributing to the program were Mr. R.G. Frank, Dr. F.N. Mazandarany and Mr. S.I. Schwartz.

The cooperation and assistance of Dr. Michael Lind of Batelle, Pacific Northwest Laboratories, who was responsible for most of the specularly measurements, is gratefully acknowledged.

## TABLE OF CONTENTS

<u>Section</u>		<u>Page</u>
1	INTRODUCTION	1
2	SELECTION OF CANDIDATE MATERIALS	3
	2.1 Enclosure Materials	3
	2.2 Reflector Materials	3
3	BIAXIAL ORIENTATION OF PVDF	5
	3.1 Background of Film Orientation	5
	3.2 Laboratory Test History	5
	3.3 Pilot Plant Experiments	6
	3.3.1 Longitudinal Stretching	6
	3.3.2 Transverse Stretching	10
	3.3.3 Product Properties	15
	3.3.4 Probable Outlook	21
4	INVESTIGATION OF METHODS FOR BONDING PLASTIC FILMS	22
	4.1 Adhesive Bonding	22
	4.2 Ultrasonic Bonding	24
	4.3 Radio Frequency Bonding	26
	4.4 Electromagnetic or Induction-Heated Bonding	28
5	DEVELOPMENT OF SPECULARLY-OPTIMIZED METALIZED FILM REFLECTORS	31
	5.1 Metalization Studies	31
	5.2 First-Surface and Pseudo-First-Surface Reflectors	33
	5.3 Second-Surface Reflectors	37
6	WEATHERING TESTS OF MATERIALS	43
	6.1 Weatherometer Tests	43
	6.2 Outdoor Exposure	43
	6.2.1 Real-Time Exposure	44
	6.2.2 Accelerated Exposures	45

TABLE OF CONTENTS (Cont.)

<u>Section</u>		<u>Page</u>
6	WEATHERING TESTS OF MATERIALS (Continued)	
	6.3 Weathering of Materials	46
	6.3.1 Weathering of a First-Surface Aluminized Reflector	46
	6.3.2 Weathering of a Pseudo-First-Surface Aluminized Reflector	48
	6.3.3 Weathering of a Second-Surface Aluminized Reflector	50
	6.3.4 Weathering of LLumar	51
	6.3.5 Weathering of Melinex OW	53
	6.3.6 Weathering of Kynar	54
	6.3.7 Weathering of LLumar Bonds	56
	6.3.8 Weathering of Kynar Bonds	59
	6.3.9 Weathering Predictions	61
7	MECHANISM OF WEATHERING DEGRADATION	67
	7.1 Experimental Equipment	67
	7.2 Test Procedure	69
	7.3 Test Results	70
8	FLAMMABILITY OF PLASTIC FILMS	77
	8.1 General Considerations	77
	8.2 Flammability of LLumar	78
	8.3 Flammability of Kynar	78
9	CONCLUSIONS AND RECOMMENDATIONS	81
	9.1 Enclosure Materials	81
	9.2 Reflector Materials	81

TABLE OF CONTENTS (Cont.)

<u>Section</u>		<u>Page</u>
<u>APPENDIXES</u>		
A	Optical Properties Measurements	83
B	Tensile Properties of Pilot Plant Kynar Film	92
C	Effect of Weathering on Tensile Properties of Potential Enclosure Materials	95
D	Effect of Weathering on Strength of Bonded Samples	97
E	Failure Mode of Weathered Bond Samples	98
F	Strength of Bonds Not Selected for Weathering	100

## Section 1

## INTRODUCTION

Solar thermal electric power plants are projected to play an important role in reducing the United States' consumption of nonrenewable fuels. However, in order for such power generation plants to become commercially attractive, they must be a cost-competitive, reliable power source. General Electric believes that the utilization of lightweight enclosed heliostats is the key to achieving a cost-competitive and reliable solar thermal power system. The cost saving that can be realized by protecting the heliostat from the environment more than compensates for the (normally) slightly lower performance of an enclosed heliostat, since it is the cost of the energy delivered that will determine the ability of a solar thermal power plant to be commercially attractive.

The development of long-life, reliable, cost-effective heliostats will require innovative design, mass production techniques, and the best possible choice of materials. The selection of the optimum materials for the major components of the heliostat system requires a thorough knowledge of materials, their behavior, their processing, their cost, and their ability to function reliably in a particular application and environment for long periods of time. The proper selection depends on the availability of an adequate data base which is, unfortunately, not always available for the materials and conditions of interest.

The inherent operational requirements of solar devices and facilities dictate that they be deployed, largely, in the very environments most degrading and hostile to their components. Therefore, the intelligent selection of functional materials for solar devices must take into account their reliability and long-term durability as well as their relevant optical, mechanical, and thermal properties. Lifetime predictions of such materials depend on the availability of accurate, well documented data on outdoor weatherability.

Outdoor weathering is a degradation-promoting process that is both qualitatively and quantitatively dependent upon the constituent factors peculiar to any particular environment. The objective of outdoor exposure testing is the determination of the weathering performance of materials for one or more reasons: to

provide statistical data regarding the prediction of the influence of weathering on materials properties, as a quality control technique, or as a research tool in the development of new or improved materials. The essential characteristics of accurate outdoor testing are: 1) that the test environment match as nearly as possible that of the anticipated end use, or more importantly, that it create in the material the same effects as the anticipated end use and 2) that the diagnostic tests, usually of relevant functional properties, be selected to assess accurately the type of degradation that has the most important effect on the choice of materials.

The objective of this program was to produce, characterize, and test enclosure and reflector materials with the purpose of establishing a firm data base for the prediction of useful life cycles and of upgrading the performance of enclosed heliostat systems, leading to a lower cost/performance ratio.

## Section 2

## SELECTION OF CANDIDATE MATERIALS

2.1 ENCLOSURE MATERIALS

During the conceptual design study of enclosed solar devices,<sup>1</sup> one primary candidate material and several alternates were identified for the major system components. Transparent materials may serve to protect a heliostat or the entire solar device from the wind, dirt, and precipitation, and may, in addition, be used to minimize radiative and convective heat losses to the environment. Reflective surfaces redirect the sunlight, normally for the purpose of concentrating it. The films selected for testing as potential enclosure materials were UV-stabilized poly(ethylene terephthalate) (PET) and poly(vinylidene fluoride) (PVDF). The stabilized polyester film appeared to be a likely candidate considering its cost, optical and mechanical properties, and its apparent weatherability (based on uncontrolled testing). Biaxially-oriented PVDF was selected as a candidate because, although not yet in commercial production, it appeared to have tensile strength approaching that of PET, extremely high clarity, and presumably good weathering resistance. While there is a great deal of data on the weatherability of PVDF in the form of protective coatings or of protective or decorative appliques, no data were available concerning the weathering properties of unsupported, biaxially-oriented film.

It is frequently necessary to refer to a material by its trade name, either for clarity or because the properties and characteristics of a particular brand and grade of material may not be the same for all generically-related materials. Trade names used in this report are listed in Table 2-1 along with brief descriptions and the manufacturers. They are used wherever chemical or generic names may not be explicit.

2.2 REFLECTOR MATERIALS

One of the chief advantages of an enclosed solar collector system is the lightweight structure made possible by the protective enclosure. Metalized

---

<sup>1</sup>"Solar Central Receiver Prototype Heliostat, Phase I Final Technical Report," SAN-1468-1, October 1978.

Table 2-1  
TRADE NAMES OF MATERIALS AND PROCESSES

<u>TRADE NAME</u>	<u>MANUFACTURER</u>	<u>DESCRIPTION</u>
Kynar	Pennwalt Corp.	Poly(vinylidene fluoride)
LLumar	Martin Processing Co.	UV-Stabilized poly(ethylene terephthalate)
Versilok	Hughson Chemicals	Acrylic adhesive
Acryloid	Rohm & Haas	Acrylic resin
Adcote	Morton Chemical Co.	Polyester adhesive
Melinex	ICI Petrochemicals & Plastics Co.	Poly(ethylene terephthalate)
Melinex OW	ICI Petrochemicals & Plastics Co.	UV-Stabilized poly(ethylene terephthalate)
Celanar 5000	Celanese Corp.	Poly(ethylene terephthalate)
EC-534	Celanese Corp.	Poly(ethylene terephthalate)
EEK	DSET Laboratories	Sample weathering technique in which insolation is always normal to sample
EMMA	DSET Laboratories	Weathering process with 10 mirrors to concentrate sunlight
EMMAQUA	DSET Laboratories	Similar to EMMA but with intermittent water spray
Tedlar	Du Pont	Poly(vinyl fluoride)

plastic films are therefore the logical choice for reflector materials. First-surface aluminized polyester, if adequately protected, would provide a low-cost highly specular reflector. Protected (second-surface) reflectors may prove necessary under some conditions where the first-surface mirror is too fragile. A number of second-surface reflectors were investigated, and a laminated aluminized PET reflector available from Martin Processing Co. was selected for testing. First-surface aluminized PET, both unprotected and protected by a thin layer of Dow Corning Q96315 resin, also were selected for testing.

### Section 3

#### BIAXIAL ORIENTATION OF PVDF

Since only very limited amounts of biaxially-oriented PVDF were available from laboratory experiments, an investigation of orientation on a pilot plant scale was initiated. This effort was designed to clarify the feasibility of commercial production of biaxially-oriented PVDF and to provide material for investigation in the weathering studies.

##### 3.1 BACKGROUND OF FILM ORIENTATION

Plastic films, depending on their composition and intended use, may be un-oriented, uniaxially oriented, or biaxially oriented. Blown film is produced by extrusion of the plastic through an annular die and inflation of the resulting tube. This process is often used for the production of plastic bags or for very wide film. However, blown film is difficult to produce in a biaxially-oriented form which is orthotropic. Most truly biaxially-oriented film, such as thermo-plastic polyester and polypropylene, is produced by extrusion through a flat die with subsequent orientation first on longitudinal stretch rolls and subsequently in the transverse direction on a tenter frame. Orientation of the polymer molecules in the plane of the film has a number of desirable effects. The tensile strength of the polymer film is greatly increased, as is the clarity of the film. Frequently, orientation also has the desirable effect of increasing the impact resistance of the film, particularly at low temperatures.

##### 3.2 LABORATORY TEST HISTORY

Late in 1977, researchers at Pennwalt Corporation produced laboratory samples of biaxially-oriented Kynar PVDF. The usual unoriented film has a tensile strength between 41-76 MPa (6-11 ksi), a yield strength about 41 MPa (6 ksi), and an ultimate elongation between 300-500%. The total hemispherical transmittance of the unoriented film is about 0.85-0.90. The laboratory samples of biaxially-oriented film had tensile strengths on the order of 131-138 MPa (19-20 ksi), 100% elongation at break, and transparency of about 87% at 0.076 mm (0.003 in.) thickness.

Detailed studies of the orientation process have since been reported<sup>2</sup> which make it clear that some of the conditions employed in this study were not optimum. For example, the temperatures employed in the orientation procedures in this work appear to have been higher than desirable. The observed tensile strength of Kynar 460, about 155 MPa (23 ksi), is higher than would have been expected from reported experiments with a T.M. Long orientation machine, but is much lower than the 170-212 MPa (24.6-30.7 ksi) tensile strengths that were observed in some domes thermoformed from Kynar 460.

It is evident that much more work is needed in optimizing the orientation process to produce the strongest and clearest possible PVDF film.

### 3.3 PILOT PLANT EXPERIMENTS

Virgin Kynar pellets, grade 460 natural, lot 78-5334, were extruded by the Research and Development Division of Pennwalt Corp. in King of Prussia, Pa., into sheet 1.52 mm (0.060 in.) thick by 0.48 m (19 in.) wide. This sheet was shipped to the film orientation laboratory of Marshall & Williams Co. in Providence, R.I., where film orientation experiments were performed on pilot plant equipment.

#### 3.3.1 LONGITUDINAL STRETCHING

Longitudinal orientation of the Kynar sheet was obtained with a modified Marshall & Williams Model D-7700 longitudinal stretch machine. The necessary modification of the machine consisted of the addition of infrared preheater panels which were placed in line ahead of the first preheat roll. The modified machinery is shown schematically in Figure 3-1.

A view of the feed end of the longitudinal stretcher is shown in Figure 3-2. In the foreground is a roll of extruded Kynar sheet. In the background the sheet is passing over the heated rollers, its surface temperature monitored by an infrared sensor.

Figure 3-3 is a closer view of the infrared preheaters, the infrared sensor, and the sheet passing around the hot rolls. Figure 3-4 shows the output end of the longitudinal stretch machine where the uniaxially-oriented sheet is slit and wound preparatory to being stretched laterally. The difference between the clarity of the unoriented sheet shown in Figure 3-2 and the uniaxially-oriented sheet in

---

<sup>2</sup>"One-Piece Dome Fabrication Study Final Report," SAND78-8184, December, 1979.

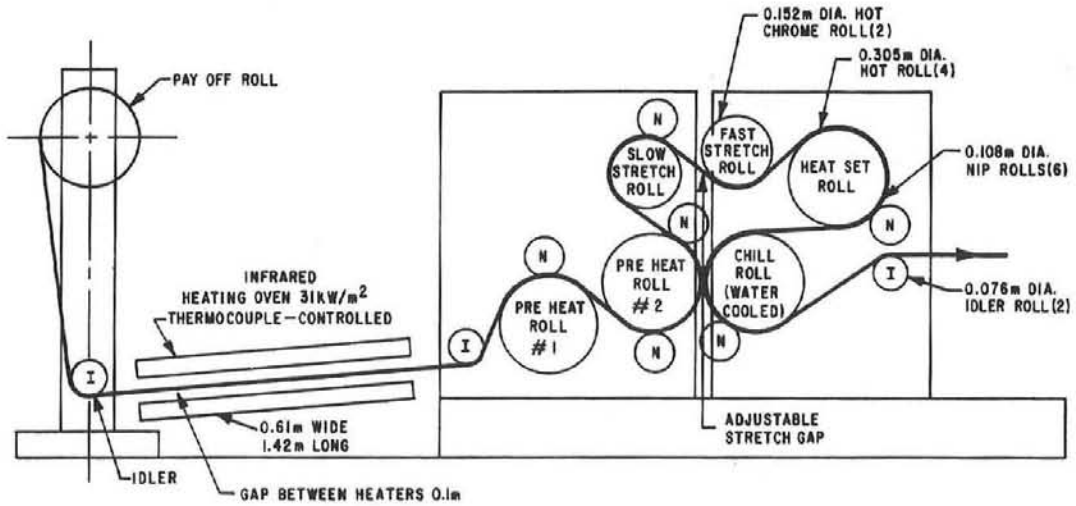


Figure 3-1. Modified Longitudinal Stretch Machine (Schematic)

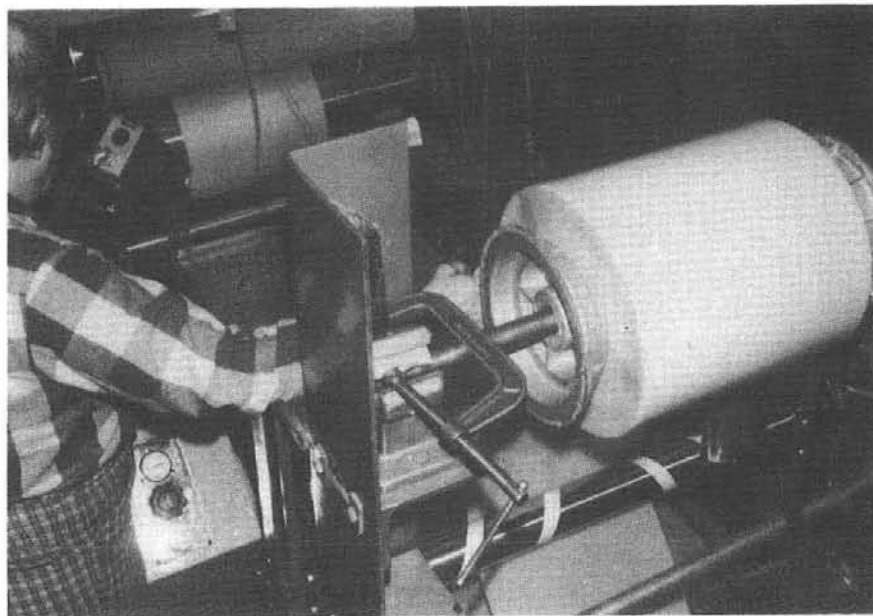


Figure 3-2. Feed End of Longitudinal Stretch Machine

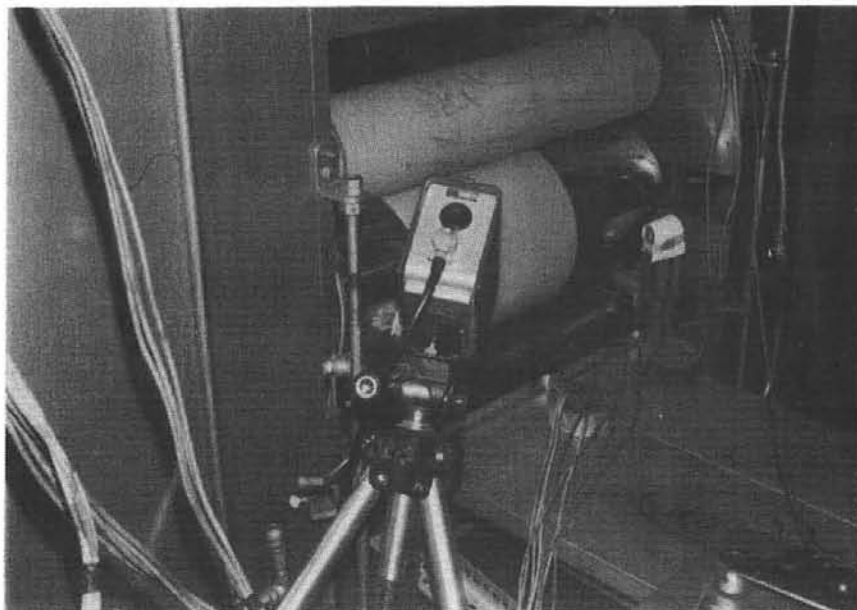


Figure 3-3. Kynar Sheet and Preheat Section of Longitudinal Stretch Machine

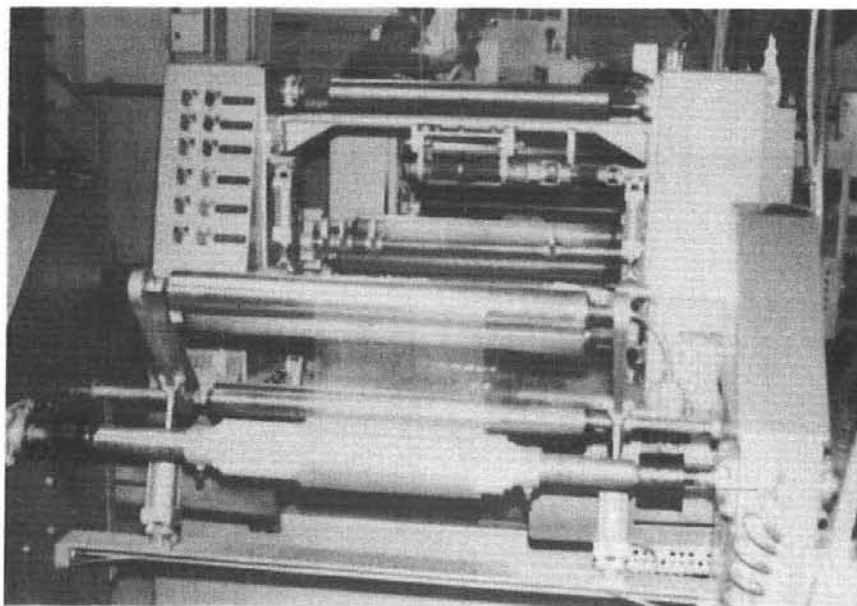


Figure 3-4. Output End of Longitudinal Stretch Machine

Figure 3-4 is noteworthy. A closeup view of the transformation from opaque to transparent is shown in Figure 3-5. The arrow in the figure designates the point where stretching occurs and the change in optical properties takes place.

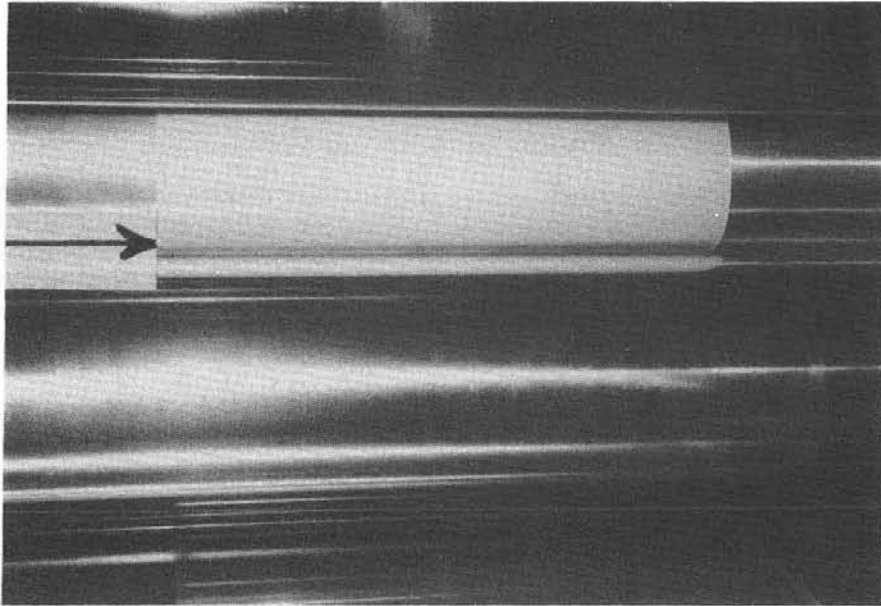


Figure 3-5. Longitudinal Stretching of Sheet

With the infrared preheaters in place and with the longitudinal stretcher operating at its lowest speed, it was possible to introduce a 4:1 longitudinal stretch in the 1.52 mm (0.060 in.) sheet. The product, uniaxially-oriented sheet, had a thickness of 0.41 mm (0.016 in.) and a width before slitting of 0.446 m (17-9/16 in.). Then, this was slit to a final width of 0.387 m (15-1/4 in.). Details of the operation of the longitudinal stretcher are included in Table 3-1. Two factors limited the rate of throughput of sheet through the stretching machine. One limitation was the rate of heat transfer through the plastic sheet. This limitation, however, could be overcome simply by adding more preheating elements. The second limitation was the power of the stretch machine itself. Kynar film is very tough at the temperature used for orientation, and the stretch machine was operated at the slowest possible speed. This is probably the reason that a sort of slip/stick motion was observed in the machine, resulting in transverse striations in the uniaxially-oriented polymer sheet.

Table 3-1

## ORIENTATION OF KYNAR 460 SHEET ON A LONGITUDINAL STRETCHER

Thickness In, mm	1.524
Thickness Out, mm	0.406
Input, meters/ min.	0.229
Output, meters/min.	0.914
Stretch Ratio	4:1
Temp., 0.305 m Rolls, °C	152.8
Temp., 0.152 m Rolls, °C	152.8
Temp., 0.152 m Fast and 0.305 m Heatset Rolls, °C	132.2
Surface Temp. after IR Preheat, °C	151.7
Ammeter, Input Section	8
Ammeter, Output Section	20
Stretch Gap, mm	4.32
Let-off, MPa	0.207
Winder, MPa	0.262
Input Width, m.	0.483
Output Width, m	0.446
Slit Width, m	0.387

## 3.3.2 TRANSVERSE STRETCHING

The uniaxially-oriented sheet described in Section 3.3.1 was converted to biaxially-oriented film on a tenter frame. A tenter frame consists of two continuously moving belts of film clips which grasp the edges of the uniaxially-oriented sheet. The distance between the two belts of film clips is variable at will. A typical film clip is shown in Figure 3-6, and a sketch of the arrangement of film clips into two continuous moving belts is shown in Figure 3-7. Operation of the tenter frame may be clarified by reference to Figure 3-8. A closeup view of one of the continuous belts of film clips is shown in Figure 3-9, and the process of feeding uniaxially-oriented sheet into the tenter frame for lateral stretching to form biaxially-oriented film is shown in Figure 3-10.

The tenter frame operating conditions used to produce biaxially-oriented Kynar are summarized in Table 3-2. These conditions are not necessarily optimum. The ratio of stretch, which is the relation between the delivered width of the film and the entering width was 3.70 to 1. This is believed to be near optimum; but no investigation was made of the effect of rate of stretch, which is the

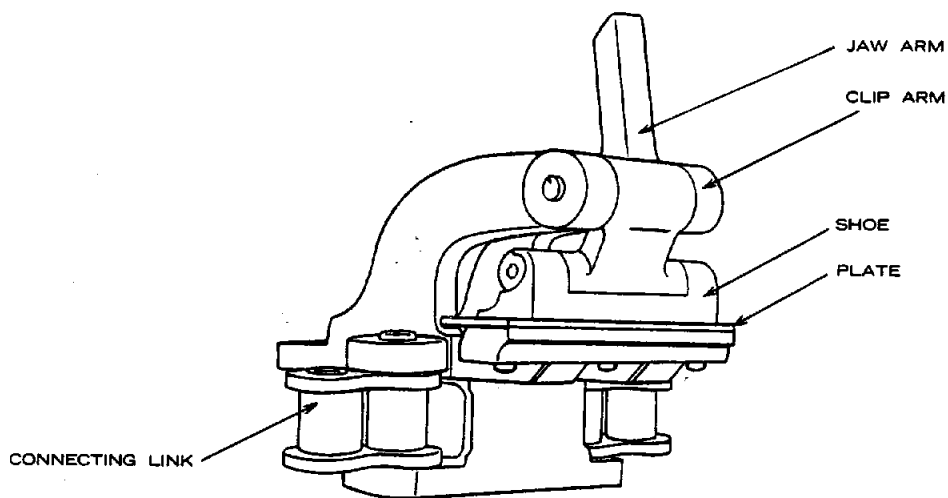


Figure 3-6. Typical Film Clip

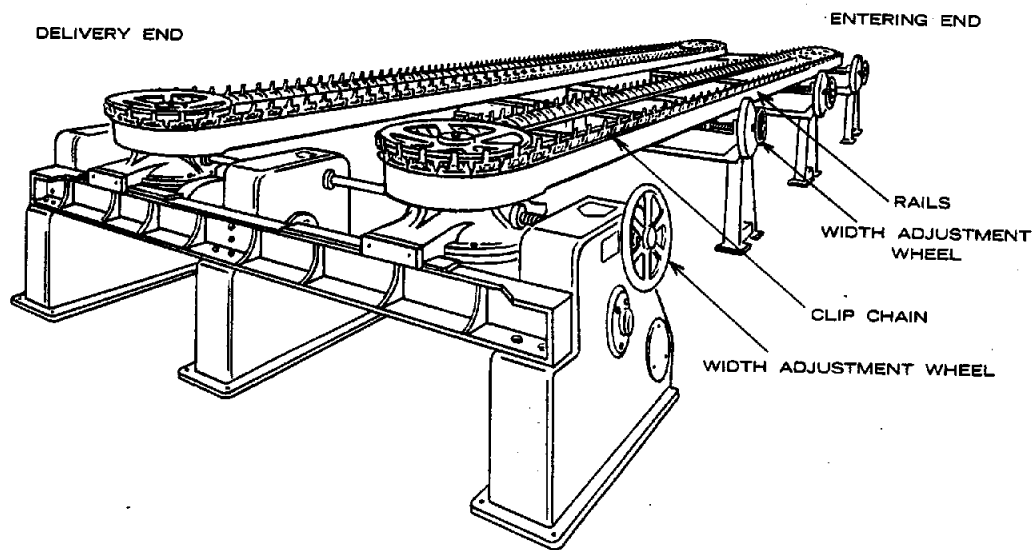


Figure 3-7. Typical Lateral Stretcher

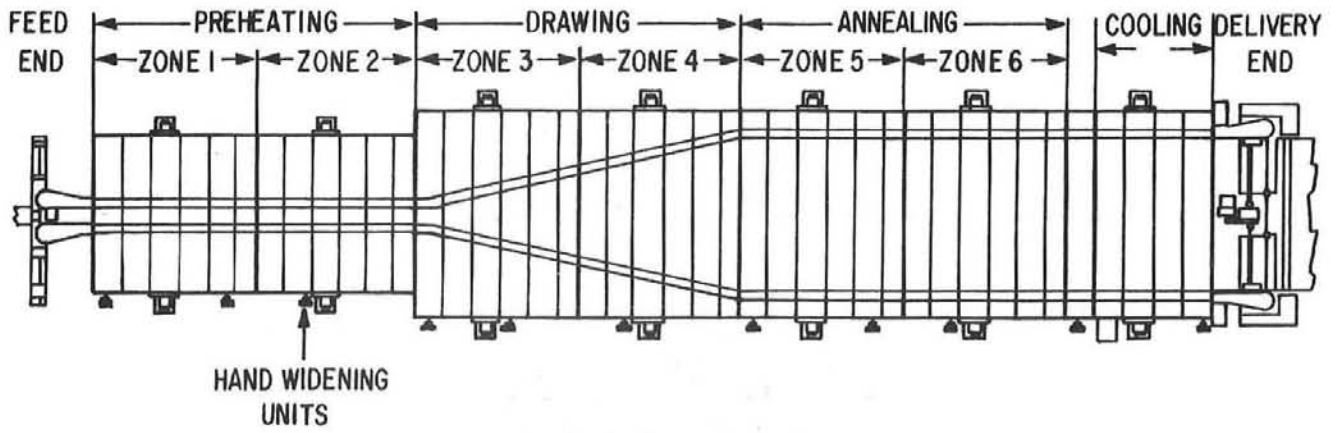


Figure 3-8. Typical Tenter Frame, Plan View

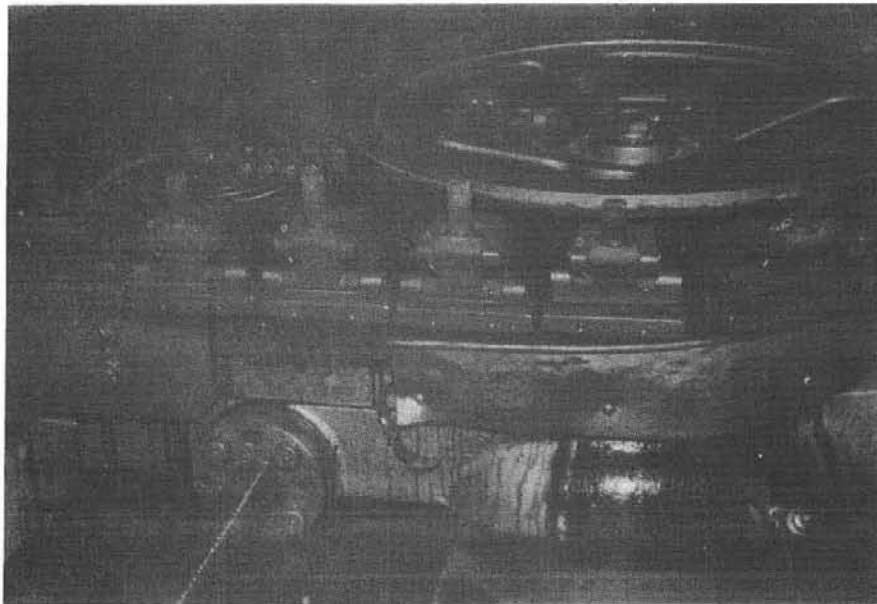


Figure 3-9. Closeup View of Tenter Frame Film Clips

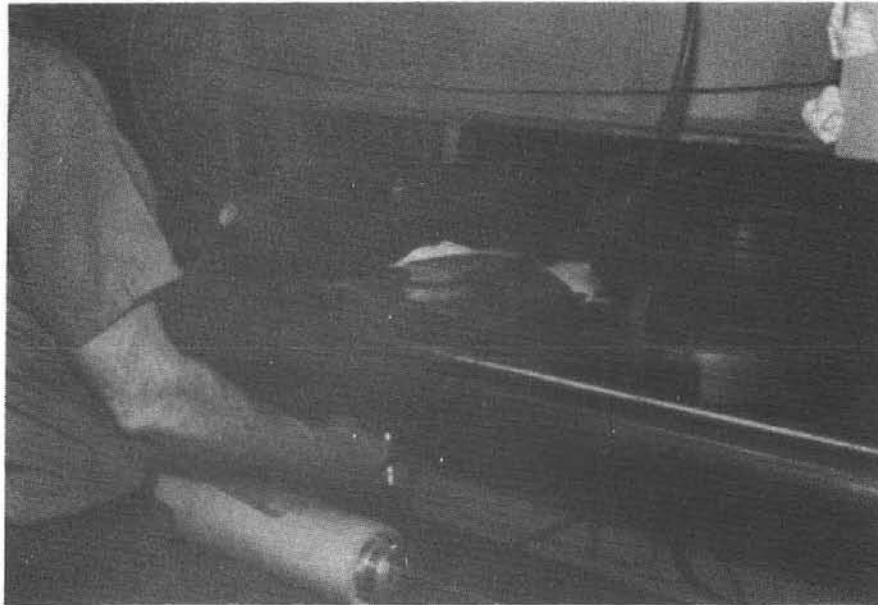


Figure 3-10. Uniaxially-Oriented Sheet Being Fed Into Tenter Frame

Table 3-2

ORIENTATION OF KYNAR 460 ON A TENTER FRAME

Entering Width, m.	0.387
Input Rate, m/min.	0.127
Temp., Pre-heat, °C	151.7
Temp., Stretch, °C	154.4
Temp., Heat-set, °C	151.7
Widths, m.	
Station #1	0.343
#2	0.356
#3	0.381
#4	0.406
#5	0.610
#6	0.813
#7	1.016
#8	1.219
#9	1.321
#10	1.270

relation between the distance and time required to go from minimum to maximum width; nor was any investigation undertaken of the effects of different contours of stretch, which is the pattern the film is made to follow while being stretched. The range of conditions that could be investigated was limited somewhat by the toughness of the Kynar film referred to earlier. Problems were frequently encountered during the stretching operation when one or more film clips let go of the edge of the film. The normal result was a chain reaction involving the entire stretched film, with catastrophic loss of all the material in the tenter frame. This is not believed to be a problem inherent in the processing of Kynar, but rather is due to the fact that the desired product in this case was a relatively heavy film between 0.089-0.102 mm (0.0035-0.004 in.) thick, while the equipment was more suited to the processing of thinner gauges of more tractable materials (e.g., polypropylene). A second problem that was encountered in the transverse orientation process was the lack of uniformity of thickness of the finished product from one side to the other. This was easily shown to be due to a transverse temperature gradient in the tenter frame oven. Cursory attempts to improve the heat balance across the oven were to no avail. As shown in Figure 3-11, gauge control was good ( $0.096 \pm 0.002$  mm ( $0.0038 \pm 0.0001$  in.) over 0.66 m (26 in.) of the 0.84 m (33 in.) width strip, the problem being confined to 0.178 m (7 in.) along one edge). No measurable variation in thickness was detected in the longitudinal direction of the film. Table 3-2 summarizes the operating conditions of the tenter frame used in the production of the biaxially-oriented Kynar film.

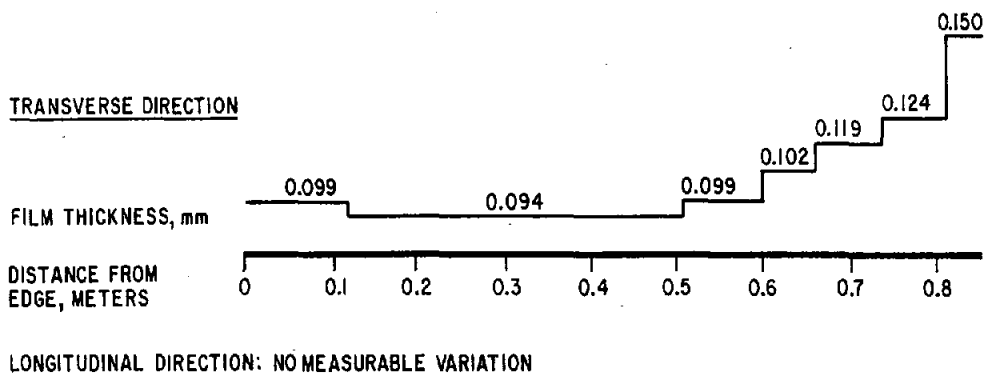


Figure 3-11. Thickness Uniformity of Kynar Film

### 3.3.3 PRODUCT PROPERTIES

#### 3.3.3.1 Optical Properties

The biaxially-oriented Kynar film prepared in the Marshall & Williams Co. pilot plant facility had a tensile strength of 158-172 MPa (23-25 ksi). Elongation at break was 88% in the machine direction (the direction of the original extrusion) and 59% in the transverse direction. Solar transmittance was 0.93 with a 1 sigma specularly  $< 0.62$  milliradians. The transverse striations described in Section 3.3.1 persisted through the transverse orientation step. The striations were expected to have no significant effect on any property except specularly. Qualitatively, the film was water-white and was visually free of the haze that had sometimes characterized earlier oriented PVDF film. The cause of the haze is not known with certainty, but it is probably due to excessive temperature at some stage of the processing.<sup>2</sup> The transmission spectrum of the film is shown in Figure 3-12 and the specularly in Figure 3-13. Specularly is plotted as the fractional intensity of light within a given cone angle relative to the intensity of light within a 28 milliradian cone angle. The high solar transmittance of the film is, of course, an important consideration in its proposed use as an enclosure for solar collectors. In order to confirm the validity of the initial transmittance measurement (0.93), six additional samples were taken at random from the same lot of film, and the transmittances were measured and compared on a statistical basis. The transmittance measurements were all made at DSET Laboratories, and the data were digitized and computer-analyzed relative to the AM 1.5 solar spectrum. The results are shown in Table 3-3 for the six new samples, designated Kynar 1-6, along with the original sample, designated Kynar 0. For an assumed Gaussian distribution, the transmittance of the Kynar had a mean value of 0.9301 and a standard deviation of 0.002. The original reported value was, therefore, verified.

#### 3.3.3.2 Behavior Under Stress

For most design purposes, the yield strength of a material is as important as its ultimate strength since the application of a stress in excess of the yield stress would be expected to lead to permanent deformation. Biaxially-oriented Kynar, however, does not appear to have a well-defined yield point, but rather a continually varying ratio of stress to strain. It was, therefore, important to determine what stress could be applied to the film without causing a permanent deformation. Application of a 77 MPa (11.2 ksi) stress to a Kynar sample resulted in a 20% elongation; upon release of the load, a 7.0% deformation remained.

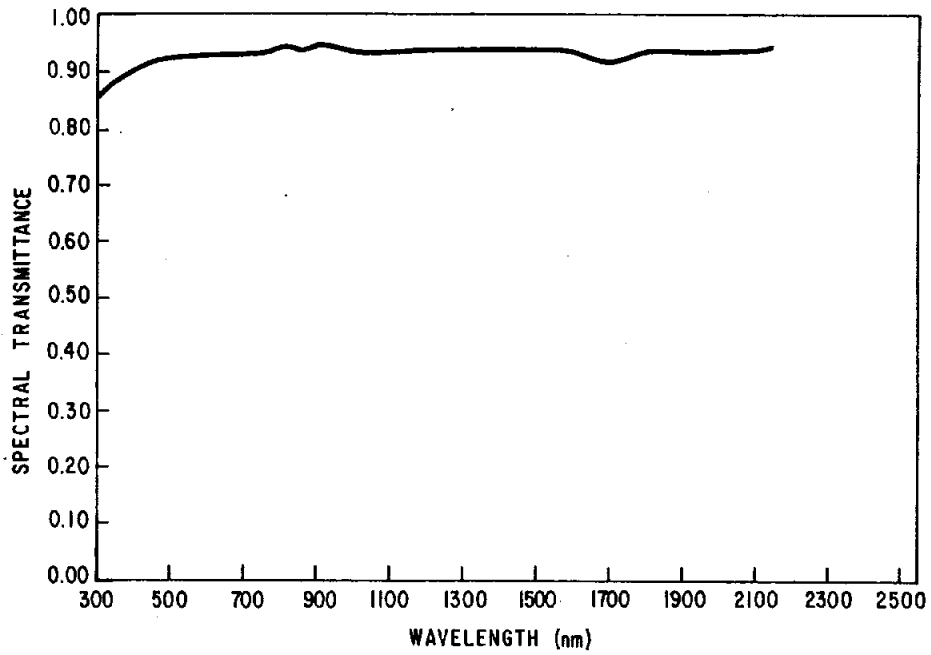


Figure 3-12. Transmittance of Kynar Film

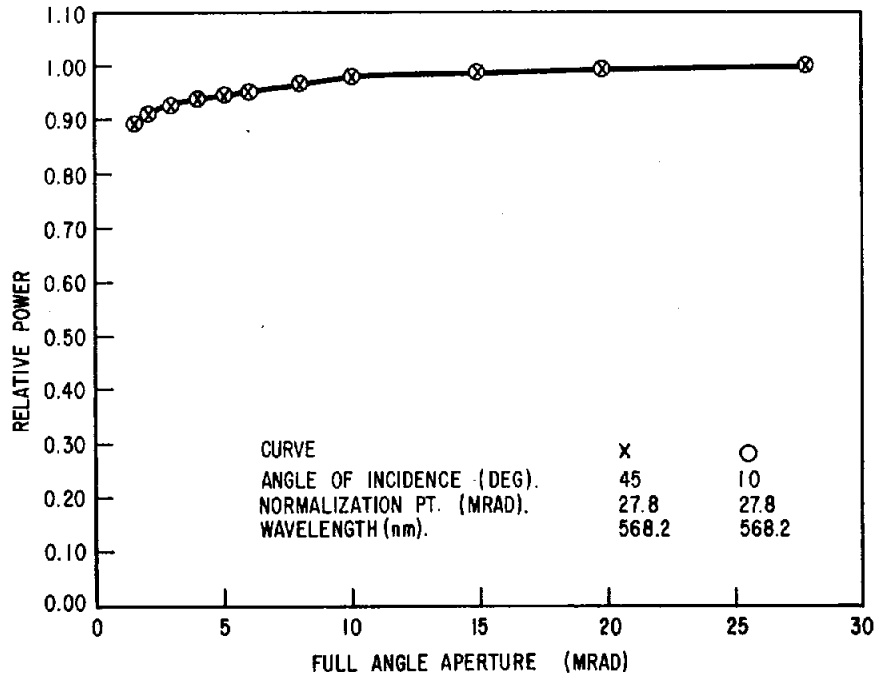


Figure 3-13. Specularity Plot of Kynar 460

Table 3-3  
INITIAL TRANSMITTANCE OF KYNAR

<u>SAMPLE NO.</u>	<u>TRANSMITTANCE @ AM 1.5</u>	<u><math>(x-\bar{x})^2</math></u>
KYNAR-0	.9329	$7.84 \times 10^{-6}$
KYNAR-1	.9313	1.44
KYNAR-2	.9256	20.25
KYANR-3	.9312	1.21
KYNAR-4	.9287	1.96
KYNAR-5	.9279	4.84
KYNAR-6	.9330	8.41
TOTAL	6.5106	$45.95 \times 10^{-6}$

$$\bar{x} = \text{means} = \frac{\sum x}{n} = \frac{6.5106}{7} = .9301$$

$$\sigma = \text{standard deviation} = \left( \frac{\sum (x-\bar{x})^2}{n-1} \right)^{\frac{1}{2}} = \left( \frac{45.95 \times 10^{-6}}{6} \right)^{\frac{1}{2}} = .0028$$

Successive applications of the same force, 72.9 N (16.4 lb), resulted in residual deformation of 4.3%, 3.0%, 2.5%, 2.0%, and 2.0%, so that after six applications of the original force an apparent permanent deformation of 20.8% was observed. Figure 3-14 is a plot of force versus distance, traced from the Instron strip chart recorder. The strain rate was 50.8 mm/min (2 in./min) over a gauge length of 101.6 mm (4 in.), and there was no appreciable "hold time" in the stressed condition.

However, further investigation indicated that the residual deformation was not permanent and disappeared over a period of time. Another sample of Kynar was elongated 20.3 mm (0.8 in.), 20% of the 101.6 mm (4 in.) gauge length, by application of a tensile stress of 76.5 MPa (11.1 ksi). A nominally 25.4 mm (1 in.) gauge near the center of the sample was observed through a cathetometer. Before any elongation of the sample, the cathetometer reading was 0.985. After the first elongation of 20%, the reading was 1.033; after four applications of the same loading, the cathetometer reading was 1.088. Tension was removed from

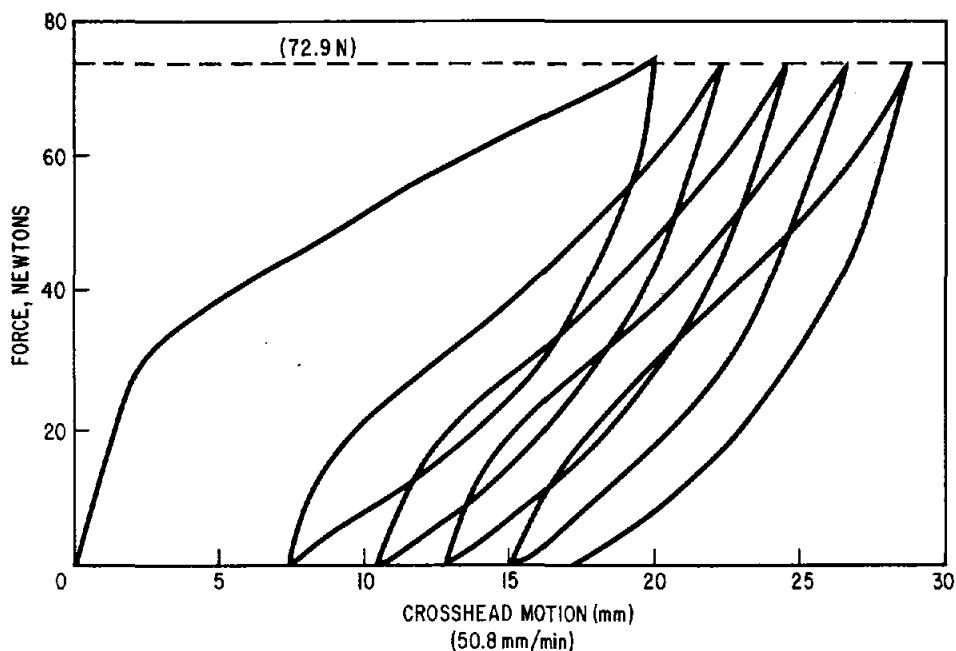


Figure 3-14. Effect of Cyclic Stress on Strain of Kynar

the sample and readings were repeated at intervals. After 10 minutes the reading was 1.064; after 45 minutes, 1.033; and after 3 hours 45 minutes, 1.026. The sample was once more stressed to 76.5 MPa (11.1 ksi), but this time the Instron crosshead was reversed just until a no-load condition was reached. The crosshead was stopped and the development of a tensile stress in the sample was observed. Within minutes, the Kynar film developed a stress of 6.65 MPa (965 psi); after 90 minutes the stress had increased 9.86 MPa (1430 psi); after 5 hours it was 10.3 MPa (1500 psi); and after 19 hours it was 13.8 MPa (2000 psi).

In similar fashion, experiments were conducted at 25%, 30% and 33% elongation. The latter corresponds approximately to a 20% offset yield and required a tensile stress of 103 MPa (15 ksi). In every case a "permanent" deformation was observed after the first application of stress; but additional deformation due to a second application of the same load essentially disappeared, in all cases, within 4 hours. The deformation resulting from the first stress may also disappear in time.

It appears that biaxially-oriented Kynar 460 can recover from at least 33% elongation or 103 MPa (15 ksi) tensile stress at room temperature without major distortion lasting more than 4 hours. Indications are that the recovery continues well beyond 4 hours and perhaps up to 19 hours.

### 3.3.3.3 Creep

A plastic subjected to a specific static load deforms rapidly to a strain predictable from its appropriate modulus, then continues to deform at a lower rate over a long period of time or, if the load is high enough, until rupture occurs. This behavior is creep. Creep curves (strain vs time) generally show three distinct stages: a first stage characterized by large and rapid deformation; a second stage in which deformation continues at a slow and constant rate; and a third stage characterized either by increasing rate of deformation leading to rupture or by abrupt rupture without warning. A complete characterization of the creep behavior of a material entails the development of creep-rupture envelopes at a number of temperatures. Such an effort was beyond the scope of the present work, and creep testing of Kynar film was limited to 1000-hour tests with three different loads at room temperature and one load at 50°C. The creep rate of Kynar film proved to be much lower than had been expected from the lack of a definable tensile modulus and the creep behavior of most fluorinated polymers. The creep behavior is summarized in Figure 3-15. In addition to the experiments at 18.4 MPa (2666 psi), 50 MPa (6666 psi), and 69 MPa (10,000 psi), a test was conducted at 9.2 MPa (1333 psi), but the total strain was only 0.05%. Another feature evident in Figure 3-15 is the lack of permanent distortion resulting from prolonged stress. Removal of the load after 1000 hours at 69 MPa (10 ksi) resulted in almost complete recovery of the film within 24 hours.

### 3.3.3.4 Abrasion Resistance

The resistance of materials to abrasion by blowing sand and dust is a major concern in all concentrating solar systems. Scattering of light can have deleterious effects on the efficiency of the system. Unfortunately, there does not appear to be a known correlation between any standard abrasion test method and the expected lifetime of a particular solar collector system in a particular locale. Therefore the abrasion problem was scoped in a qualitative manner by examining the effect of falling abrasive on glass, on PET film, and on Kynar film in accordance with ASTM Standard Test Method D673. As is shown in Figure 3-16, the Kynar film exhibited a much lower "loss of gloss" (or loss of specularity) than did the LLumar polyester film but a higher loss than glass. It will remain for future studies to determine the severity of the abrasion problem in practice, or whether the problem exists.

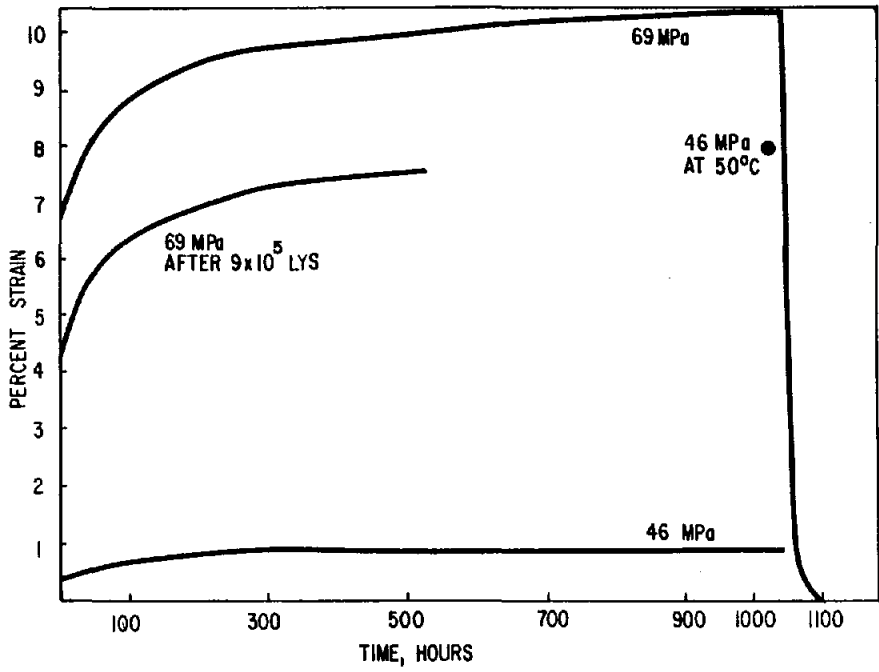


Figure 3-15. Creep Behavior of Kynar

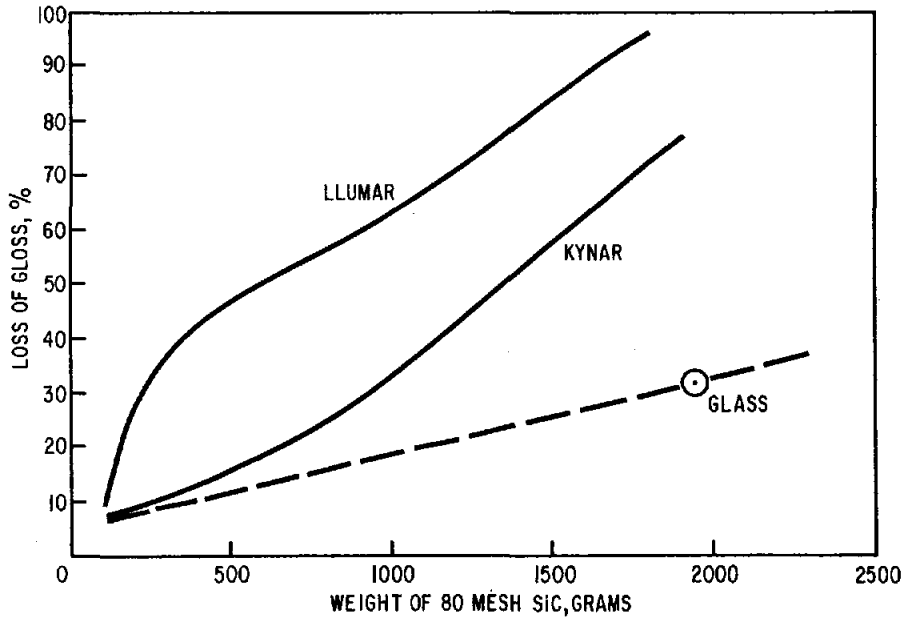


Figure 3-16. Mar Resistance of Materials (ASTM D673)

### 3.3.3.5 Tear Resistance

A characteristic shared by many oriented films is low propagating tear strength. PVDF shares this characteristic. Propagating tear strength in the transverse direction was 459 g/mm (11.6 g/mil) and 550 g/mm (13.9 g/mil) in the machine direction.

Other mechanical properties of the biaxially-oriented Kynar are described in Section 6.2 - Outdoor Exposure, particularly those properties which were measured in comparison with the properties of other candidate enclosure materials.

### 3.3.4 PROBABLE OUTLOOK

It has been demonstrated that PVDF can be biaxially-oriented in a process analogous to that used commercially for the production of other films such as polypropylene and PET. Further refinement of the process parameters such as temperature control, draw ratio, and draw contour will undoubtedly lead to improved product properties. Since the process is now used to produce PET in thicknesses to at least 0.254 mm (0.01 in.), it is reasonable to expect that it can be used to produce PVDF film in any desired thickness and in widths of at least 2 m. Heavy duty equipment of the type used for the orientation of PET film will be required.

## Section 4

## INVESTIGATION OF METHODS FOR BONDING PLASTIC FILMS

4.1 ADHESIVE BONDING

Adhesive bonding is often an efficient, economical, and durable method for joining plastic film. Many techniques are available for adhesive application, each of which offers advantages for particular types of adhesives or plastic assemblies. Many of these methods can be easily factored into automated production lines. Therefore, the adhesive bonding of LLumar PET film and Kynar PVDF film was investigated. The Kynar film used in the bonding studies was nominally 0.1 mm (0.004 in.) thick. Lap bonds approximately 4.8-6.4 mm (3/16-1/4 in.) wide were made in both the machine and transverse directions of the film.

The first adhesive systems tried on the Kynar film were Versilok types 551 and 506 acrylic adhesive systems. No significant adhesion to the Kynar film could be obtained. Lap bond strengths on the order of 875.5 N/m (5 lb/in.) of bond length were obtained with a lap bond of 4.8-12.7 mm (3/16-1/2 in.) No etching of the Kynar surface took place, resulting in complete separation of the adhesive from the film surfaces. A film surface treatment with dimethylacetamide (DMA) or the addition of this solvent to the adhesive may be possible. This solvent will attack the Kynar surface and may produce some surface etching to give the adhesive a bondable surface. This treatment was not tested with the Versilok systems but may be of interest in the future.

An adhesive incorporating dimethylacetamide as a solvent was evaluated. This system was suggested by Pennwalt Corp. The adhesive is 20% by weight solids made up of 80% Acryloid B44 and 20% Kynar 301F. The solvents in this system are 70% methyl cellosolve acetate and 30% dimethylacetamide. At room temperature, this material is a gelatinous mass. The two resin components appear to separate at room temperature (<30°C), but heating of the mixture to approximately 35°-40°C partially fluidizes the mixture and permits recombination of the system. Tensile tests of Kynar film bonded with this adhesive demonstrated excellent strength, greater than 12.2 kN/m (70 lb/in.) of bond length.

The manufacturer, Pennwalt, recommended application of this adhesive to both surfaces to be bonded, allowing the solvents to evaporate until the surfaces were tacky, and pressing together and heating for 10 to 15 minutes at 115°C. Optimum lap joints were formed when the adhesive was first heated at 35°C and mixed. This produced a stable, uniform mixture that could be spread on the bonding surfaces without immediate solvent flashoff.

It was found that a polyethylene squeeze bottle with a conical tip cut off at an angle to expose a 1.6 - 2.4 mm (1/16 - 3/32 in.) orifice provided the best applicator. At the suggested application temperature, 35°C, the mixture is still gelatinous, requiring a pressure-feed applicator that the polyethylene squeeze bottle provided. Adhesive spread and solvent flashoff were found to be improved if the two film surfaces also were held at 35° to 45°C. Film temperature lower than this caused the adhesive not to wet the film surface and the two solid components to separate on the surface. The suggested film bonding temperature of 115°C resulted in heavy wrinkling of the films near the bond line. Absorption of the solvents into the films resulted in shrinkage of the films at the bond lines during the terminal bonding cycle. It was found that lowering the bonding temperature to 90°C alleviated, but did not totally eliminate, this wrinkling. Lowering the bonding temperature below 90°C resulted in poor bond tensile strength, <12.2 kN/m (<70 lb/in.). Secondly, extending the solvent flashoff so that the adhesive was no longer tacky also reduced the bond strength.

Pressure was applied to the bond line during the heating cycle. Optimum bond lines were achieved with a load of 0.15 MPa (20 psi). Pressures higher than this had a tendency to cause a flow of the film material in the solvent-affected regions, resulting in a reduction of the film thickness. Pressures lower than this resulted in incomplete bonding due to gas bubble entrapment in the bond.

It is recommended that if further work is done with this system, solvents be found that would be less active in causing wrinkling. Pennwalt personnel suggest dimethyl phthalate rather than the DMA.

A Morton Chemical Company adhesive, Adcote 76M5 with a 9H1 catalyst, was used for bonding of LLumar polyester. This is a two-component polyester-based adhesive containing 20% solids in a methylene chloride solvent.

The manufacturer's recommended application of this adhesive system is by coating both surfaces of the film, allowing to dry to a tack-free surface and then combining at 150° - 177°C for "a few seconds." The adhesive had a pot

of approximately 8 hours and the bonding should take place within 24 hours of application.

The difficulty in the use of this material was in the application of the adhesive to the polyester film. Methylene chloride as a solvent presents application problems because of its rapid evaporation. Pressure-fed glass and Dacron felt wipers were tried, along with brushing and spraying. All these methods suffered from clogging or very erratic thickness of adhesive film. Narrow striping rolls also were tried. These left chunks of resin along both edges of the rolled stripe. The intent was to apply a narrow uniform band, approximately 4.8 mm (3/16 in.) wide, of adhesive along an edge of the film. Of the unsuccessful methods listed above, spray application may have some merit if a miniature external mix pressure spray head is available. The unsuccessful spray system tried was an internal mix air brush. Heavy clogging, spattering or webbing resulted from the internal mix spray nozzle that was available. A K&E<sup>TM</sup> inking pen head also was tried, but clogging of the space between the barrel and plunger of the pen occurred within a minute on exposure to the air. It was found, however, that an applicator made from a medicine dropper worked well. When the end of a medicine dropper was flame polished so that a 0.25-0.38 mm (0.01-0.015 in.) diameter hole remained, capillary action held the adhesive in the barrel. Contact of the flame-rounded end of the glass to the plastic film provided a smooth applicator tip that fed through the capillary section from the barrel.

The adhesive stripe produced by the modified medicine dropper was about 2.4 mm (3/32 in.) wide. Rate of application and consequently film thickness could be controlled by the speed at which the tip was drawn over the polyester film sheet. To obtain the 4.8-6.4 mm (3/16-1/4 in.) wide stripe for bonding, two passes on each film edge were used.

The results of adhesive bonding experiments are summarized in Table 4-1.

#### 4.2 ULTRASONIC BONDING

Ultrasonic assembly of thermoplastic film is a clean, fast, readily automated process capable of handling high volume production. High frequency mechanical vibrations are utilized in ultrasonic bonding to melt the joining surfaces of the thermoplastic films and to fuse them together with a strong molecular bond. Friction and the alternating high frequency stress produced by the vibrations generate heat in the plastic at the interface and cause it to melt.

Table 4-1  
ADHESIVE BOND STRENGTHS

Sample #	Film	Failure Load		Bond Strength		Bond Strength	
		N	(lb)	MPa	(psi)	kN/m	(lb/in. length)
3-2-1-1	LLumar, M.D. (a)	184	(41.3)	1.86	(270)	10.4	(59.4)
-2		183	(41.2)	3.34	(485)	10.3	(59.1)
-3		179	(40.3)	4.03	(584)	10.2	(58.1)
-4		166	(37.4)	3.68	(534)	9.4	(53.8)
-5		184	(41.3)	1.95	(283)	10.4	(59.6)
Average				2.97	(431)	10.2	(58.0)
3-2-2-1	LLumar, T.D. (b)	167	(37.5)	1.05	(152)	9.4	(54.0)
-2		163	(36.7)	1.10	(160)	9.3	(52.9)
-3		148	(33.3)	1.05	(153)	8.4	(48.1)
-4		174	(39.2)	1.10	(159)	9.9	(56.3)
-5		170	(38.2)	1.14	(165)	9.7	(55.3)
Average				1.09	(158)	9.3	(53.3)
3-7-1-1	Kynar, T.D.	269	(60.5)	1.85	(268)	15.4	(88)
-2		293	(66.0)	1.88	(273)	16.6	(95)
-3		262	(59.0)	1.84	(267)	15.2	(87)
-4		100	(22.5)	0.66	(96)	5.8	(33)
-5		87	(19.5)	0.54	(78)	4.9	(28)
Average				1.35	(196)	11.6	(66)
3-7-2-1	Kynar, M.D.	--	--	--	--	--	--
-2		248	(55.8)	2.10	(305)	14.0	(80)
-3		274	(61.5)	2.21	(320)	15.6	(89)
-4		227	(51.0)	2.01	(291)	13.0	(74)
-5		220	(49.4)	1.90	(276)	12.6	(72)
Average				2.05	(298)	13.8	(79)

(a) Machine Direction  
(b) Transverse Direction

Ultrasonic bonding was studied as a means of joining films of Melinex OW, LLumar, and Kynar. In this particular application a flat anvil and rounded horn were used. The two films to be joined were overlapped approximately 0.79 mm (1/32 in.). Bonded samples were provided by several potential vendors, all skilled in the art of ultrasonic assembly. By far, the most satisfactory results were obtained by Ultra Sonic Seal Co. in Broomall, Pa.

Ultrasonic seals would have at least two distinct advantages in heliostat enclosures. First, the bond line is about 0.79 mm (1/32 in.) wide, creating a minimum of shadowing interference. Second, no foreign substance is introduced into the bond; the only material present is the material of the plastic film itself.

None of the ultrasonic bonds produced in this study was as strong as the adhesive bonds; the major difficulty with the ultrasonic bonds was the extremely low tear strength found in every case. It appeared that the sealing process had in some way damaged the plastic film adjacent to the bond area.

Because of the potential advantages mentioned above, ultrasonic bonding of the plastic films deserves further attention. However, for the purposes of this program, ultrasonic bonds were not considered further in the test program. The results of tensile tests of the ultrasonic bonds are summarized in Table 4-2.

#### 4.3 RADIO FREQUENCY BONDING

High frequency or radio frequency (RF) sealing fuses two or more films of thermoplastic by means of heat and pressure. RF sealing takes advantage of the high dielectric loss characteristics of certain plastics. When the material is placed in a radio frequency field, internal friction develops between the molecules of the plastic, causing heat to be produced. PET does not have a high dielectric loss at the 27.12 MHz frequency normally used in RF bonding, so no attempt was made to bond LLumar or Melinex OW by RF bonding.

An attempt was made to RF seal Kynar film with a machine normally used for sealing heavy gauge poly(vinyl chloride) swimming pool liners. The machine appeared to have to effect whatever on the Kynar. Therefore, samples of film were sent to Solidyne, Inc., Bay Shore, N.Y., who tried sealing with a 65 MHz machine. The seam made with the high frequency machine had a tensile strength of 10.8 kN/m (62 lb/in.), but unfortunately, a very low tear strength. RF bonding was not pursued further.

Table 4-2  
ULTRASONIC BOND STRENGTHS

Sample #	Film	Failure Load		Bond Strength		Bond Strength	
		N	(lb)	MPa	(psi)	kN/m	(lb/in. length)
3-1-2-1	Melinex OW	93	(21.0)	4.26	(618)	5.4	(31)
-2		107	(24.1)	4.75	(689)	6.1	(35)
-3		99	(22.2)	4.37	(634)	5.8	(33)
-4		98	(22.0)	4.34	(629)	5.6	(32)
-5		89	(20.1)	3.96	(574)	5.1	(29)
Average					4.34	(629)	5.6
3-1-3-1	LLumar	118	(26.5)	4.35	(631)	6.6	(38)
-2		112	(25.3)	4.25	(617)	6.5	(37)
-3		135	(30.3)	4.97	(721)	7.7	(44)
-4		143	(32.2)	5.29	(767)	8.2	(47)
-5		145	(32.5)	5.34	(774)	8.2	(47)
Average					4.84	(702)	7.5
3-4-1-1	Kynar	138	(31.0)	3.10	(449)	7.9	(45)
-2		101	(22.7)	2.27	(329)	5.8	(33)
-3		87	(19.5)	1.95	(283)	4.9	(28)
-4		117	(26.4)	2.64	(383)	6.6	(38)
-5		159	(35.8)	4.05	(587)	9.1	(52)
Average					2.80	(406)	6.8
3-1-1-1	LLumar	75	(16.9)	2.12	(307)	3.0	(17)
-2		67	(15.0)	1.85	(268)	2.6	(15)
-3		70	(15.8)	1.98	(287)	2.8	(16)
-4		68	(15.3)	1.92	(278)	2.6	(15)
-5		72	(16.2)	2.03	(295)	2.8	(16)
Average					1.98	(287)	2.8

#### 4.4 ELECTROMAGNETIC OR INDUCTION-HEATED BONDING

In the electromagnetic or induction-heated bonding process, magnetic fields are used to melt a thermoplastic layer containing paramagnetic micrometer-size or sub-micrometer-size particles. When the composition is placed between the surfaces to be bonded and is exposed to an alternating magnetic field, heat develops at the interface, causing melting and fusion of the intervening layer. LLumar, Melinex OW, and Kynar all were successfully bonded by this technique.

The method has been described by Leatherman<sup>3</sup> in some detail: "A typical bonding agent for the process consists of a layer of thermoplastic, selected to make a good weld, into which has been dispersed one-half to six percent by volume of very fine magnetic iron oxide powder. The iron oxide has the characteristic of becoming hot in a short time as a result of magnetic loss when exposed to a high-frequency magnetic field of proper type. Such excitation typically can be provided by a conventional induction coil operating at a frequency of 2 to 7 MHz. The magnetic-loss phenomenon permits the heat-generating iron oxide powder to be used in submicron size and to be mixed into bonding agents by normal dispersing and compounding methods.

"To make a bond in thermoplastic, two materials to be joined are brought together with a layer of bonding agent between them [as in Figure 4-1]. The induction coil, which supplies the magnetic excitation field to produce the heat, can be simply a loop or 'hairpin' of copper tubing, shown in cross-section. When the coil is energized, the bonding agent (tape, coating, or ink with the iron oxide constituent) rapidly melts and fuses adjacent substrates. Modest pressure completes the weld with virtually no distortion or squeezeout, since the major portion of the substrate thickness is still cold."

The polyester films were bonded using a film-type bonding agent proprietary to HELLERBOND. Bonding tape starting dimensions were 0.15 x 2.4 mm (0.006 x 0.094 in.) and the heat cycle was 0.6 seconds. Tensile strength of this bond was as high as 12.6 kN/m (72 lb/in.). However, later it was determined that the 0.6 second heat cycle did not appear to provide the desirable high level of reliability. In subsequent experiments, the heating cycle of 1.5 seconds was used. While this increased heating cycle appeared to improve the reliability

---

<sup>3</sup>A.F. Leatherman, "Magnetic Heat Bonding," Modern Packaging, June 1974.

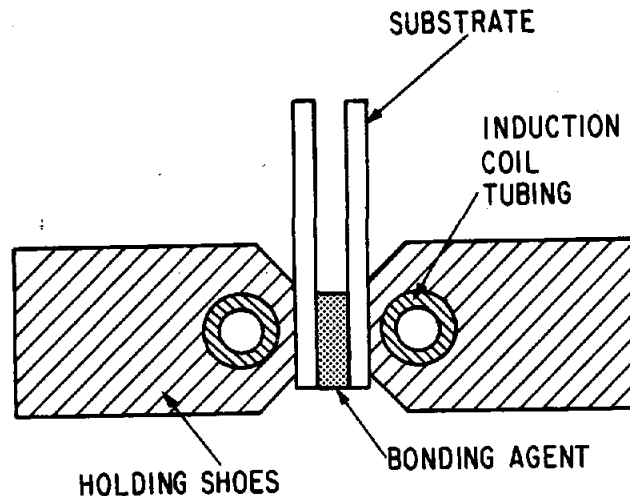


Figure 4-1. Schematic Arrangement of Magnetic Heat System

of the bond, the average strength decreased to 8 kN/m (46 lb/in.). It may be that the longer heating cycle resulted in some damage to the film and that the optimum heat cycle is between 0.6 and 1.5 seconds. Kynar film was bonded using a bonding tape made from Kynar resin with approximately the same dimensions as the polyester bonding agent. A heating cycle of 0.75 seconds was used. A tensile strength of 13.8 kN/m (79 lb/in.) was obtained with the Kynar bond. Tensile failure of all the bond samples occurred immediately adjacent to the bond line. A fractured sample is shown in Figure 4-2. The actual bond length in this sample was 17.5 mm (0.69 in.). It is believed that the location of the failure is due to stress concentration at the bond. The average stress in the film at the time of failure was approximately 145 MPa (21 ksi). Bonds made by other methods such as ultrasonic or RF welding also were observed to fracture adjacent to the bond line. This, too, may be due to stress concentration, but also may be due to physical damage to the polymer film by the sealing technique.

Both adhesive and electromagnetic bonding techniques appear useful in bonding LLumar and Kynar. Ultrasonic and RF techniques have certain potential advantages if tear strengths can be improved.

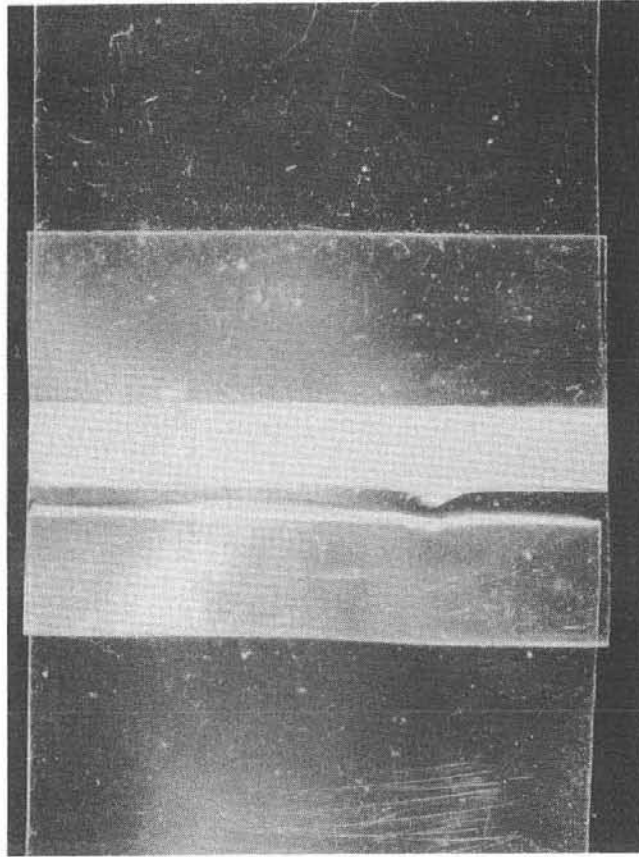


Figure 4-2. Fracture of an Electromagnetic Bond in Kynar

## Section 5

## DEVELOPMENT OF SPECULARLY-OPTIMIZED METALIZED FILM REFLECTORS

High power, high temperature solar thermal systems generally depend on the use of large areas of highly reflective material. Although glass and anodized aluminum have obvious merits in this application, metalized plastic films have the added potential to be very low cost and very low weight. The challenge is to make metalized plastic films as reflective, specular, and stable as the competing materials. It frequently has been assumed that first-surface aluminized film would be adequate in enclosed reflector systems. Therefore, it seemed appropriate to start the investigation with a study of the metalization process since the results would presumably be applicable regardless of whether a first-surface or a second-surface reflector were eventually chosen.

5.1 METALIZATION STUDIES

During an earlier program, data were obtained which seemed to indicate a high degree of dependence of the specularity of reflected light on the thickness of the vapor-deposited aluminum of a first-surface mirror. To determine whether this really is an important consideration, samples were taken from a single roll of polyester, Celanese EC534, which was metalized in a single production run using a variety of conditions, such as angle of deposition, vacuum level, and rate of motion of the film through the metalizer. Samples were taken from this film, and specular and hemispherical reflectance measurements were made to determine whether deposition conditions of the aluminum have a strong effect on specular reflectance. The results of the study were convincing evidence that, under good commercial production conditions, neither rate of deposition, system pressure, nor angle of incidence has any detectable effect on the reflectance of vapor-deposited aluminum. The results are summarized in Table 5-1. The system pressure is necessarily qualitative, since there is no pressure sensor in the deposition region of the equipment. The deposition rates were approximately  $10^2$  and  $10^5$  nm/sec.

It is, however, easy to show that in both first- and second-surface reflectors the choice of substrate is critical to the performance of the reflector. Reflectors #1 and #4 in Table 5-2 were prepared by the same converter as those in Table 5-1,

Table 5-1

EFFECT OF DEPOSITION CONDITIONS ON ALUMINUM REFLECTANCE  
(Commercial Deposition Equipment, EC 534 Polyester Substrate)

<u>Variable Studied</u>	<u>2.5° Specular Solar Reflectance (AM 1.5)</u>
Angle of Incidence	
Grazing	0.91
45°	0.90
Normal	0.92
System Pressure	
High	0.92
↓	0.91
↓	0.91
↓	0.91
↓	0.91
Low	0.91
Rate of Deposition	
High	0.92
Low	0.92

which were prepared on Celanese EC534, a smooth, clear film. Celanar 5000 apparently contains a filler which reduces its smoothness, although it appears superficially to be a smooth, clear, transparent film. Melinex 442 is a commercial film not intended for demanding optical applications. The differences in specular reflectance are obvious.

Nothing in the above discussion should be taken to mean that deposition process parameters have no effect on the reflectance of vapor deposited aluminum. In fact, the laboratory studies summarized in Table 5-3 showed, as expected,<sup>4,5</sup> an optimum thickness of aluminum and an effect due to chamber pressure. The only surprise was the higher reflectance obtained with some oxygen in the chamber compared to the reflectance obtained at the system base pressure  $1.33 \times 10^{-4}$  Pa ( $10^{-6}$  torr).

<sup>4</sup>L. Holland, J. of Optical Soc. of Amer. 43, (1953), p. 376.

<sup>5</sup>G. Mass, J. of Optical Soc. of Amer, 45, (1955), p. 945.

Table 5-2  
CANDIDATE REFLECTORS

<u>Sample Number</u>	<u>First Surface, Polyester Substrates</u>	<u>2.5° Specular Solar Reflectance (AM 1)</u>
1	Celanar 5000/Al	0.71
2	Melinex OW/Al	0.87
3	Melinex 531/Al	0.86
4	(a) Melinex 442/Al	0.87
5	Mylar D/Ag/Al <sub>2</sub> O <sub>3</sub> .SiO <sub>2</sub>	0.92
6	Mylar D/Al/Al <sub>2</sub> O <sub>3</sub> .SiO <sub>2</sub>	0.37
7	(a) Melinex 442/DC Q9-6315	0.88 (AM 1.5)
<u>Second Surface</u>		
8	(a) Martin Processing	0.82
9	Dunchrome	0.82 (Hemispherical)
10	Ag/LLumar	0.81
11	Al/Kynar	0.12
12	Ag/Kynar	0.18
<u>New Second-Surface Samples</u>		
13	Ag/LLumar	0.91
14	Ag/Tedlar	0.81

(a) Selected for Weathering Tests

It can be concluded that with proper technique and choice of materials, AM 1.5 solar reflectance of 0.90 to 0.91 can be obtained consistently with vapor-deposited aluminum.

## 5.2 FIRST-SURFACE AND PSEUDO-FIRST-SURFACE REFLECTORS

While a study of aluminum deposition is a necessary part of the investigation of plastic film reflectors, unprotected aluminum is probably not stable enough for solar collectors, regardless of whether they are enclosed. Therefore, the major interest is in second-surface reflectors or reflectors with a protective layer over the metal.

Table 5-3

## EFFECT OF LABORATORY DEPOSITION CONDITIONS ON THE REFLECTANCE OF ALUMINUM VAPOR-DEPOSITED ON MELINEX 442 POLYESTER

<u>Al Thickness, nm</u>	<u>Oxygen Pressure</u>		<u>2.5° Specular Solar Reflectance (AM 1)</u>
	<u>Pa</u>	<u>(torr)</u>	
50	$<1.3 \times 10^{-4}$	$(<10^{-6})$	0.83
125	$<1.3 \times 10^{-4}$	$(<10^{-6})$	0.84
200	$<1.3 \times 10^{-4}$	$(<10^{-6})$	0.80
125	$6.6 \times 10^{-3}$	$(5 \times 10^{-5})$	0.87
125	0.04	$(3 \times 10^{-4})$	0.61
125	0.07	$(5 \times 10^{-4})$	0.63

One approach to developing a lightweight reflector material entails a metalized plastic film and a thin protective layer over the metal, a configuration for which the term "pseudo-first-surface reflector" has been coined. Silver and aluminum were vapor-deposited on LLumar film, and successive layers about 50 nm each of aluminum oxide and silicon dioxide were deposited by Magnetron sputtering over the metal. (Table 5-2, reflectors #5 and #6.) The aluminum reflector was essentially diffuse, having a 2.5° specular solar reflectance of only 0.37. The silver reflector, however, had an encouraging 0.92 specular AM 1 solar reflectance. The reflectance spectrum is shown in Figure 5-1. The specularity, however, was not as high as had been expected. Figure 5-2 is a plot of the relative specularity. Since the durability of this reflector is doubtful and the processing cost would be high even in mass production, this reflector was not investigated further. Instead, aluminized LLumar was coated (on the aluminum side) with Dow Corning's Q9-6315 resin, (Table 5-2, reflector #7) which decreased the measured AM 1.5 solar specular reflectance from 0.90 to 0.88. The flat spectral response of this reflector can be seen in Figure 5-3. The specularity of the reflector before coating is shown in Figure 5-4. Comparison with Figure 5-5 shows that the Dow Corning coating had little adverse effect on the specularity. However, the coating should improve the abrasion-resistance of the reflector and will probably inhibit the oxidation that is expected to limit the lifetime of unprotected aluminum reflector surfaces. The Dow Corning coating may provide a very satisfactory solution to the oxidation and abrasion sensitivity of first-surface aluminized reflectors.

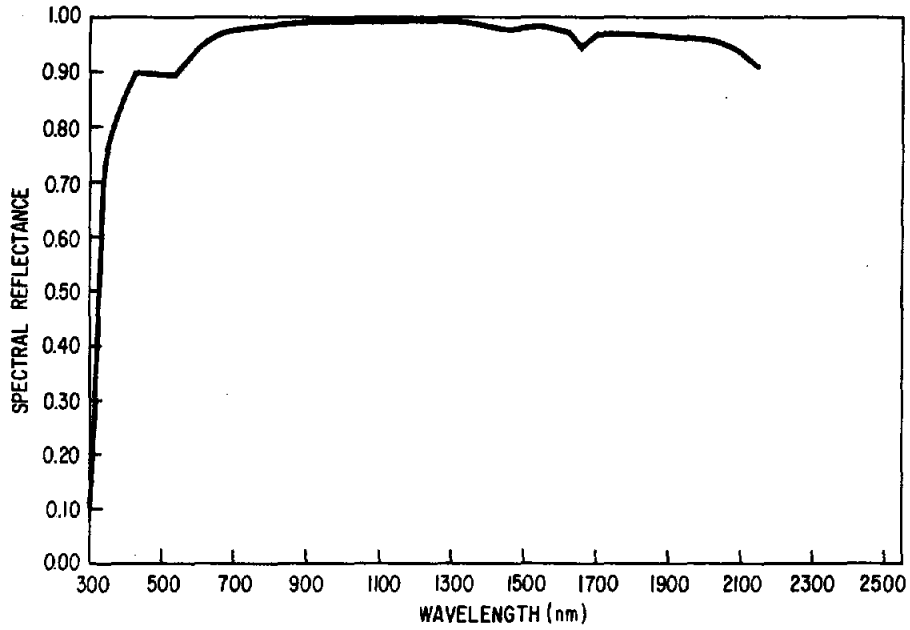


Figure 5-1. Reflectance of Pseudo-First-Surface Silver Reflector

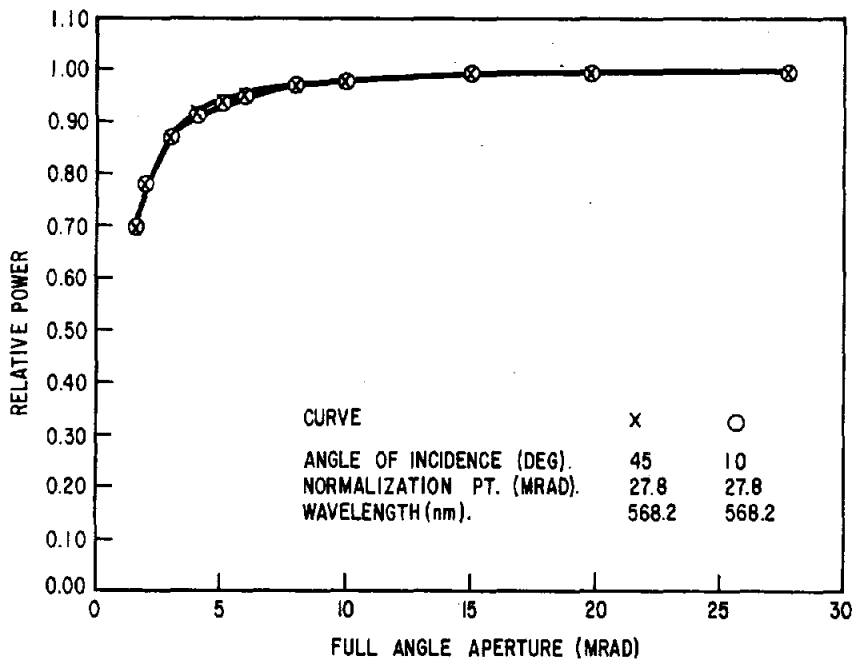


Figure 5-2. Specularity of Pseudo-First-Surface Silver Reflector

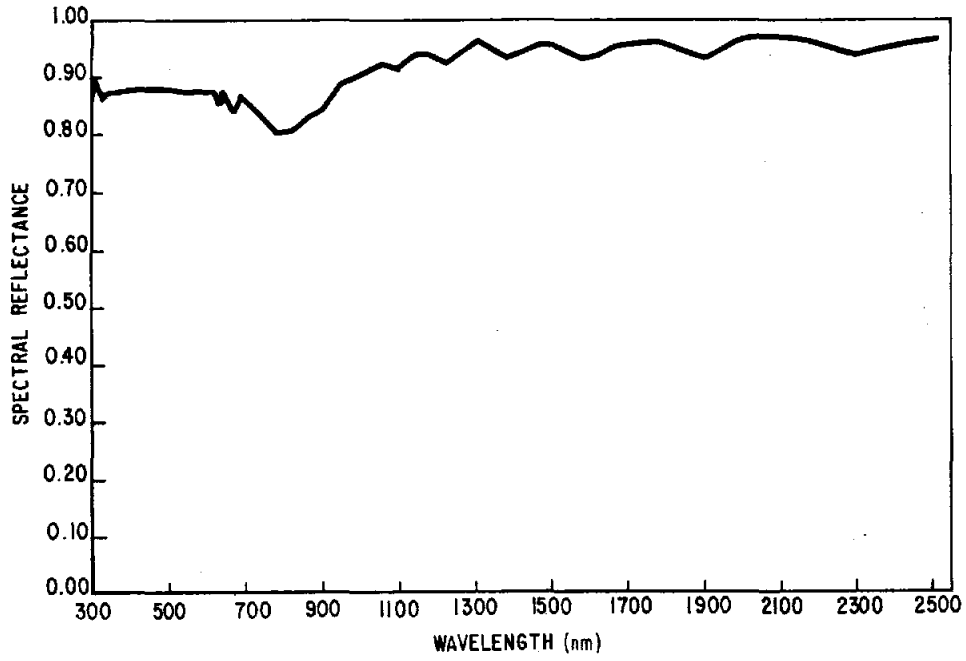


Figure 5-3. Reflectance of Aluminized LLumar Overcoated with Dow Corning 096315 Resin

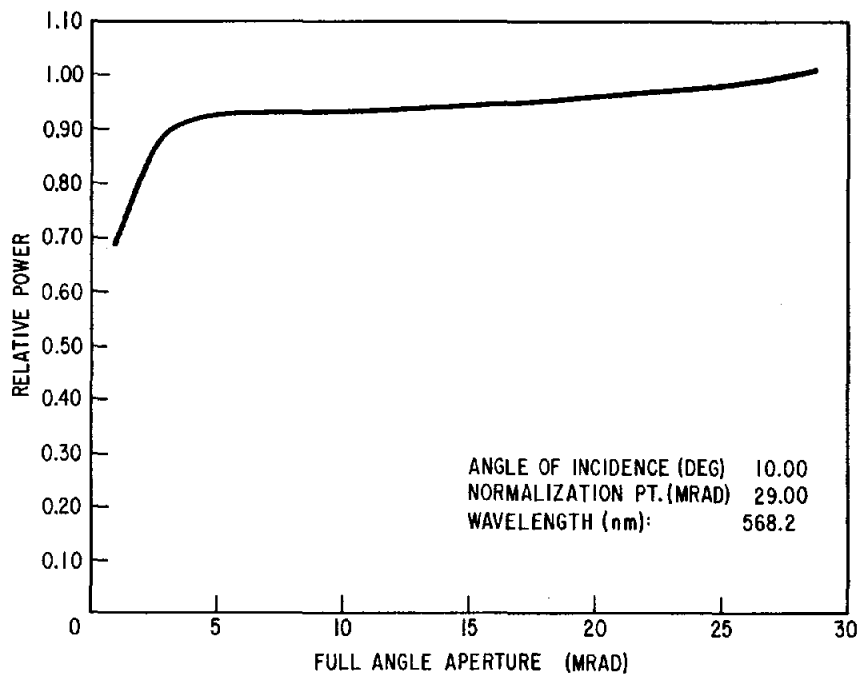


Figure 5-4. Specularity of Aluminized LLumar Before Overcoating with Dow Corning 096315 Resin

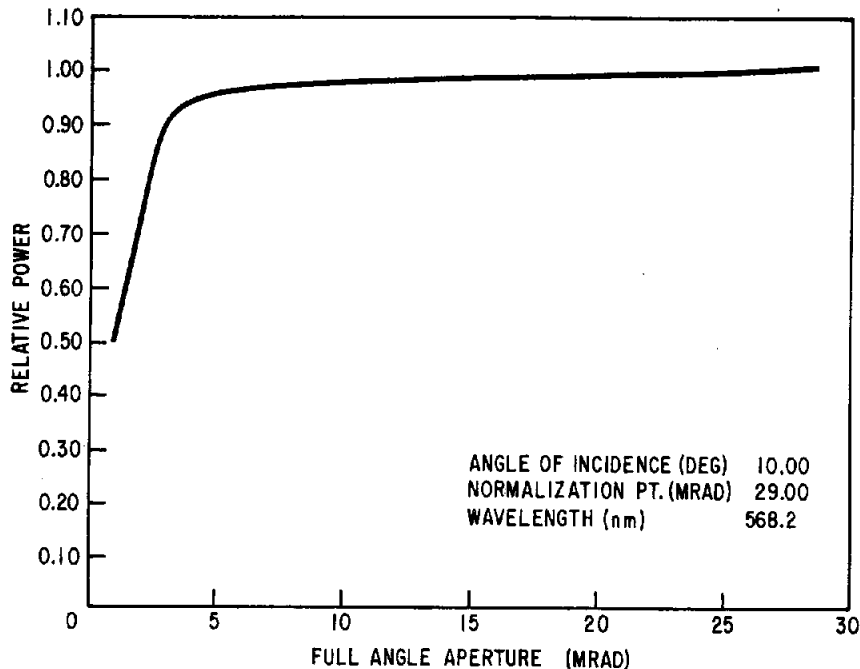


Figure 5-5. Specularity of Aluminized LLumar Overcoated with Dow Corning Q96315 Resin

### 5.3 SECOND-SURFACE REFLECTORS

Two second-surface metalized film reflectors commercially available are made by Martin Processing Company and by Dunmore Corporation. Both use stabilized polyester as the first surface, though major differences exist between the methods of preparation and the finished products. The Martin Processing reflector uses a LLumar stabilized polyester film as the front surface. It has an air mass 1 solar reflectance of about 0.81, and when made with the proper polyester film, is specular within about 1.5 milliradians half-cone angle. The reflectance spectrum is shown in Figure 5-6. It shows the characteristic strong absorption of LLumar at 400 nm. The reflector material used in the early studies of this program was made from Melinex 442. The specularity of this reflector is adequate for most purposes. It is shown in Figure 5-7. Later in the program, a similar reflector was made based on Melinex 516. The improvement in specularity can be seen by comparing Figures 5-7 and 5-8.

The reflector made by Dunmore Corporation was intended to be included in the weathering program. It has approximately the same AM 1 solar reflectance as the Martin Processing product with a similar short wavelength cut-off (Figure 5-9). Unfortunately the specularity, as shown in Figure 5-10, is low for heliostat use.

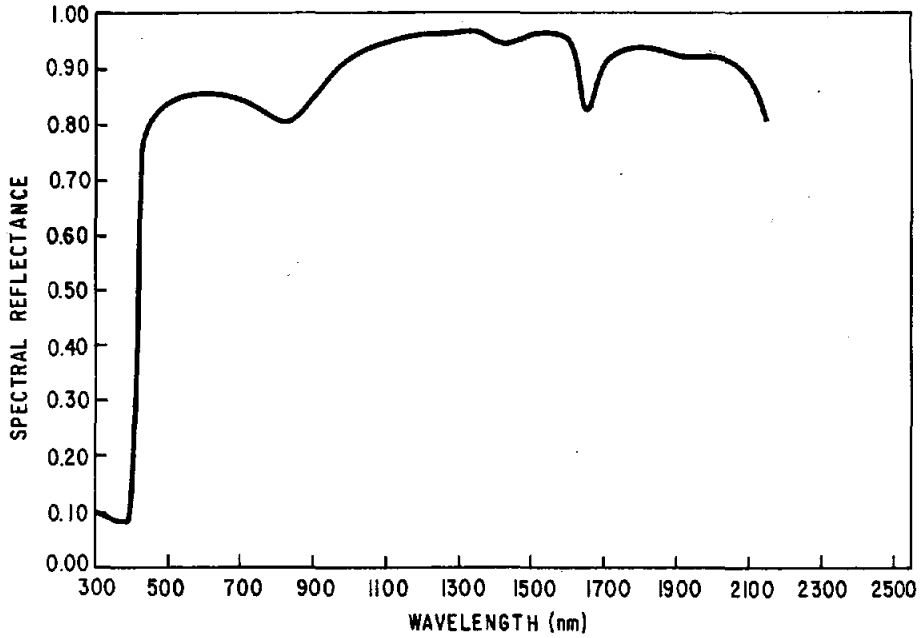


Figure 5-6. Reflectance of Martin Processing Company Reflector

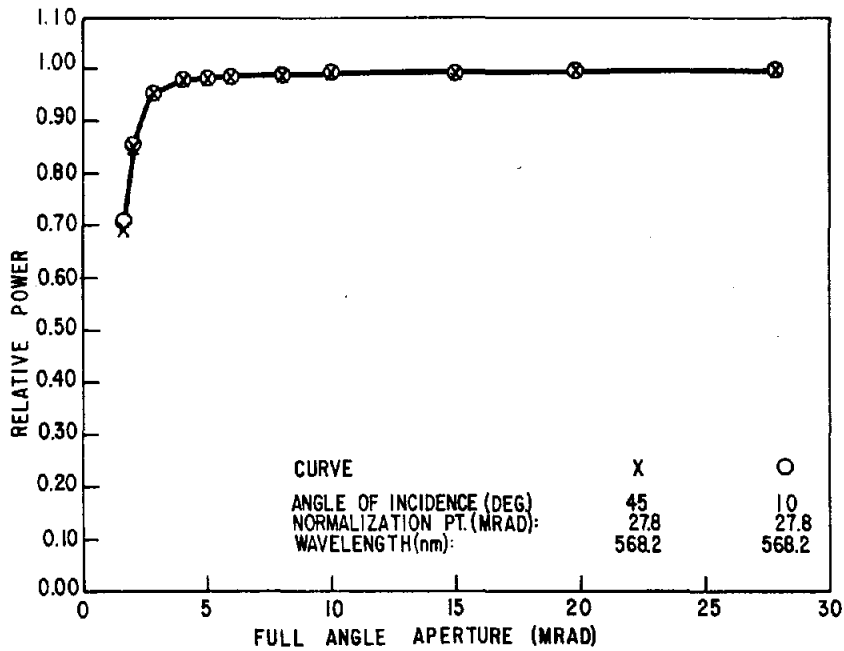


Figure 5-7. Specularity of Martin Processing Company Reflector

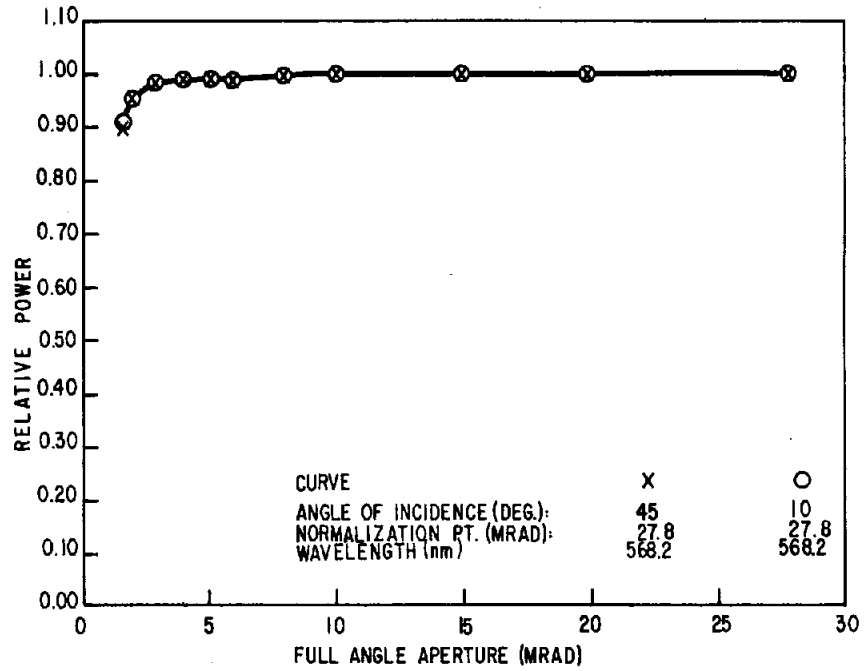


Figure 5-8. Specularity of Martin Processing Company Reflector Made from Melinex 531

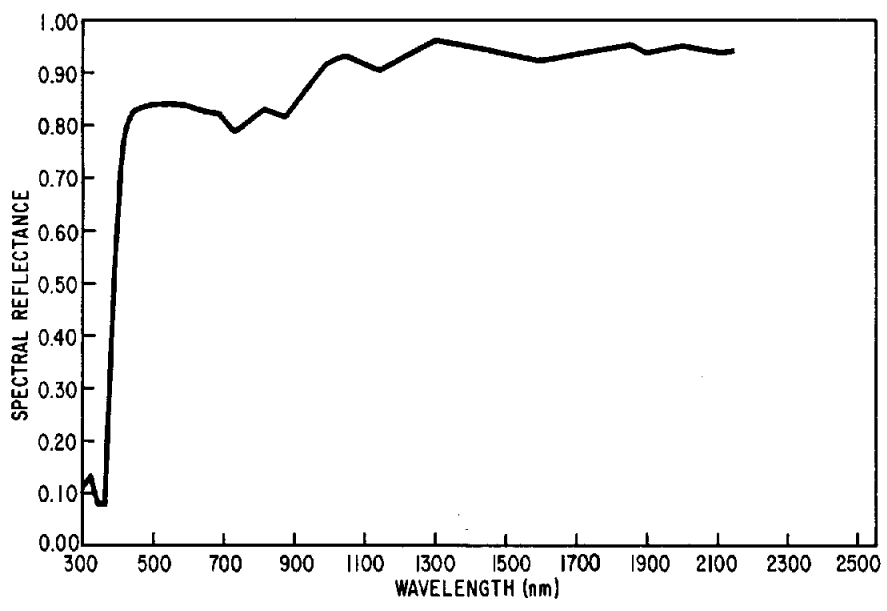


Figure 5-9. Reflectance of Dunchrome DL 50

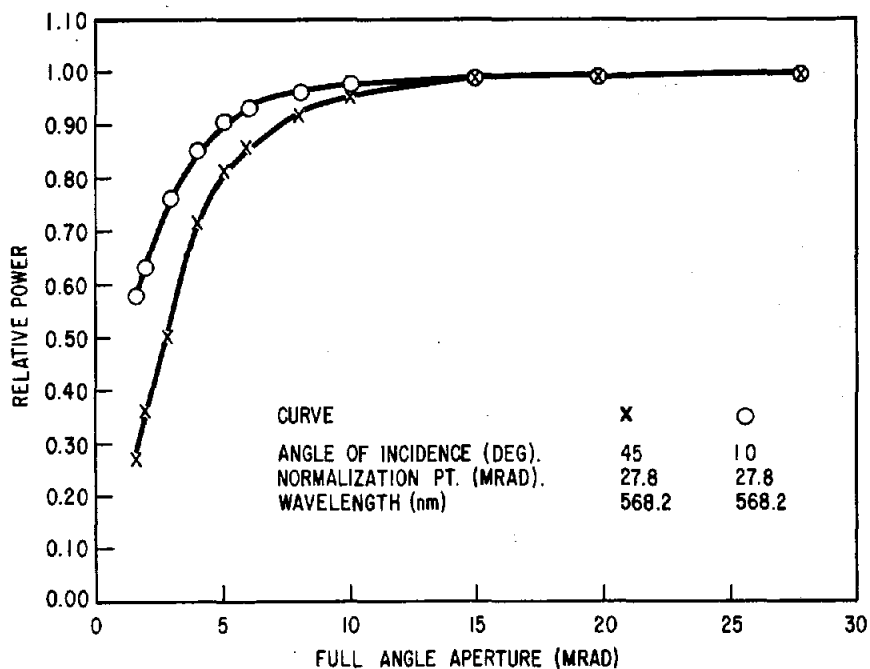


Figure 5-10. Specularity of Dunchrome DL 50

An obvious variant of the Martin Processing Company reflector would be silvered LLumar. The only LLumar available at the time of the experiment was made from Melinex 442, so a slightly lower specularity was expected than had been obtained by the better of the two Martin Processing Company reflectors. This was, in fact, observed as seen by comparing Figures 5-8 and 5-11. The first silvered LLumar samples were prepared by a General Electric laboratory (Table 5-2, reflector 10). While the specularity was qualitatively high, there was some obvious discoloration, and the AM 1 solar reflectance was 0.81. A second sample was made from the same materials by a commercial metalizer more experienced at depositing silver (Table 5-2, reflector #13). The AM 1 solar reflectance of this sample was 0.91, shown in Figure 5-12.

A significant improvement in reflectance could be obtained by increasing the reflectance at the short wavelength end of the solar spectrum. The sharp decrease in reflectance at 400 nm, shown in Figure 5-12, is due to a strong absorption inherent in the LLumar superstrate. Since PVDF appears to be very stable and weatherable, it might be useful as a substitute for LLumar in this application. Figure 5-12 shows a distinct potential advantage of Kynar 460 over LLumar in this application. It has no major absorption in the solar

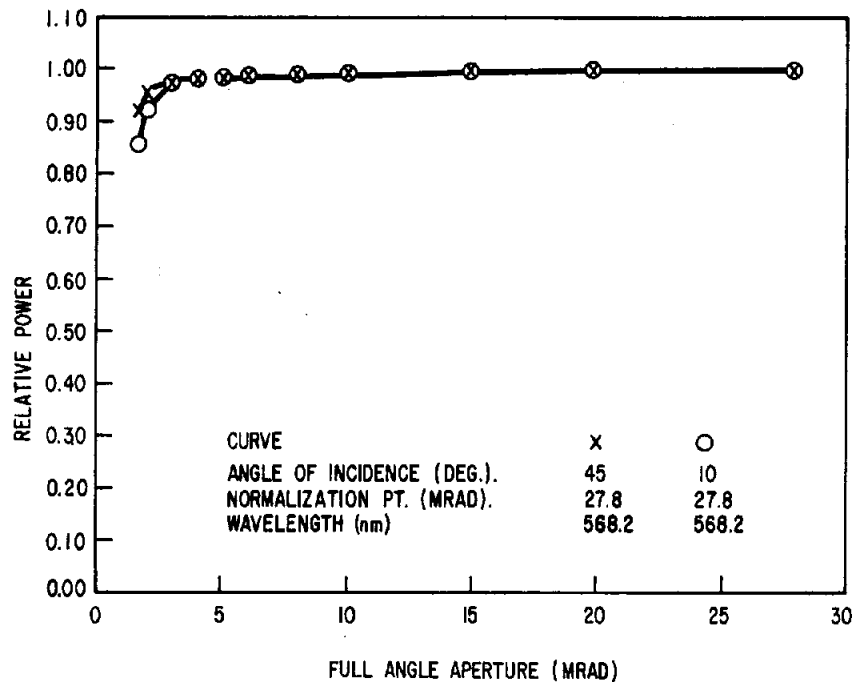


Figure 5-11. Specularity of Second-Surface LLumar/Ag Reflector

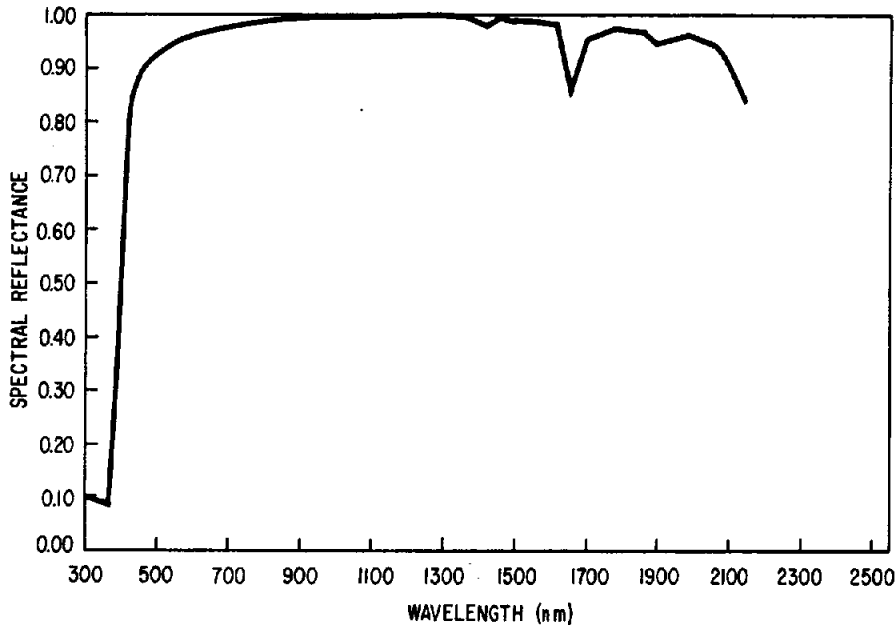


Figure 5-12. Reflectance of Second-Surface LLumar/Ag Reflector

spectral region. LLumar's sharp cutoff at 400 nm would thus be eliminated, giving a potential increase in solar reflectance of about 3%. Unfortunately, initial attempts at metalizing Kynar led to disappointing reflectance and unsatisfactory specularity, the cause of which has not been determined, (Table 5-2, reflectors #11 and #12).

It seemed possible that the problems encountered in metalizing Kynar might be due to a rough surface on this still developmental film. Therefore, an attempt was made (by the metalizer mentioned above) to deposit silver on a high clarity Tedlar film (Table 5-2, reflector #14). The specularity was much higher than had been observed with deposition on Kynar, but a noticeable discoloration was evident and led to a solar reflectance of 0.81. The low reflectance in the visible portion of the spectrum shown in Figure 5-13 is evidence of the discoloration.

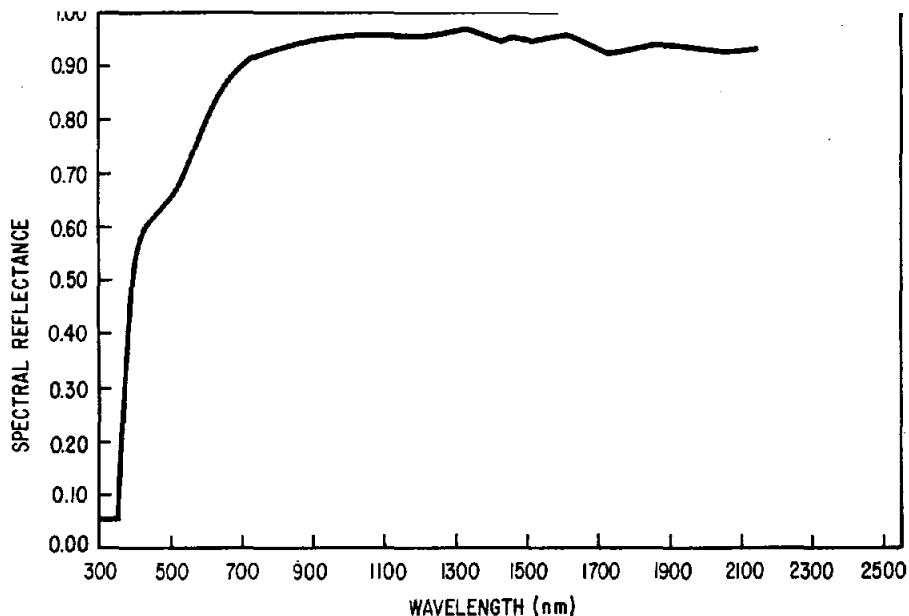


Figure 5-13. Reflectance of Silvered Tedlar

At present, metalized LLumar appears to be the material of choice for second-surface thin film reflectors. Further development of Kynar or the metalizing of Kynar, however, could produce significantly improved reflectors.

## Section 6

## WEATHERING TESTS OF MATERIALS

6.1 WEATHEROMETER TESTS

Laboratory Weatherometer tests were conducted to provide a basis for correlating accelerated laboratory weathering data with outdoor weathering. Such tests are known not to be representative of actual outdoor exposure conditions, but with knowledgeable assessment and correlation with outdoor exposure data they can serve to rank the materials in order of relative performance for long service lives.

One thousand hour Weatherometer exposure of LLumar, Melinex OW, and Kynar was carried out at a General Electric facility in Schenectady, N.Y. The test exposures were of limited value because of extensive residues deposited from the water used as an intermittent spray in accordance with normal Weatherometer operation. There was such a heavy deposit, particularly on the polyesters, that the amount of ultraviolet light actually reaching the sample is very uncertain. Nevertheless, as evident in Table 6-1, some damage was done to all three materials by the exposure. Both tensile strength and ultimate elongation were markedly affected, with the apparent amount of damage increasing in order: Kynar < LLumar < Melinex OW.

6.2 OUTDOOR EXPOSURE

The most reliable outdoor testing is obviously real-time testing in actual use. It is equally obvious that such testing alone cannot serve adequately in the present program. Therefore, a variety of exposure techniques available at DSET Laboratories, Inc. was used. The various materials were exposed to EEK, a seasonally-adjusted real-time (1-fold) exposure test. In order to obtain data for extrapolation of materials degradation to longer times, samples also were exposed in EMMA (Equatorial Mount with Mirrors for Acceleration) and EMMAQUA (similar but with a water spray) machines. These devices provide approximately an 8-fold concentration of sunlight. Additionally, an EMMAQUA machine was modified to provide 4-fold and 16-fold concentrations of sunlight. Samples thus were exposed to help improve the validity of the extrapolation of material degradation to longer times.

Table 6-1

MECHANICAL PROPERTIES OF SAMPLES FROM WEATHEROMETER EXPOSURE

<u>MATERIAL</u>	<u>EXPOSURE, HOURS</u>	<u>TENSILE STRENGTH,</u>		<u>ELONGATION</u>
		<u>MPa</u>	<u>(ksi)</u>	<u>%</u>
Kynar	0	156	(22.6)	87.8
	300	145	(21.0)	64.4
	600	132	(19.1)	63.1
	1000	133	(19.2)	51.0
LLumar	0	172	(25.0)	120.0
	300	123	(17.9)	85.9
	600	119	(17.3)	95.3
	1000	116	(16.9)	80.0
Melinex OW	0	179	(26.0)	130.0
	300	104	(15.1)	70.0
	600	94	(13.6)	39.3
	1000	102	(14.8)	44.7

Samples of Kynar, LLumar, Melinex OW, three selected reflector materials, and four bonds were exposed outdoors at intensity levels of 1, 4, 8 and 16 suns as discussed above. Optical measurements (reflectance and transmittance) were made on the exposed samples at approximately equal levels of insolation, whether obtained in real-time or accelerated exposure. A schedule for the measurements is shown in Table 6-2. Mechanical properties, specular reflectance, and specular transmittance were measured on samples before exposure and on samples with the longest exposure times. The test procedures conformed in general to the accepted standard methods below:

- Tensile strength - ANSI/ASTM D882-75b
- Creep - ANSI/ASTM D2990-76
- Tear - ANSI/ASTM D1938-67
- Mar - ANSI/ASTM D673-70

6.2.1 REAL-TIME EXPOSURE

Several techniques are available for exposing samples to normal sunlight. The samples may be mounted at 5°, 34°, or 45°, south-facing. In New River, Arizona, such rack-mounted samples are exposed to about  $1.9 \times 10^5$  Langleys/year. Slightly higher insolation rates can be achieved without artificial concentration by mounting the samples on a device that follows the sun so that the sunlight is always incident normal to the sample. This technique is referred to

Table 6-2  
SOLAR EXPOSURE LEVELS FOR OPTICAL DATA ANALYSIS

<u>INSOLATION, 10<sup>5</sup> LANGLEYS</u>			
<u>1X</u>	<u>4X</u>	<u>8X</u>	<u>16X</u>
0.48			
0.95			
1.27	1.27	1.27	
1.9	1.9	1.9	1.9
	2.5	2.5	2.5
	3.8	3.8	
	5.1	5.1	5.1
	6.3	6.3	
	7.6	7.6	7.6
		10.1	10.1
		12.7	12.7
			15.2
			17.7
			20.3
			22.8
			25.3

as EEK. In this study, some samples were exposed at 34°S, other replicates on an EEK apparatus.

### 6.2.2 ACCELERATED EXPOSURES

Acceleration of the weathering process is accomplished at DSET Laboratories by concentrating sunlight with aluminum mirrors. There are two versions of the standard 8-fold accelerated testing, EMMA and EMMAQUA. In both, the samples are mounted inverted on an air-cooled channel as shown in Figure 6-1. The device tracks the sun in azimuth and is adjusted seasonally in elevation. The two tests differ in that EMMAQUA includes an intermittent spray with water purified by reverse osmosis.

If the degradation of a given material depends uniquely on the accumulated insolation in a 1:1 relationship and not at all on the degree of acceleration of the testing, then lifetime predictions can be made with confidence from the results of accelerated testing. But if the relationship is not 1:1, lifetime

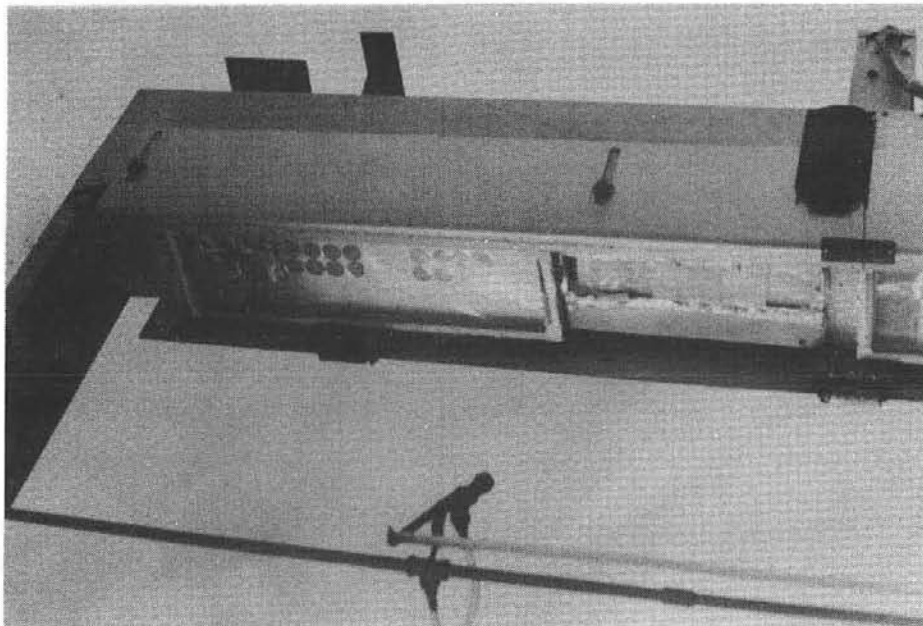


Figure 6-1. Weathering Test Samples Mounted Inverted on an EMMAQUA Machine

predictions become much less certain. In order to assist in defining the relationship between weathering rates and concentration of sunlight, testing was performed at 4-fold and 16-fold concentrations of sunlight. Thus, data were obtained from exposures at 1, 4, 8, and 16-fold concentrations of sunlight. This was accomplished by modifying an EMMA/EMMAQUA machine as shown in Figure 6-2. At one end, 5 mirrors concentrated the sunlight 4-fold (80% reflectance), while 20 mirrors at the other end produced a 16-fold concentration. Tracking in both azimuth and elevation ensured the proper exposure of all the samples. Standard EMMA/EMMAQUA machines are visible in the background of Figure 6-2.

### 6.3 WEATHERING OF MATERIALS

The effects of outdoor weathering at DSET Laboratories near Phoenix, Arizona, are described below for samples which included three reflectors, three transparent materials, and four types of bond specimens. In the following discussions, the optical results of material weathering tests are presented in terms of AM 1.5 data reduced from graphical measurements as described in Appendix A.

#### 6.3.1 WEATHERING OF A FIRST-SURFACE ALUMINIZED REFLECTOR

In spite of some reservations about the durability of first-surface aluminized reflectors, even inside an enclosure, the low cost and relatively high reflectance of first-surface aluminized PET reflectors such as those described

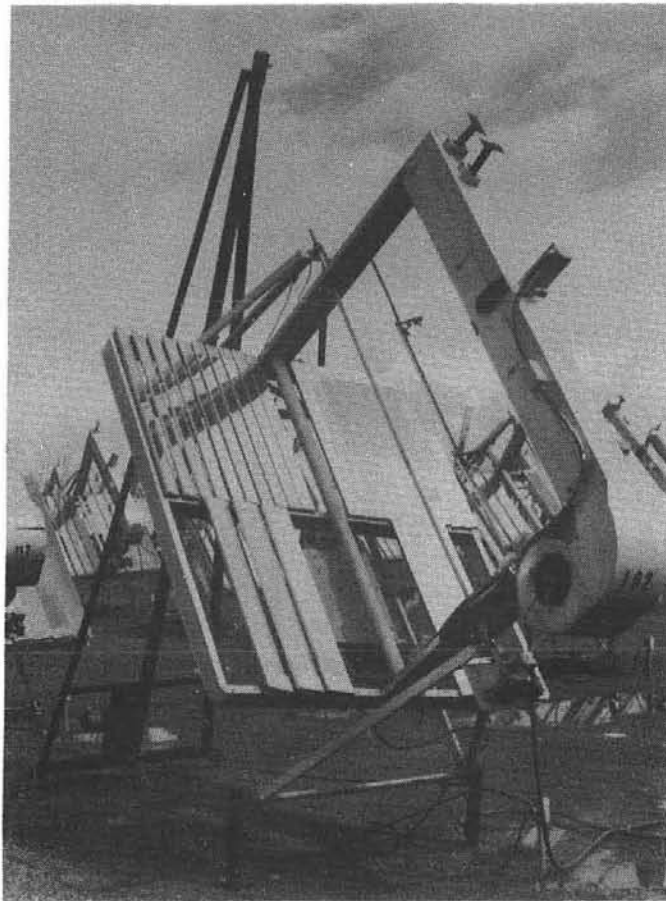


Figure 6-2. Modified EMMAQUA Machine

in Section 5.2 made weathering tests seem worthwhile. Such reflectors would not survive direct exposure to the weather for long periods of time, so all weathering tests were conducted behind Kynar films. Kynar was selected as the protective film because it would present a worst-case situation, being transparent throughout the solar spectrum and, in fact, transparent to below 220 nm. Therefore it would not be expected to screen out any damaging solar radiation. On the other hand, a protective film of LLumar, Melinex OW, or Tedlar UT, all of which have strong absorption in the ultraviolet region of the spectrum, would provide significant protection from short wavelength solar radiation for the reflector sample. Reflector samples were exposed on 34° south-facing racks, on EEK machines, on EMMA machines, and on EMMAQUA machines at 4-, 8-, and 16-fold concentrations of sunlight. Insolations up to  $7.6 \times 10^5$  Langley had no apparent deleterious effect on the reflectance of the first-surface aluminized LLumar. The results are summarized in Table 6-3.

Table 6-3

## REFLECTANCE OF A WEATHERED FIRST-SURFACE ALUMINIZED REFLECTOR

<u>INSOLATION, 10<sup>5</sup> LANGLEYS</u>	<u>CONCENTRATION OF SUNLIGHT</u>	<u>AM 1.5 SOLAR REFLECTANCE</u>
0		0.91
0.5	1X	0.89
1.3	4X	0.90
1.3	8X	0.91
1.9	4X	0.90
1.9	8X	0.91
2.5	8X	0.91
2.5	16X	0.91
3.8	8X	0.90
5.5	16X	0.90
7.6	16X	0.91

This study shows, as expected, that an aluminum reflector surface is not sensitive to sunlight alone. It also shows one of the hazards of accelerated weathering tests. All possible forms of weathering may not be equally accelerated, leading to possibly erroneous predictions.

## 6.3.2 WEATHERING OF A PSEUDO-FIRST-SURFACE ALUMINIZED REFLECTOR

Samples of the pseudo-first-surface reflector described in Section 5.2 were exposed to outdoor weathering at DSET Laboratories. A very limited amount of sample was available and it became available relatively late in the program. Therefore, the extent and variety of weathering studies done with this material were less than with other materials. However, it is evident from the data in Table 6-4 that  $4.5 \times 10^5$  Langleys insolation had no detectable effect on the reflectance of this material. Furthermore, one sample of this reflector was exposed on an EEK machine for approximately six months without being protected from the weather by a Kynar film. The objective of this experiment was to assess the capability of the Dow Corning Q9-6315 resin to protect the aluminum surface. The aluminum reflective layer was completely destroyed near one edge of the sample, possibly because of a crack or other defect in the coating. However, no effect on

Table 6-4

REFLECTANCE OF A WEATHERED PSEUDO-FIRST-SURFACE ALUMINIZED REFLECTOR  
(PROTECTED WITH DOW CORNING Q9-6315 RESIN)

<u>INSOLATION, 10<sup>5</sup> LANGLEYS</u>	<u>CONCENTRATION OF SUNLIGHT</u>	<u>AM 1.5 SOLAR REFLECTANCE</u>
0		0.88
0.6	1X	0.88
1.5	8X	0.87
3.0	8X	0.87
4.5	8X	0.88

the reflectance of the remainder of the sample was observed. Figure 6-3 shows two specimens of the pseudo-first-surface reflector mounted on an EEK machine. Both specimens were wet from a recent rain storm. The specimen at the top of the figure is enclosed in a protective box behind a Kynar film. The photograph shows the loss of aluminum along the left-hand edge of the lower sample, and a one-inch hole near the right side of the lower sample where a sample had been removed for measurement. Although the extent of weathering studies is limited, the Dow Corning coating looks promising in enclosed reflector applications and perhaps in exposed reflector applications.

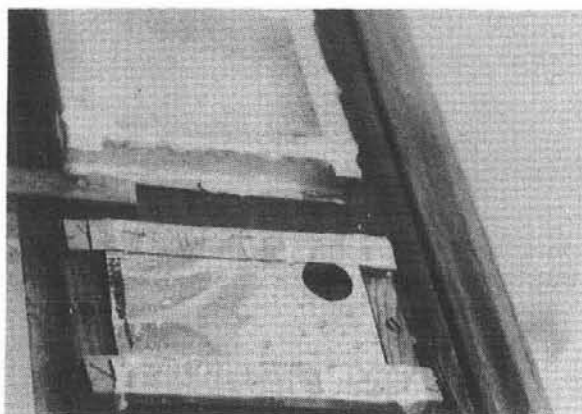


Figure 6-3. Pseudo-First-Surface Reflector Samples on an EEK Machine

## 6.3.3 WEATHERING OF A SECOND-SURFACE ALUMINIZED REFLECTOR

The second-surface aluminized LLumar reflector made by Martin Processing Company and described in Section 5.3 was exposed to outdoor weathering in the same manner as described in Section 6.3.1 for the weathering of a first-surface reflector. Although the laminated second-surface reflector was expected to be much more resistant to environmental attack than the first-surface aluminized reflector, it too was exposed behind a protective Kynar film. As explained in Section 6.3.1, this was intended to simulate the exposure of the reflector inside a protective enclosure. Some of the weathering studies with bond samples (discussed in Section 6.3.7) indicate that LLumar degrades more rapidly on an EMMAQUA machine than it does on an EMMA machine. The implication is that the moisture, at least the type of moisture encountered during EMMAQUA testing, accelerates the degradation of the material. Therefore, although the data in Table 6-5 indicate that no change in solar reflectance was caused by insolation up to  $7.6 \times 10^5$  Langleys, concurrent exposure to moisture may have caused significant change in the solar reflectance. If this is proven by further studies, it may indicate that LLumar will perform better as an enclosed reflector than in exposed applications.

Table 6-5

## REFLECTANCE OF A WEATHERED SECOND-SURFACE ALUMINIZED LLUMAR REFLECTOR

<u>INSOLATION, 10<sup>5</sup> LANGLEYS</u>	<u>CONCENTRATION OF SUNLIGHT</u>	<u>AM 1.5 SOLAR REFLECTANCE</u>
0		0.81
0.5	1X	0.80
1.3	4X	0.81
1.3	8X	0.80
1.9	4X	0.81
1.9	8X	0.81
2.5	8X	0.81
2.5	16X	0.81
3.8	8X	0.81
5.5	16X	0.81
7.6	16X	0.81

#### 6.3.4 WEATHERING OF LLUMAR

LLumar stabilized PET film was considered a possible candidate for use as a heliostat enclosure material. Therefore, it was exposed to weathering studies on 34° south-facing racks, on EEK machines, and on EMMAQUA machines at 4-, 8-, and 16-fold concentrations of sunlight. Initially, it was believed that changes in the solar transmittance of the film would provide the most sensitive indicator of degradation. Therefore, transmittance measurements were made at appropriate intervals as indicated in Table 6-2. The results of transmittance measurements of weathered LLumar samples are summarized in Table 6-6. The loss of transmittance of the samples after as much as  $12.7 \times 10^5$  Langleys of insolation amounted to about 2 to 3%. However, mechanical properties rather than transmittance proved to be the most sensitive to weathering.

The data in Table 6-7 indicate that both the tensile strength and the elongation at break of LLumar were markedly affected by weathering.

A graphic demonstration of the degradation of mechanical properties of LLumar occurred when a hailstorm struck the exposure site approximately seven months after initiation of the weathering tests. Figure 6-4 shows some of the film samples mounted on an EEK machine shortly after the hailstorm. The rectangle at the bottom had been a sample of Melinex OW film, the one above it a sample of LLumar film, and above it a sample of Kynar. The sample at the top of the EEK machine is unidentified. To the left of the film samples can be seen four bond samples, at least one of which has been destroyed. It is believed that the destroyed sample was electromagnetically-bonded LLumar.

A close view of the damage to the Melinex OW and LLumar films is in Figure 6-5. Again, the Melinex OW is the lower sample, the LLumar sample occupying the rectangular space above it. Beads of water are evident on all the samples.

Finally, Figure 6-6 shows a 34° south-facing rack which had contained three rows, one each of LLumar, Kynar, and Melinex OW. The LLumar is the vertical row to the left in the photograph. Extensive damage to most of the samples is obvious.

Table 6-8 characterizes, as far as the facts are known, the hailstorm that caused the damage described above. The storm has been described by personnel at the test site as "severe, but certainly not unprecedented." The results of weathering tests indicate that the lifetime of LLumar as a heliostat enclosure would be very limited.

Table 6-6

EFFECT OF WEATHERING ON THE SOLAR TRANSMITTANCE OF LLUMAR

<u>INSOLATION, 10<sup>5</sup> LANGLEYS</u>	<u>CONCENTRATION OF SUNLIGHT</u>	<u>AM 1.5 SOLAR TRANSMITTANCE</u>
0		0.86
0.5	1X	0.86
0.9	1X	0.86
1.3	1X	0.86
1.3	4X	0.86
1.3	8X	0.86
1.8	1X	0.86
1.9	4X	0.86
1.9	8X	0.86
1.9	16X	0.86
2.5	4X	0.86
2.5	8X	0.86
2.5	16X	0.86
3.8	8X	0.84
5.1	8X	0.84
5.1	16X	0.85
6.3	8X	0.82
7.5	8X	0.80
7.6	16X	0.77
8.8	8X	0.78
10.1	16X	0.81
12.7	16X	0.83

Table 6-7

## EFFECT OF WEATHERING ON THE MECHANICAL PROPERTIES OF LLUMAR

<u>INSOLATION, 10<sup>5</sup> LANGLEYS</u>	<u>CONCENTRATION OF SUNLIGHT</u>	<u>TENSILE STRENGTH MPa (ksi)</u>	<u>YIELD STRENGTH MPa (ksi)</u>	<u>ELONGATION AT BREAK, %</u>
0		183 (26.5)	61 (8.9)	99
0.5	1X	174 (25.2)	77 (11.2)	105
0.9	1X	135 (19.6)	70 (10.1)	56
1.3	8X	96 (13.9)	59 (8.6)	40
1.8	1X	128 (18.5)	76 (11.0)	53
1.9	8X	87 (12.6)	67 (9.7)	15
2.5	8X	96 (13.9)	67 (9.7)	20
3.4	4X	98 (14.2)	66 (9.5)	13
3.8	8X	88 (12.8)	55 (8.0)	6
8.8	8X	84 (12.2)	59 (8.5)	5
13.1	16X	80 (11.6)	58 (8.4)	4

## 6.3.5 WEATHERING OF MELINEX OW

The weathering properties of Melinex OW were studied in parallel with the weathering studies on LLumar described in Section 6.3.4. In a similar fashion it was determined that change in the transmittance of Melinex OW is less pronounced than changes in the mechanical properties after weathering. While the changes in both materials were qualitatively the same, the changes may have occurred somewhat more rapidly in Melinex OW than in LLumar. The hailstone damage to Melinex OW shown in Figure 6-5 can be seen to consist of apparently brittle fracture of the film as well as two distinct holes where material was removed from the film by the hailstones. In Figure 6-6, the Melinex OW samples had originally been on the right-hand side of the picture. As can be seen, every sample was completely destroyed. A close view, Figure 6-7, illustrates the type of apparently brittle fracture that occurred in the Melinex OW film during the hailstorm. Measured changes in the solar transmittance and mechanical properties of the Melinex OW film as a result of weathering are summarized in Tables 6-9 and 6-10.

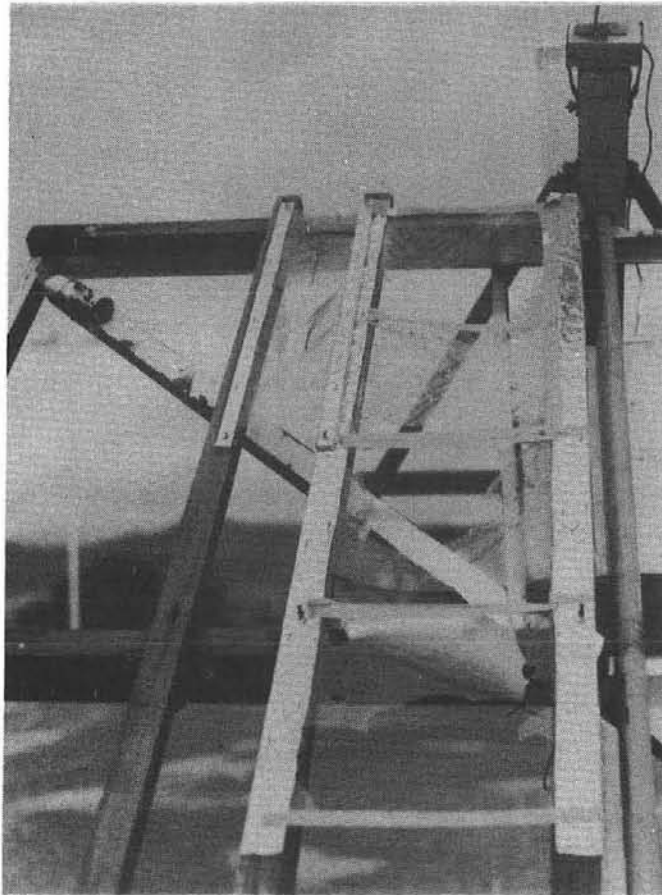


Figure 6-4. Film Samples on EEK Machine After Hailstorm

#### 6.3.6 WEATHERING OF KYNAR

The primary candidate for an enclosure material in this study was Kynar. Samples of Kynar were subjected to weathering at DSET Laboratories on 34° south-facing racks, on EEK machines, and on EMMAQUA machines at 4-, 8- and 16-fold concentration of sunlight. All the Kynar used in this study was from the lot of material described in Section 3.3.3. The data reported in Table 6-11 indicate that no significant change in solar transmittance of Kynar was observed in any of the weathering studies. As discussed in Section 6.3.9, statistical analysis of the transmittance data carried out to three significant figures indicates a trend toward decreasing transmittance on weathering. It is believed that with sufficient care, transmittance data can be obtained in which the third decimal place has some significance. This, however, is a measure of precision

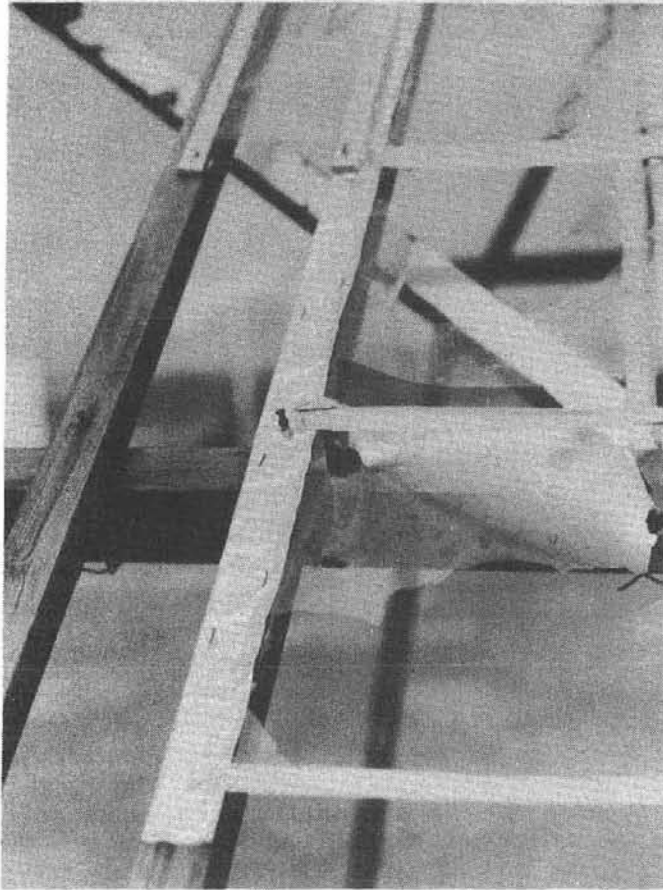


Figure 6-5. Hailstorm Damage to PET Films

of measurement rather than accuracy, which is probably limited to two significant figures. The tensile properties of Kynar, shown in Table 6-12, were slightly affected by weathering. Both tensile and yield strengths showed a slight tendency to decrease with insolation up to  $13 \times 10^5$  Langleys.

The hailstorm that destroyed most of the PET samples had no apparent effect on any of the exposed Kynar samples. Exposed Kynar samples after the storm can be seen at the top of Figures 6-4 and 6-5 and the center row in Figure 6-6. Moisture on the samples is particularly evident in Figure 6-6.

Figure 3-15, showing the effects of weathering on the creep properties of Kynar film, indicates that cross-linking is the major structural change effected by weathering. If chain scission predominated, the creep rate would be expected to increase after weathering, but, in fact, exposure to  $9 \times 10^5$  Langleys reduced the amount of creep observed at 69 MPa by about 25%.

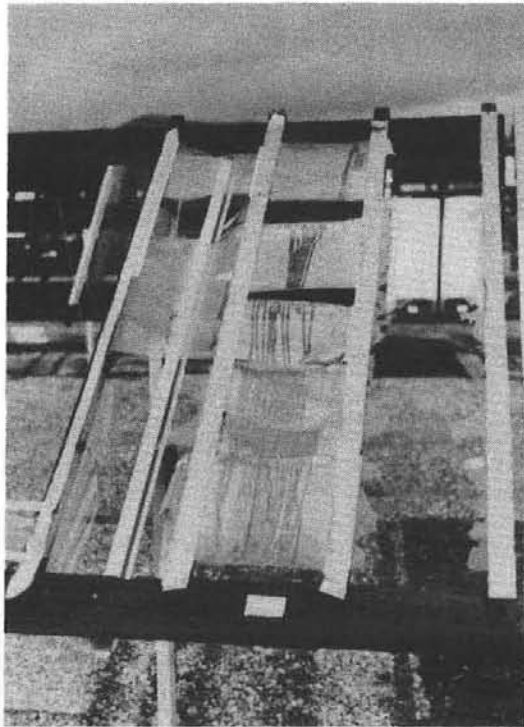


Figure 6-6. Film Samples on 34° South-Facing Rack After Hailstorm

Kynar has demonstrated remarkable stability in the weathering tests conducted to date. Continued testing is imperative to assess the importance of the observed trends in tensile properties.

#### 6.3.7 WEATHERING OF LLUMAR BONDS

Samples of LLumar bonded with Adcote 76M5 and bonded electromagnetically were exposed at DSET Laboratories on 34° south-facing racks, on EEK machines, and on EMMAQUA machines at 4-, 8-, and 16-fold concentrations of sunlight. The samples on the 34° south-facing racks and the electromagnetically bonded samples on the EEK machine were all destroyed by the hailstorm described in Section 6.3.4. After exposure to  $3.4 \times 10^5$  Langleys on a modified EMMAQUA machine, the electromagnetically-bonded LLumar samples had lost a major portion of their strength.

Table 6-8  
 CHARACTERISTICS OF HAILSTORM AT NEW RIVER, ARIZONA

Date: January 18, 1980

Duration: 15-20 minutes

Ambient Temperature: 12.8<sup>0</sup>C (55<sup>0</sup>F)

Hailstone diameter:

Average	9.5 - 12.7 mm	(3/8 in - 1/2 in )
Maximum	15.9 - 19 mm	(5/8 in - 3/4 in )

Character: Hard

Accumulation: 12-25 mm (1/2 in - 1 in )

Other local damage:

- Dents in auto sheet metal
- Breakage of 3.18 mm (1/8 in ) thick window glass
- Breakage of 6.36 mm (1/4 in ) thick glass in two 1.22 x 2.44 m (4 ft x 8 ft) solar collectors
- Dimpling of aluminum mirrors on numerous EMMA and EMMAQUA machines.

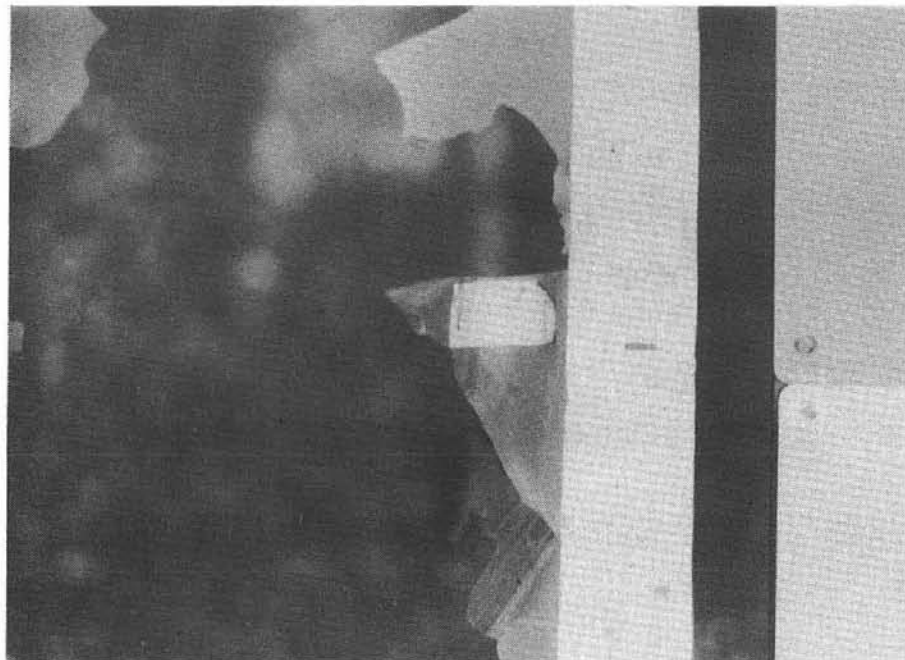


Figure 6-7. Remnants of Melinex OW After Hailstorm

Table 6-9

EFFECT OF WEATHERING ON THE SOLAR TRANSMITTANCE OF MELINEX OW

<u>INSOLATION, 10<sup>5</sup> LANGLEYS</u>	<u>CONCENTRATION OF SUNLIGHT</u>	<u>AM 1.5 SOLAR TRANSMITTANCE</u>
0		0.86
0.5	1X	0.87
0.9	1X	0.87
1.3	1X	0.87
1.3	4X	0.88
1.3	8X	0.87
1.8	1X	0.88
1.9	4X	0.87
1.9	8X	0.87
1.9	16X	0.87
2.5	4X	0.87
2.5	8X	0.86
2.5	16X	0.87
3.8	8X	0.79
5.1	8X	0.77
5.1	16X	0.81
6.3	8X	0.79
7.5	8X	0.80
7.6	16X	0.77
8.8	8X	0.79
10.1	16X	0.79
12.7	16X	0.81

Table 6-10

EFFECT OF WEATHERING ON THE MECHANICAL PROPERTIES OF MELINEX OW

<u>INSOLATION, 10<sup>5</sup> LANGLEYS</u>	<u>CONCENTRATION OF SUNLIGHT</u>	<u>TENSILE STRENGTH MPa (ksi)</u>	<u>YIELD STRENGTH MPa (ksi)</u>	<u>ELONGATION AT BREAK, %</u>
0		187 (27.1)	74 (10.8)	131
0.5	1X	88 (12.7)	68 ( 9.8)	9
0.9	1X	89 (12.9)	57 ( 8.3)	7
1.3	8X	90 (13.1)	54 ( 7.9)	10
1.8	1X	85 (12.3)	54 ( 7.9)	6
1.9	8X	89 (12.9)	59 ( 8.5)	8
2.5	8X	85 (12.3)	55 ( 8.0)	6
3.4	4X	84 (12.2)	58 ( 8.4)	4
3.8	8X	71 (10.3)	47 ( 6.8)	7
8.8..	8X	71 (10.3)	46 ( 6.7)	4
13.1	16X	61 ( 8.9)	43 ( 6.3)	3

In almost every case, failure of the electromagnetically-bonded sample occurred either in the bond or immediately adjacent to it. On the other hand, failure of the adhesively-bonded LLumar samples occurred almost exclusively in the gauge length, indicating that the strength of the material itself was the limiting factor in the strength of these samples.

Electromagnetic bonds of LLumar appear to be degraded rapidly by exposure to sunlight. This method is probably not useful in solar applications where the bond line is exposed to sunlight.

6.3.8 WEATHERING OF KYNAR BONDS

Samples of Kynar bonded electromagnetically and with an experimental adhesive were exposed to weathering in the same fashion as the bonded LLumar samples. As was true of all Kynar samples, no damage was evident as a result of the hailstorm described in Section 6.3.4. Weathering increased the strength of the electromagnetically-bonded Kynar samples, though it also is possible that this was merely an aging phenomenon. All the weathered electromagnetically-bonded Kynar samples failed in the gauge length when tested to destruction,

Table 6-11

EFFECT OF WEATHERING ON THE SOLAR TRANSMITTANCE OF KYNAR 460

<u>INSOLATION, 10<sup>5</sup> LANGLEYS</u>	<u>CONCENTRATION OF SUNLIGHT</u>	<u>AM 1.5 SOLAR TRANSMITTANCE</u>
0		0.93
0.5	1X	0.93
0.9	1X	0.93
1.3	1X	0.93
1.3	4X	0.93
1.3	8X	0.93
1.8	1X	0.93
1.9	4X	0.93
1.9	8X	0.93
1.9	16X	0.93
2.5	4X	0.92
2.5	8X	0.94
2.5	16X	0.93
3.8	8X	0.93
5.1	8X	0.93
5.1	16X	0.93
7.6	16X	0.92
6.3	8X	0.93
7.5	8X	0.93
8.8	8X	0.93
10.1	16X	0.93
12.7	16X	0.93

Table 6-12  
EFFECT OF WEATHERING ON THE MECHANICAL PROPERTIES OF KYNAR 460

INSOLATION, 10 <sup>5</sup> LANGLEYS	CONCENTRATION OF SUNLIGHT	TENSILE STRENGTH		20% OFFSET YIELD STRENGTH		ELONGATION AT BREAK, %
		MPa	(ksi)	MPa	(ksi)	
0		163	(23.6)	104	(15.1)	93
0.5	1X	153	(22.2)	102	(14.8)	90
0.9	1X	150	(21.7)	104	(15.1)	83
1.3	1X	155	(22.5)	101	(14.7)	95
1.3	8X	143	(20.7)	88	(12.8)	118
1.9	8X	139	(20.2)	94	(13.6)	106
2.5	8X	143	(20.8)	92	(13.3)	115
3.4	4X	137	(19.9)	90	(13.1)	91
3.8	8X	130	(18.8)	89	(12.9)	88
5.1	8X	146	(21.2)	65	(9.46)	124
6.3	8X	132	(19.2)	86	(12.5)	107
7.5	8X	126	(18.3)	92	(13.4)	75
8.8	8X	128	(18.5)	88	(12.8)	95
9.0	8X	143	(20.8)	89	(12.9)	115
13.1	16X	134	(19.4)	98	(14.2)	60

while the unexposed samples failed adjacent to the bond line as shown in Figure 4-2. The adhesively-bonded Kynar samples proved to be the strongest of the four types chosen for weathering studies. Failure of these samples occurred almost universally at the bond interface or adjacent to the bond line. The strengths of these bonds were generally in the 12-16 kn/m (68-91 lb/in.) range. There did not appear to be a significant effect of weathering even at the level of 13.1 x 10<sup>5</sup> Langleys.

Both adhesive and electromagnetic bonds of Kynar appear to have high resistance to weathering degradation. Both appear suitable for use in solar applications.

### 6.3.9 WEATHERING PREDICTIONS

One of the primary objectives of the weathering program was the development of confidence in the prediction of long-term weathering behavior of materials. For this purpose, it was necessary to determine the relationship between the degree of concentration of sunlight and the degree of acceleration of the

weathering process. In the simplest case, the logarithm of the measured solar transmittance or reflectance would be a linear function of the accumulated solar insolation. The most practical means of determining the relationship is by a statistical regression analysis in which all known variables are considered. For our purpose, the variables to be considered are:

- Dependent Variable - logarithm of measured solar property
- First Independent Variable - accumulated insolation (Langleys)
- Second Independent Variable - solar concentration ratio
- Third Independent Variable - artificial water spray (yes, no, or natural exposure)

The last two independent variables are a function of the type of exposure to which the material is subjected. Table 6-13 contains a listing of these assumed variables as used in the regression analysis. A statistical regression analysis was performed using the STAREG program. This is a General Electric Mark III Computer Program that does multiple regression analyses and fits a linear model of the form:

$$Y = \beta_0 + \beta_1 X_1 + \beta_2 X_2 + \dots + \beta_n X_n$$

to the observed data. The statistical significance of assumed independent variables is established and the coefficients,  $\beta$ , of the regression model are obtained by a least squares approach.

Table 6-13  
2ND AND 3RD INDEPENDENT VARIABLES

<u>EXPOSURE TYPE</u>	<u>X<sub>2</sub></u>	<u>X<sub>3</sub></u>
EEK	1	0
Modified EMMAQUA	4	1
EMMA	8	-1
EMMAQUA	8	1
Modified EMMAQUA	16	1

Using the AM 1.5 data from Tables 6-6, 6-9 and 6-11, the necessary regression analyses have been accomplished. Sufficient solar transmittance data were available to make a reasonable prediction of the future behavior of Kynar, LLumar and Melinex OW. The initial output of the STAREG computer program for Kynar is shown in Table 6-14. The statistical significance of the independent variables is first determined. This is done by noting the absolute value of the t-statistic. If the absolute value is larger than about 2.0, the corresponding term in the regression model is statistically significant at the 5% significance level. As in Table 6-14, the absolute value of the t-statistic exceeds 2.0 only for variable  $X_1$  (accumulated insolation). Therefore, variables  $X_2$  and  $X_3$  are not significant in this analysis. This means that the change in solar transmittance does not depend upon the presence or absence of an artificial water spray nor on the degree of concentration of sunlight, but only on the total accumulated insolation. This conclusion, illustrated for Kynar, is perhaps not true for LLumar. The statement was made in Section 6.3.3 that LLumar degrades more rapidly on an EMMAQUA machine than it does on an EMMA machine. The fact is that the specular transmittance of some LLumar bond samples, as determined by visual inspection, was greatly affected by the presence or absence of water spray. No such difference can be documented in the optical data since EMMA exposure of the PET samples was not carried out. There is some indirect evidence to support the hypothesis of the importance of water in the degradation of LLumar. The transmittance of LLumar decreased 5% after exposure to  $7.5 \times 10^5$  Langleys insolation with water spray, but  $7.6 \times 10^5$  Langleys insolation without water had no effect on the reflectance of a second-surface LLumar reflector (hence, presumably, no effect on the transmittance of the LLumar superstrate).

Table 6-14  
"STAREG" - PARTIAL OUTPUT FOR KYNAR

	<u>INDEX OF VARIATE</u>	<u>COEFFICIENT</u>	<u>CHECK</u>	<u>STANDARD ERROR</u>	<u>T-STATISTIC</u>
(a)	1	-6.99011746E-09	-1.79E-04	2.96083E-09	-2.36086E+00
	2	4.67751108E-05	-4.47E-08	1.23149E-04	3.79826E-01
	3	4.038/2001E-04	-1.98E-22	1.49457E-03	2.70226E-01
	INTERCEPT	1.96975200E+00			
(b)	1	-5.66873355E-09	2.68E-03	2.01690E-09	-2.81062E+00
	INTERCEPT	1.97010790E+00			

The regression model is next reanalyzed after excluding the insignificant variables, namely,  $X_2$  and  $X_3$ . The resulting output from STAREG is shown in (b) of Table 6-14. The absolute value of the t-statistic for variable  $X_1$  again exceeds 2.0, reaffirming its significance in the regression model. The equation  $Y = 1.9701 - 5.6687 \times 10^{-9} X_1$  is obtained from (b) of Table 6-14 where  $Y = \log$ -arithm of solar transmittance of Kynar, and  $X_1 =$  accumulated insolation in Langleys.

This equation, the required linear relationship, was used to predict future changes in the solar transmittance of Kynar. The results are shown in Figure 6-8 where the actual data obtained are shown with an appropriate symbol to indicate the concentration of sunlight.

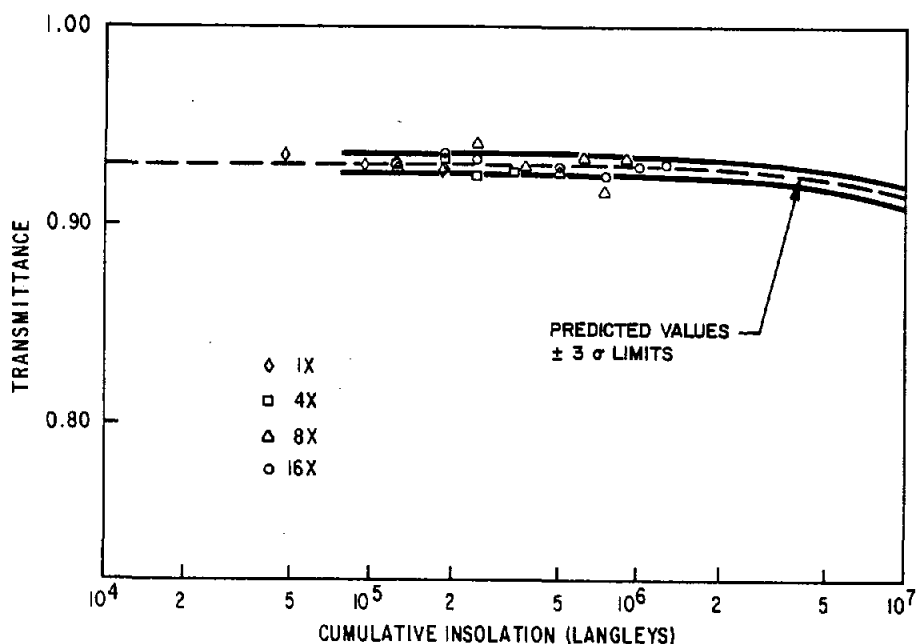


Figure 6-8. Solar Transmittance of Kynar

Similar regression analyses were performed on the LLumar and Melinex OW data. The results for these two materials are shown in Figures 6-9 and 6-10. The three figures include  $\pm 3\sigma$  standard deviations.

DSET Laboratories records indicate that the Phoenix, Arizona area receives insolation at an average rate of  $2 \times 10^5$  Langleys per year. This rate has been used to convert the predicted transmittance curves from Figures 6-8, 6-9, and 6-10 to a time basis. Transmittance as a function of predicted exposure time

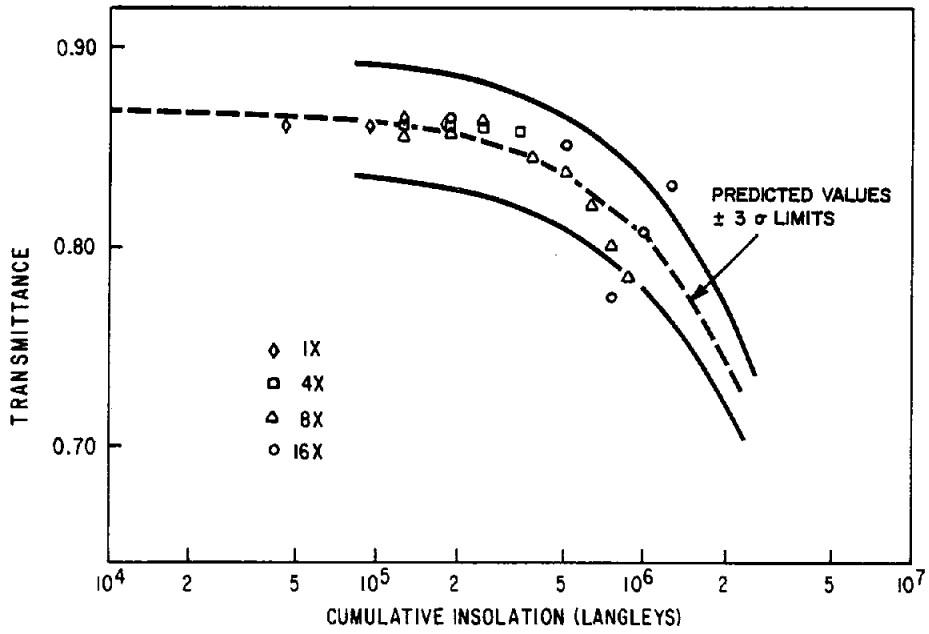


Figure 6-9. Solar Transmittance of LLumar

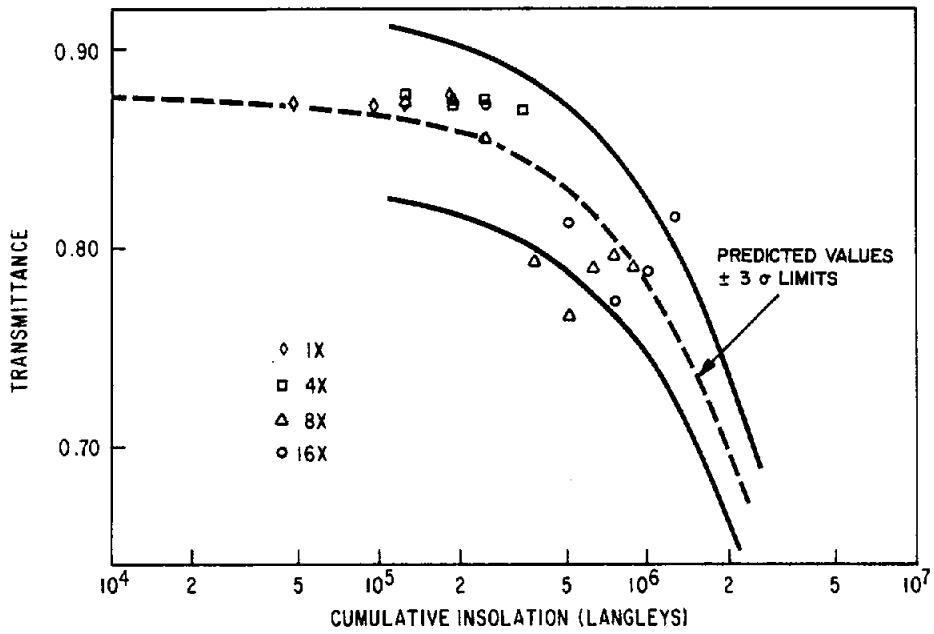


Figure 6-10. Solar Transmittance of Melinex-OW

is shown in Figure 6-11 where all available data have been included for the three materials. It must be remembered that these predictions are based solely on insolation, and take no account of other forms of degradation such as roughening by abrasion, loss of mechanical strength, or chemical reactions such as oxidation. For this reason lifetime predictions of reflectors are not made. For example, extrapolation of the data obtained on the reflectance of the first-surface aluminized polyester film indicates that 5% loss in reflectance might be expected in about 25 years. However, such an extrapolation does not take into account the known sensitivity of the thin aluminum film to oxidation in the presence of moisture.

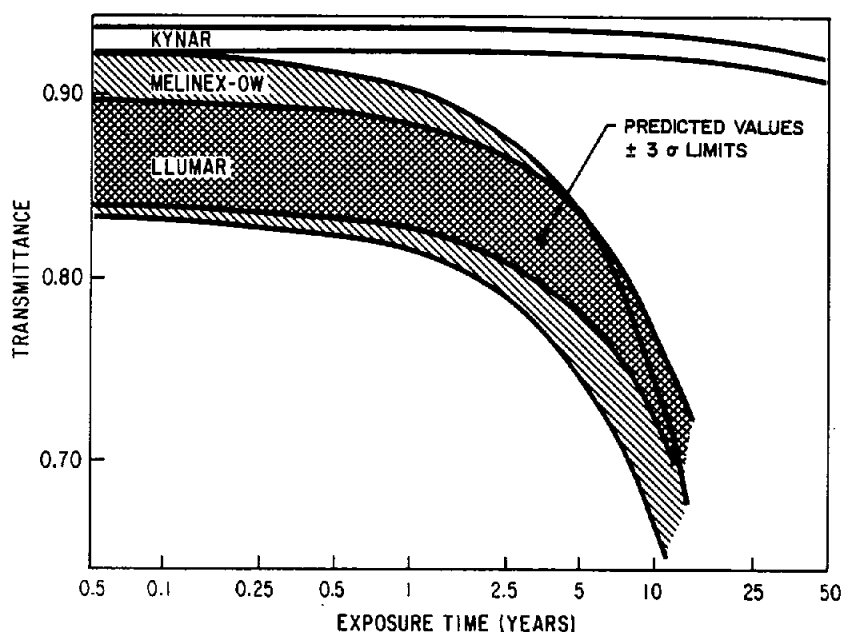


Figure 6-11. Predicted Solar Transmittance

Statistical analysis of optical data indicates that the useful lifetime of Kynar as an enclosure material should be much longer than that of stabilized PET. Indications, however, are that changes in mechanical properties will limit useful lifetimes of both PVDF and PET films rather than changes in optical properties. An extended weathering and testing program will be necessary for prediction of the useful mechanical lifetime of PVDF films.

## Section 7

## MECHANISM OF WEATHERING DEGRADATION

Kynar films were exposed to ultraviolet and visible light in the presence of air in a specially-designed, air-tight container. Degradation products were collected and analyzed by gas chromatograph/mass spectrometer (GC/MS). The evolved hydrogen fluoride was trapped and quantified using a special buffer solution and fluoride-ion-specific electrode. The exposed films also were analyzed for degradation after exposure by use of differential infrared analysis and by ultraviolet and visible spectrometry.

7.1 EXPERIMENTAL EQUIPMENT

Two Kynar films 127 mm (5 in.) diameter and 0.1 mm (0.004 in.) thick were cleaned and dried at 45°-50°C in a vacuum oven overnight. A chromel/alumel thermocouple was sealed between the two films using a plastic bag sealer. The lead wires from the sandwiched thermocouple were run through a ceramic insulator inserted into a 6.35 mm (1/4 in.) hole in the sample container.

The sample container was an aluminum dish "hogged out" to provide a 140 mm (5-1/2 in.) diameter sample chamber (see Figures 7-1 and 7-2). Holes were drilled on opposite sides of the dish to provide an air inlet and outlet. The holes were tapped to accept a pipe to Swagelok fitting. This fitting was drilled through so that 6.35 mm (1/4 in.) Teflon tubing could be pushed until flush with the inside surface of the dish. Teflon ferrules were used to seal the tubing in the dish.

The inside of the sample container was gold-plated and fitted with a 3.18 mm (1/8 in.)-thick fused silica cover glass held in place with an aluminum retaining ring. Cover gaskets were cut from a thin sheet of Teflon FEP. A silicone O-ring was used between the Teflon gasket and the silica cover glass. A heavy wire mesh (gold-plated) was used to hold down the Kynar film in the sample chamber to get as much dish-to-film contact as possible for temperature control.

Ultraviolet light was supplied by a Hanovia 2.5 kilowatt type 929 B009  $\mu$  mercury-xenon lamp with Pyrex filter. The sample container was mounted on a stage that could be moved up and down to provide the required energy density. For these tests the maximum energy available, 3 suns, was used.

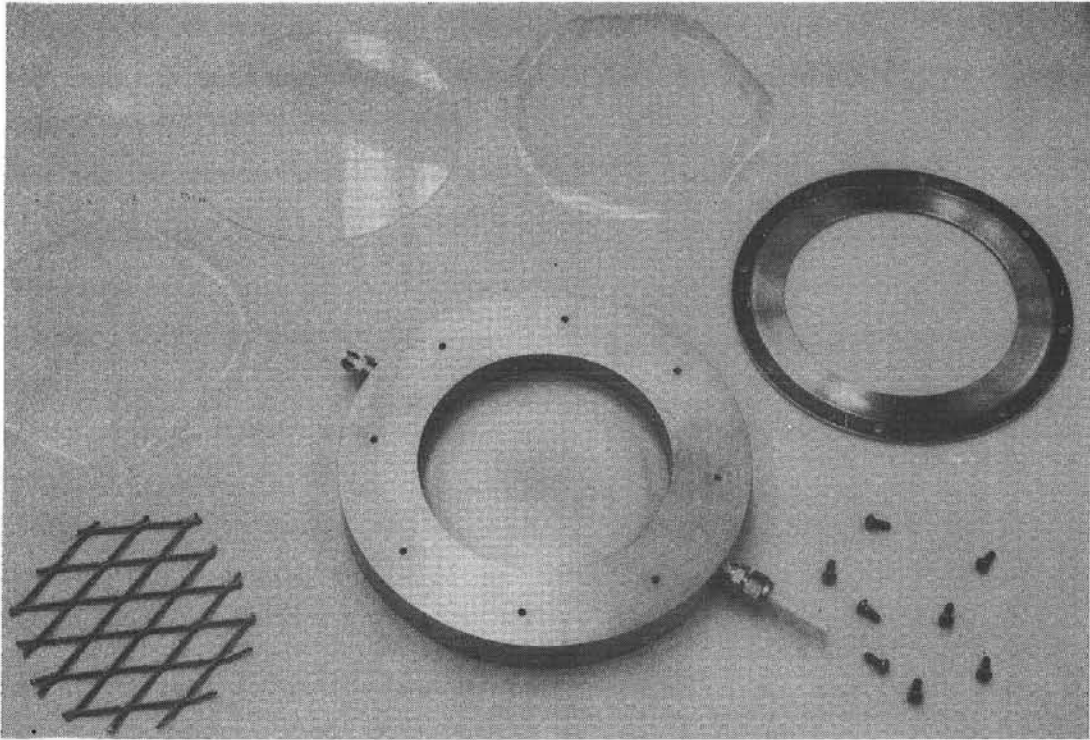


Figure 7-1. Components of Sample Chamber

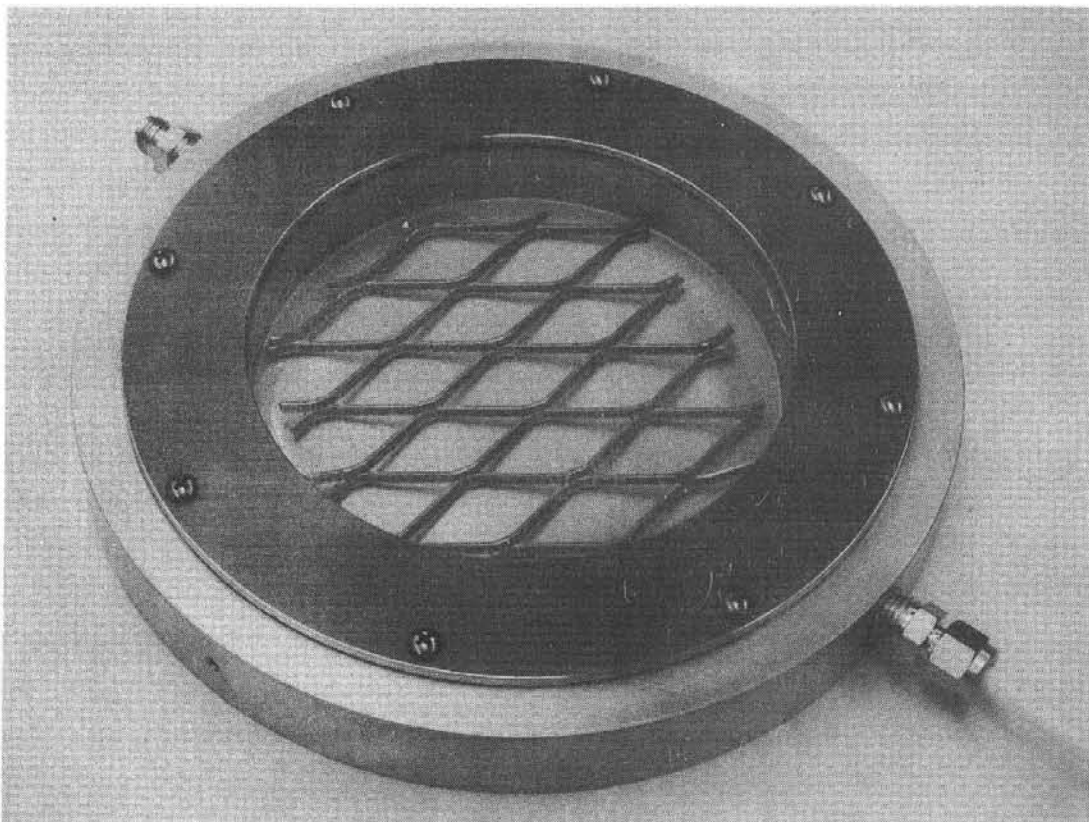


Figure 7-2. Assembled Sample Chamber

Air from a compressed air tank was run through polyethylene tubing to a column of Molecular Sieve type 5A, 45/60 mesh in a 6.35 x 305 mm (1/4 in. x 12 in.) copper tube previously rinsed with carbon tetrachloride and dried. Outlet tubing for the air flow was Teflon, similarly cleaned. Air from the sample compartment was bubbled through a polyethylene gas dispersion tube immersed in 230 ml of 1:1 Orion TISAB II buffer/water contained in a one-liter Nalgene graduated cylinder.

Tenex polymer contained in 6.35 x 76 mm (1/4 in. x 3 in.) stainless steel tubing was used to collect volatile degradation products other than HF. These traps were inserted in the line between the dispersion tube and the sample container at specific times to collect degradation products. The trapped compounds were desorbed at 185°C in flowing helium and flushed into a Perkin Elmer Hitachi RM 50 gas chromatograph/mass spectrometer for identification and quantification. Temperature of the sample was maintained using a cold plate supplied with a water/ethylene glycol mixture from a constant temperature bath and circulated by a peristaltic pump.

A pH meter (Corning model 119) equipped with a fluoride electrode (Orion model 96-09) was connected to an Esterline Angus Servo Recorder for continuous monitoring of hydrogen fluoride. Two chromel-alumel thermocouples, one inserted in the dish and the other sandwiched between the two Kynar films, were connected to a Digitec Datalogger 1000 temperature recorder.

Infrared spectra were run on a Perkin Elmer Model 283 with IR reduction, replot and differential data obtained via a PDP 11/55 computer. Ultraviolet spectra were run on a Beckman model 5240 spectrometer.

## 7.2 TEST PROCEDURE

Two Kynar films 127 mm (5 in.) diameter were rinsed with carbon tetrachloride (122°C and 101°C runs), reagent grade methanol (77° run), or both (153°C run) and dried under vacuum overnight at 45°C. The pieces were weighed as one sample and heat-sealed to the thermocouple in the sample compartment. Gold-plated mesh was placed on top of the sample.

The sample container, previously rinsed with methanol, was assembled and the screws torqued to 0.28 Nm (40 in. ozf). The container, connected to the Molecular Sieve column and the Teflon outlet tubing, was sealed in a plastic bag, and air was allowed to pass through the compartment at  $8.5 \times 10^{-3} \text{ m}^3/\text{hr}$

(0.3 SCFH) for 1/2 hour. If no leaks were detected, the sample container was removed from the bag and placed on the cold plate under the lamp, centered, and surrounded with aluminum foil. Connection was made to the dispersion tube and the tube was placed in 230 ml of 1:1 TISAB II buffer/water. Air flow was adjusted to  $8.5 \times 10^{-3} \text{ m}^3/\text{hr}$  (0.3 SCFH).

The lamp was turned on and power output was gradually brought to operating conditions. The thermocouple at the sample was connected to the temperature recorder. Occasionally the thermocouple in the dish was connected to the recorder to monitor dish temperature. The desired temperature was obtained by adjusting the flow of liquid through the cold plate and altering the temperature of the liquid in the bath. Some slight change in temperature was generally noted during the night, probably because of changes in power to the test equipment.

The fluoride ion electrode was generally calibrated after the lamp was turned on, as well as at the end of the test run. The electrode was placed in the collection buffer for the duration of the test run. Tenex tubes were inserted in the effluent line at the end of the run for 1/2 to 1-1/2 hours.

Exposed samples were weighed and examined for changes. Post-exposure testing included visual examination, infrared, visible and ultraviolet spectrographic analysis of the Kynar polymer film and gas chromatographic/mass spectrometric analysis of the degradation products collected on the Tenex traps.

### 7.3 TEST RESULTS

The results of studies of the evolution of HF from Kynar during irradiation are summarized in Table 7-1. Details of the four most significant experiments are summarized in Tables 7-2 through 7-5.

The GC/MS analysis of degradation products failed to find any hydrocarbon or fluorocarbon compounds. The only compounds found were traces of common solvents used in the laboratory and apparently adsorbed on the surface of the components of the test dish and/or Kynar film. The lack of fluorocarbon degradation products indicates that the only degradation product was hydrogen fluoride.

Infrared spectra of Kynar film were measured before and after exposure in both transmission and attenuated total reflectance. No difference could be found between exposed and virgin film. The production of either cross-links or isolated unsaturation by elimination of HF is consistent with these findings

Table 7-1  
PHOTOLYSIS OF KYNAR

TEST NO.	TEMPERATURE, °C	HF Evolution Rate	
		μg F <sup>-</sup> /hr	μg F <sup>-</sup> /hr/g
12	77 (a)	0.27	0.05
11	103	0.41	0.09
10	123 (b)	1.8	0.4
13	153	1.8	0.4

- (a) Recorded temperature is probably low due to thermocouple pulling away from Kynar film.
- (b) Recorded temperature is definitely low due to thermocouple pulling away from Kynar film. One spot on film appeared to have melted, indicating temperature closer to 150°C in that area.

since isolated double bonds have inherently weak infrared absorption which might not be seen in film that had been exposed for such a short time. Possibly more significant was the total lack of any indication of oxidation. This would be seen as a carbonyl absorption, a very strong absorber in the region 175-168  $\text{mm}^{-1}$ . Corroborative evidence that the principal reaction is either cross-linking or production of isolated unsaturation (or both) was obtained from ultraviolet absorption spectra. No difference was observed in absorption spectra before and after exposure, between 250 and 750 nm, a fact which effectively rules out the presence of conjugated unsaturation containing more than two double bonds.

The effect of weathering on creep behavior of Kynar (Section 6.3.6) indicates that, at least in the early stages of degradation, cross-linking probably predominates over chain scission. Therefore, at least part of the HF evolved must come from intermolecular elimination, but there does not appear to be enough information to define the ratio of intermolecular to intramolecular reaction.

The degradation reaction, as measured by the evolution of HF, appears to follow a normal Arrhenius temperature-dependence of the form:

$$k_t = k_o e^{\frac{-E_a}{RT}}$$

Table 7-2  
RESULTS OF IRRADIATION OF KYNAR AT 123°C

<u>Elapsed Time, Hours</u>	<u>Chart Reading</u>	<u>Hydrogen Fluoride Collected</u>		<u>Notes</u>
		<u>µg/230 ml</u>	<u>µg/hr</u>	
2	25.3			Temp Avg 122°C
3	24.3	0.9		
5-1/2	22.1	3.8	1.19	Temp 124°C
11-1/2	18.2	15.6	1.7	
14-1/2	17.4	20.2	1.6	Temp Avg 122°C
17-1/2	(16.7)	25.3		
18-1/2	16.2	29.9 (c)		
21	(15.9)	39.6 (c)	1.6	
23	(15.1)	42.5		
23-1/2 (a)	14.9	45.1		
23-1/2	14.5	51.0	ND	
24-3/4 (b)	14.5	51.1		
23-3/4 (a)	14.5	51.1	ND	
25-3/4 (b)	14.5	51.1		

- (a) Tenex Inserted
- (b) Tenex Removed
- (c) Unexplained sudden jump in HF reading

Initial Weight of Kynar film 4.396 g  
Final Weight of Kynar film 4.399 g

Table 7-3

RESULTS OF IRRADIATION OF KYNAR AT 103°C

Elapsed Time Hours	Chart Reading	Hydrogen Fluoride Collected		Notes
		$\mu\text{g}/230 \text{ ml}$	$\mu\text{g}/\text{hr}$	
2-1/4	27.3	-		Temp Avg 101°C
3-1/4	27.0	-		
3-3/4	26.8	-		
16-1/2	22.0	3.6		Temp Avg 103°C
28-1/2 (a)	19.9	8.5	0.41	
28-1/2	19.4	10.1		Temp Avg 101°C
29 (b)	19.4	10.1	ND	

(a) Tenex Inserted  
(b) Tenex Removed

Initial Weight of Kynar film 4.654 g  
Final Weight of Kynar film 4.654 g

A least squares analysis of the experimental results yielded a value of 8.33 Kcal/mole for the activation energy,  $E_a$ , and a value of  $k_o = 7.24 \times 10^3 \mu\text{g HF/g Kynar/hr}$ . A rather crude estimate of the quantum yield can be made with the following assumptions:

1. 10% of the incident light was energetic enough to break the weakest polymer bond (85 Kcal/mole or 336 nm)
2. Total radiation was 3 suns or  $3 \text{ KW/m}^2$
3. Sample area was  $8.1 \times 10^{-3} \text{ m}^2$
4. 5% of the incident damaging light was absorbed

With these assumptions, it is possible to calculate that at 77°C the quantum yield of HF was  $10^{-5}$ . This is reasonable, considering the nature of the assumptions, since it is about 1/50 of the quantum yield of PET.<sup>6</sup>

<sup>6</sup>K.R. Osborn, J. Poly. Sci 38, 357 (1959).

Table 7-4  
RESULTS OF IRRADIATION OF KYNAR AT 77°C

Elapsed Time Hours	Chart Reading	Hydrogen Fluoride Collected		Notes
		μg/230 ml	μg/hr	
0				Temp up to 86°C
6-1/2	26.2			Avg 81°C
8-1/4	25.2			Temp Avg 76°C
9-1/4	24.8			
10-1/4	24.4		0.27	
10-3/4	24.2	0.4		
18-1/2 (a)	21.5	5.1		Temp Avg 76°C
18-1/2	20.8	6.6		
19-1/2 (b)	20.8	6.6		
19-1/2	20.8	6.6		Temp Avg 77°C
20-1/2	20.7	9.1		

(a) Tenex Inserted  
(b) Tenex Removed

Initial Weight of Kynar film 4.908  
Final Weight of Kynar film 4.909

The low activation energy, 8.33 Kcal/mole, is also reasonable for a photochemical reaction. Reactions which are thermally activated normally have activation energies two to five times as high. The observed activation energy is of the proper magnitude for a second-order reaction involving radicals.<sup>7</sup> These facts can be interpreted to mean that a quantum of light occasionally breaks a C-H bond, liberating a hydrogen atom. The rate-determining step is, then, the abstraction of a fluorine atom by the hydrogen to form HF. Also, it is possible that the formation of HF is concerted and the apparent activation energy of the

<sup>7</sup> A.A. Frost and R.G. Pearson, Kinetics and Mechanism, John Wiley & Sons, New York, 1953, page 102.

Table 7-5  
RESULTS OF IRRADIATION OF KYNAR AT 153°C

<u>Elapsed Time Hours</u>	<u>Chart Reading</u>	<u>Hydrogen Fluoride Collected</u>		<u>Notes</u>
		<u>μg/230 ml</u>	<u>μg/hr</u>	
4-3/4	24.9	0.7	1.7	Temp Avg 153°C
7	22.5	4.5	1.8	
8-3/4	21.3	6.9	1.7	
10-3/4	20.1	10.3	1.8	
13-3/4	18.8	15.6		Temp to 159°C
16-1/2 (a)	17.8	21.4		
16-1/2	17.0	27.1	ND	Temp Avg 153°C
17 (b)	17.0	27.1		

(a) Tenex Inserted  
(b) Tenex Removed

Initial Weight of Kynar film      4.852 g  
Final Weight of Kynar film        4.876 g

reaction is really the dependence on temperature of the rate of diffusion of HF out of the polymer film.

Examination of the mechanical properties of the sample from the irradiation study at 153°C showed a remarkable increase in ultimate elongation and possibly a small loss in tensile strength. The data are summarized in Table 7-6. The changes in mechanical properties may be due to partial loss of orientation in the sample due to exposure to a relatively high temperature. In fact, the irradiation temperature was almost the same as the temperature at which the sample was originally oriented.

Table 7-6  
MECHANICAL PROPERTIES OF KYNAR  
AFTER IRRADIATION EXPERIMENT AT 153°C

	Tensile Strength		Elongation at Break, %
	MPa	(psi)	
Unexposed	161	(23,300)	87
Kynar	161	(23,300)	86.5
	168	(24,300)	104
Kynar After	156	(22,600)	171
Experiment #13	150	(21,700)	224
	152	(22,100)	183

## Section 8

## FLAMMABILITY OF PLASTIC FILMS

8.1 GENERAL CONSIDERATIONS

In recent years a considerable amount of concern has developed about the flammability of plastics in a number of end-uses. Solar collectors are one such end-use. The concern is quite justified, particularly where the proposed use is in thin films covering vast areas, as is the case with heliostats and enclosures. But concern about a problem does not necessarily provide a solution to the problem. Numerous fire research programs have been undertaken by manufacturers, insurance companies, government, testing associations, and trade associations.<sup>8</sup> The majority of these programs have been directed toward basic combustion research since the flammability of materials depends heavily on a host of variables such as configuration, environment, and ignition source. The complexity of the problem has led to the existence of a number of "accepted" flammability tests, a number of scales of flammability, and the frequent use of disclaimers in data tabulations; viz. Modern Plastics Encyclopedia, "Note: These numerical flame spread ratings are not intended to reflect hazards presented by this or any other material under actual fire conditions."<sup>9</sup>

Since actual use tests were not possible, assessment of the ignitibility of PET and PVDF films was carried out generally according to the procedure of ASTM D 1433-77. This test method is for the determination of the relative rate of burning and/or the extent of burning of flexible plastics in the form of film or thin sheeting. The ASTM test procedure specifies conditioning of specimens at  $23 \pm 2^\circ\text{C}$  and  $50 \pm 5\%$  relative humidity. However, relative humidity is probably a significant factor in the intended application, so it was included as a variable in the test matrix.

---

<sup>8</sup>J.J. Bertel et al., "Real-Life Burning Behavior of Polystyrene Home Furnishings," Modern Plastics, April 1979, p. 88.

<sup>9</sup>Modern Plastics Encyclopedia, McGraw-Hill Publishing Co., New York, 1979, pp. 543-629.

## 8.2 FLAMMABILITY OF LLUMAR

PET carries a flammability rating of UL 94-HB, which indicates that, in an Underwriters Laboratory horizontal test, burning will occur over a 3-in. span at a rate of not more than 63.5 mm/min (2.5 in./min) for specimens less than 3.05 mm (0.12 in.) thick; or extinguishment within a 101.6 mm (4 in.) span of materials that do not meet certain other flammability requirements.

Prior to the inception of this program, some uncontrolled tests had indicated that a vertical film of LLumar, ignited at the lower edge, sometimes burned completely with a smokey flame, dripping occasional flaming bits of molten plastic. On other occasions, the material was observed to be self-extinguishing under apparently identical conditions. In order to resolve the question of flammability of LLumar, studies were undertaken with a controlled, standard test procedure that would allow at least a qualitative comparison between materials. The test configuration selected was that of ASTM D 1433-77. The sample is ignited 12.7 mm (0.5 in.) above the lower edge, and the burning time and/or extent of burning are recorded. For flammable materials, the burning time is the time required for the flame to travel 152.4 mm (6 in.) along the sample held 45° above the horizontal. If the material self-extinguishes, the burning time is the length of time the sloping part of the sample burned, and the distance burned is the distance up the sloping part that the flame progressed before extinguishment. The data from the flammability testing of LLumar, summarized in Table 8-1, clearly indicate that under the test conditions LLumar is self-extinguishing.

This result probably indicates that LLumar enclosures would not be likely to burn extensively from a small ignition source. It probably has little relationship, however, to the effects of large-scale ignition sources, which are probably best evaluated in an actual end-use application.<sup>8</sup>

## 8.3 FLAMMABILITY OF KYNAR

With a Limiting Oxygen Index (LOI) of 43.7, PVDF<sup>10</sup> will support combustion only in atmospheres containing 43.7% or more oxygen. Since the flammability studies of this program were conducted in air (~ 20% oxygen), ignition of Kynar PVDF was not achieved. Thus, heliostat enclosures made of PVDF could not, of themselves, serve as fuel for a fire. If other combustibles were present, they

---

<sup>10</sup> Pennwalt Corp., Kynar Technical Data Sheet #2, July 11, 1977.

Table 8-1  
FLAMMABILITY TEST RESULTS

Material	Pretest Condition		Pretest Sample Temp	Burning Time, Sec /Distance Burned, mm (in)				
		(a)						
LLumar, Transverse Direction	1 week	5% RH	RT	$\frac{5}{6.4}$ (1/4)	$\frac{5}{9.5}$ (3/8)	$\frac{6}{9.5}$ (3/8)	$\frac{5}{9.5}$ (3/8)	$\frac{7}{6.4}$ (1/2)
	1 week	50% RH	RT	$\frac{3}{6.4}$ (1/4)	$\frac{5}{9.5}$ (3/8)	$\frac{5}{6.4}$ (1/4)	$\frac{4}{9.5}$ (3/8)	$\frac{4}{6.4}$ (1/4)
	1 week	100% RH 37°C	RT	$\frac{6}{6.4}$ (1/4)	$\frac{7}{6.4}$ (1/4)	$\frac{8}{6.4}$ (1/4)	$\frac{7}{6.4}$ (1/4)	$\frac{7}{6.4}$ (1/4)
	1 day	48.9°C	48.9°C	$\frac{5}{6.4}$ (1/4)	$\frac{5}{6.4}$ (1/4)	$\frac{5}{9.5}$ (3/8)	$\frac{18}{88.9}$ (3-1/2)	$\frac{7}{12.7}$ (1/2)
LLumar, Machine Direction	1 week	5% RH	RT	$\frac{5}{6.4}$ (1/4)	$\frac{4}{6.4}$ (1/4)	$\frac{6}{9.5}$ (3/8)	$\frac{5}{6.4}$ (1/4)	$\frac{5}{6.4}$ (1/4)
	1 week	50% RH	RT	$\frac{5}{6.4}$ (1/4)	$\frac{4}{6.4}$ (1/4)	$\frac{6}{9.5}$ (3/8)	$\frac{5}{6.4}$ (1/4)	$\frac{5}{6.4}$ (1/4)
	1 week	100% RH	RT	$\frac{26}{108.0}$ (4-1/4)	$\frac{22}{50.8}$ (2)	$\frac{5}{12.7}$ (1/2)	$\frac{6}{6.4}$ (1/4)	$\frac{4}{6.4}$ (1/4)
	1 day	48.9°C	48.9°C	$\frac{7}{6.4}$ (1/4)	$\frac{4}{6.4}$ (1/4)	$\frac{7}{9.5}$ (3/8)	$\frac{9}{12.7}$ (1/2)	$\frac{9}{19}$ (3/4)
Kynar, Transverse Direction	1 week	5% RH	RT	$\frac{0}{0}$ (0)	$\frac{0}{0}$ (0)	$\frac{0}{0}$ (0)	$\frac{0}{0}$ (0)	$\frac{0}{0}$ (0)
	1 week	50% RH	RT	$\frac{0}{0}$ (0)				
	1 week	100% RH	RT	$\frac{0}{0}$ (0)				
Kynar, Machine Direction	1 week	5% RH	RT	$\frac{0}{0}$ (0)				

(a) RH - Relative Humidity

could cause the destruction of PVDF enclosures and the production of toxic gases from pyrolysis of the resin, but the enclosures themselves could not propagate a fire. Heliostat enclosures made of PVDF do not constitute a fire hazard under any likely circumstance.

## Section 9

## CONCLUSIONS AND RECOMMENDATIONS

9.1 ENCLOSURE MATERIALS

Oriented PVDF film, such as Kynar 460, is markedly well suited to heliostat enclosure applications. Its tensile strength is among the highest of known polymer films, and it has a remarkable ability to recover its original dimensions after at least 33% strain. It has high solar transmittance and appears to maintain its high transmittance after prolonged exposure to sunlight.

Information is, at yet, inadequate to judge the importance of dirt accumulation or abrasion of a PVDF enclosure. If either proves to be a problem, no solution is at hand. The importance of abrasion and dirt retention on PVDF and other plastics should be assessed and, if necessary, remedies found for the problem.

It appears that (barring abrasion) the lifetime of PVDF enclosures may be limited by changes in mechanical properties rather than loss of solar transmittance. Low propagating tear strength is a known weakness of PVDF film. Ways should be investigated for increasing the tear strength of PVDF films or laminates. Other materials should be investigated and/or developed for use either as a laminate with PVDF or as an alternative to PVDF. It is recommended that weathering studies of Kynar films be continued, with particular emphasis placed on monitoring changes in mechanical properties.

9.2 REFLECTOR MATERIALS

Certain PET films can be aluminized to produce specular reflectors with an AM 1.5 solar reflectance  $\sim 0.90$ . Such reflectors can be protected against oxidation by Dow Corning Q96315 resin with a loss in reflectance on the order of 0.03. Weathering tests to date indicate that such reflectors are stable to extensive solar exposure and even to direct weathering. Testing of metalized film reflectors protected with Dow Corning Q96315 resin or equivalent should be continued and should be extended to include effects of film tensioning and creep.

Second-surface aluminized LLumar reflectors have an AM 1.5 solar reflectance  $\sim 0.81$ . Their stability is much higher than would be expected from tests of LLumar as an enclosure material. Second-surface metalized PVDF reflectors should have better stability and higher reflectance, but attempts to make such a reflector have not been successful. Efforts should be made to develop specular metalized PVDF film reflectors.

## Appendix A

## OPTICAL PROPERTIES MEASUREMENTS

A.1 AIR MASS 1.5 SOLAR TRANSMITTANCE AND REFLECTANCE

Optical data were received from DSET Laboratories in graphical form as recorded by a Beckman DK-2 spectrophotometer. A typical spectrum is shown in Figure A-1 in which the measured optical property (either transmittance or reflectance) is presented as a function of wavelength. The horizontal line at the top of A-1 is 97% correction curve provided to compensate for any instrument errors.

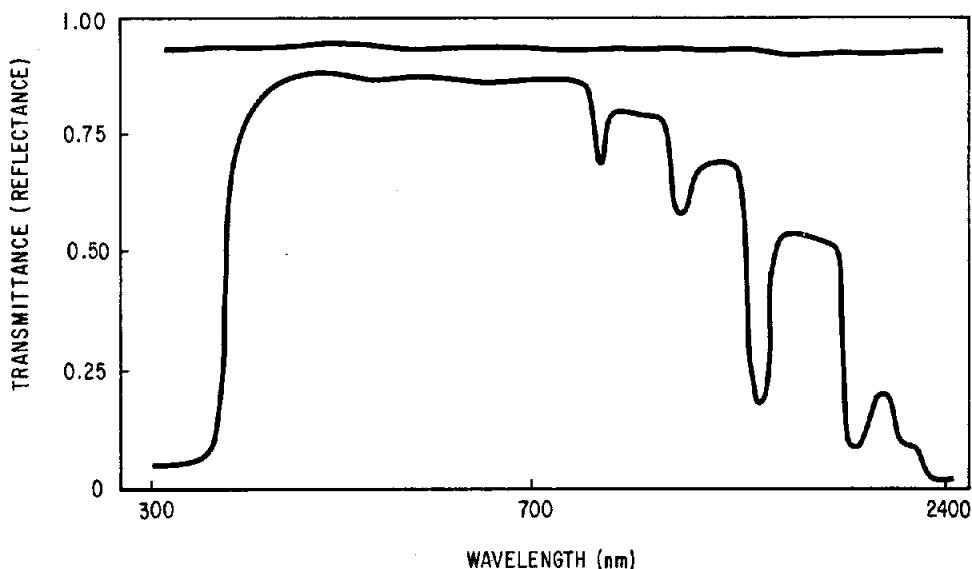


Figure A-1. Typical Optical Data as Received from DSET Laboratories

The optical data were divided into 122 equally-spaced intervals. At the end of each interval (thus giving a total of 123 data points), the value of the ordinate of both the optical property curve and the correction curve were

obtained by means of an automatic digitizing drafting table. This provided sets of data pairs. For each set, the abscissa was the wavelength of sunlight. The ordinate in one set was the corresponding solar intensity as defined by the AM 1.5 solar spectral distribution<sup>(11)</sup> and in the second set it was the amplitude of the measured optical property corrected for deviation of the 97% line.

Data reduction was accomplished in the following manner: for each x value along the abscissa a y value was determined from

$$Y_i = 0.97 + y_{\text{curve}} - y_{\text{correction}} \tag{1}$$

along with the corresponding value of solar irradiance  $B_i$  for Air Mass 1.5.<sup>(11)</sup> The dimensionless value of the measured solar property (transmittance or reflectance) was then defined by

$$\text{Solar Property} = \frac{\sum_{i=1}^n (Y_i B_i)}{\sum_{i=1}^n B_i} \tag{2}$$

where  $n = 123$  in this analysis.

A computer program, SMEDA (Solar Materials Evaluation-Data Analysis), has been written to perform the required repetitive calculations. The program (shown in A-3) was used to evaluate all optical data received from DSET Laboratories.

The AM 1.5 solar spectrum<sup>(11)</sup> extends to 295 nm, but the spectra measured by DSET Laboratories extend only to 350 nm.

Because of concern about the importance of omitting data below 350 nm, a sensitivity analysis was carried out. The absorption spectra of Kynar, LLumar and Melinex OW differ markedly in the short wavelength region. The spectrum of Kynar is relatively flat in this region while that of Melinex OW begins to drop at  $\sim 400$  nm and LLumar exhibits complete opacity between 425-375 nm.

---

<sup>11</sup>J.E.A. Selby and R.A. McClatchey, Air Force Geophys. Lab. Tech. Rep. AFGL-TR75-0255, ERP 513, AD-A017734 (1975).

The sensitivity of the analysis, to the lower end of the solar spectrum, was evaluated by assuming extreme variations in the measured data within the range 300-350 nm. This evaluation was based on the data for Kynar, and the assumed curves are illustrated in Figure A-2. As shown, the correction curve was considered to remain flat over this range. This correction curve was then combined with each of three different assumed paths of optical data (labeled A, B, and C in Figure A-2).

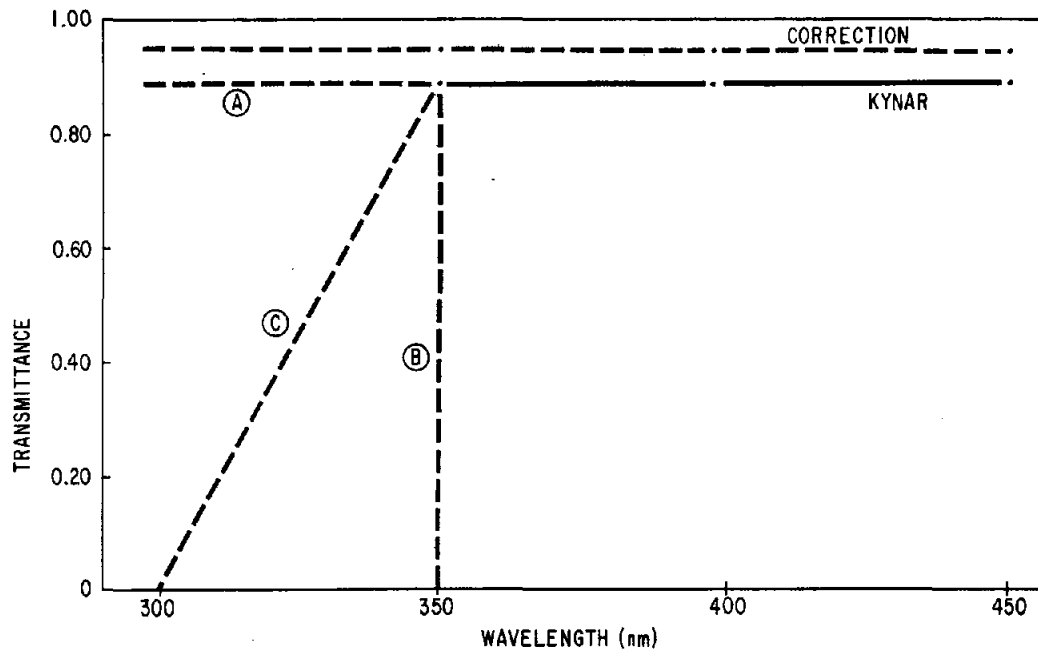


Figure A-2. Assumed Data for Kynar in the Range 300-350 nm

The results of the analysis for each of the three assumed curves are shown in Table A-1 along with the calculated transmittance for the original data as received from DSET Laboratories. Curve A, which is flat between 300-350 nm, represents the most optimistic extremum, and curve B, a sharp drop-off at 350 nm, represents the most pessimistic extremum. Curve C falls mid-way between A and B. As shown, the error in the calculated transmittance varies from 0.02% to 0.61%. Even without knowing the true shape of the curve in this region of interest, the error will probably be less than 0.25% on the assumption that the data will exhibit a smooth drop-off.

Based on the above evaluation it was concluded that the analytical approach being employed could be used without fear of causing significant errors due to neglecting the spectral range from 300-350 nm.

Table A-1  
SENSITIVITY RESULTS

<u>Curve</u>	<u>Calculated Transmittance</u>	<u>Error (%)</u>
Original	0.9329	-
A	0.9327	0.02
B	0.9268	0.61
C	0.9308	0.21

A.2 SPECULARITY MEASUREMENTS<sup>(12)</sup>

The basic principle of the specularity measurement performed at Pacific Northwest Laboratories (PNL) is illustrated in Figure A-3. A collimated, monochromatic beam of light is incident on a sample. The size, shape, and intensity profile of the beam can be tailored as desired. The beam is polarized parallel to the plane of the sample (out of the plane of the figure). The incident beam is reflected from the sample and collected with a simple plano-convex lens of focal length  $f$ .

The intensity distribution of the light in the focal plane of the collection lens contains much of the information about the reflecting surface of the sample mirror. The actual information displayed is a convolution of the intensity function of the input beam with the Fourier transform of the reflectance function of the mirror. The problem of extracting useful engineering data can be simplified by an expeditious choice of input illumination functions and image analysis techniques.

Take, for example, the case where the input beam has a uniform circular distribution and the mirror has a nonperiodic scattering function. The light scattered by the mirror surface which deviates from the specular direction by an angle  $\theta$  is displaced by a distance  $d$  in the focal plane of the collection lens. Using simple geometry, one can show that for small scattering angles,

$$d \approx f\theta \quad (3)$$

---

<sup>12</sup>Information and text provided by Dr. M. Lind, Battelle Pacific Northwest Laboratories.

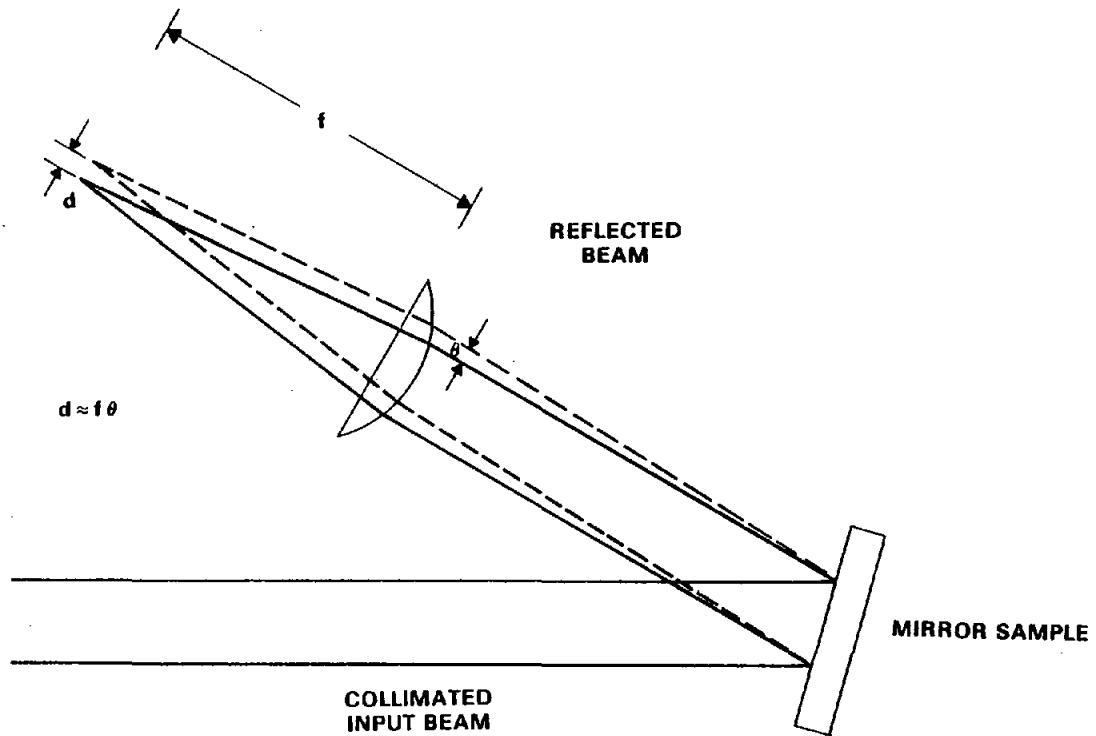


Figure A-3. Basic Principle of Specularity Measurement

where  $f$  is the focal length of the lens. Thus, by measuring the distribution of light at the focal plane, one can determine the scattering distribution of the mirror.

In actual practice it is difficult to measure the intensity distribution accurately for various reasons. One technique PNL is using to circumvent the problem and still obtain useful engineering data employs a variable circular aperture centered on the specular point at the focal plane. One then measures the integrated intensity as a function of aperture radius for some arbitrarily small value to another arbitrarily large value which collects all the scattered light. The present PNL setup measures the scattered light for  $\theta = 0.5$  to 15 milliradians. This range of angles is sufficient to characterize most materials of interest.

The actual system used for making the measurements is slightly more complicated. It is shown schematically in Figure A-4. The principle of operation is the same as described above. The additional equipment is required to perform the experiment with reasonable accuracy in the laboratory.

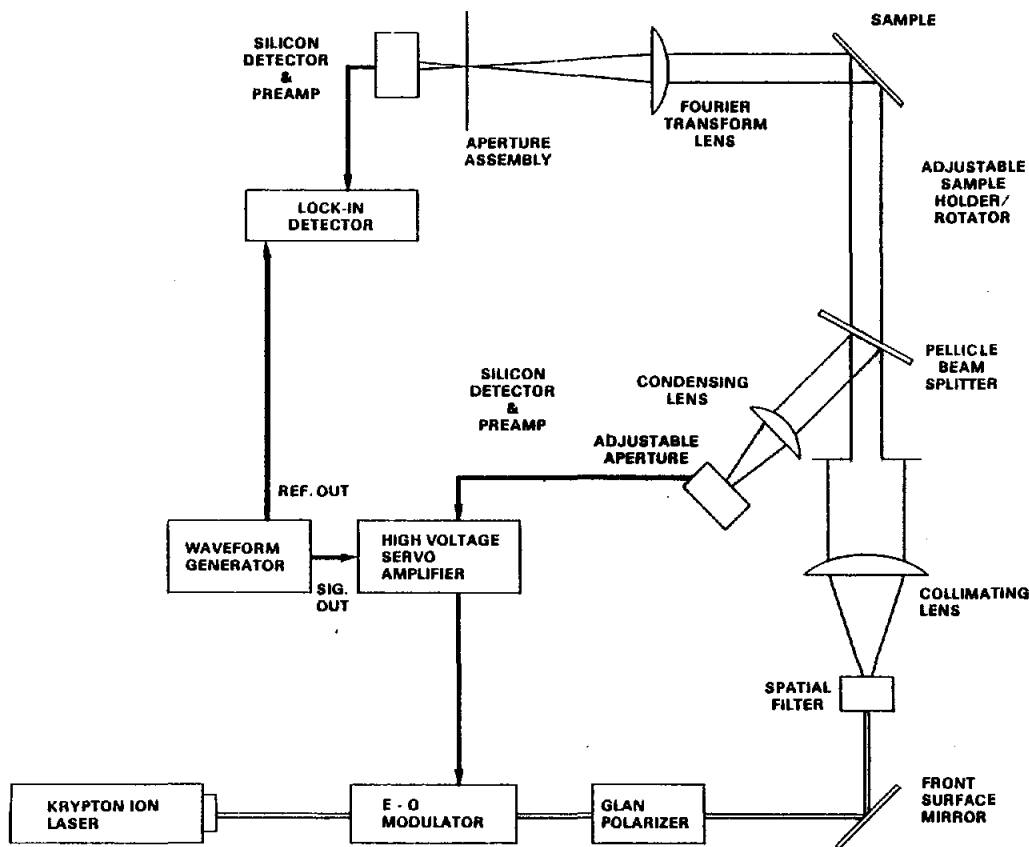


Figure A-4. Optical Configuration for Specularity Measurement

The raw data that is produced is affected not only by the light scattered from the mirror, but also by light scattered from other sources such as the collimating lens and the spatial filter. This "background" scatter may be quantified and subtracted out by measuring a reference mirror or measuring the straight-through beam. (PNL uses a well-characterized reference mirror).

For most specular materials of interest, the amount of reflex flux contained in a cone of 28 mrad ( $\theta = 14$  mrad) is within 1% of the flux measured in a hemispherical reflectance measurement. It is therefore convenient to normalize the data to the full aperture value (28 mrad). The corrected and normalized data can then be plotted as a function of angular aperture size ( $2\theta$ ). It should be noted that in using this procedure, large errors can result if the materials are nonspecular and the flux contained in the 28 mrad is not close to the hemispherical flux value.

Many surfaces tend to possess Gaussian scattering distribution because the statistics of the surface roughness can be represented by Gaussian distributions. Although this is not generally true, it is still convenient to use the

notion of a standard deviation for engineering calculations. Therefore, the standard deviation ( $\sigma$ ) also is reported as the value of  $\theta$  that corresponds to 68.3% of the total flux normalized to a 28 mrad full aperture value.

Thus, PNL presently reports a  $\sigma$  value which corresponds to half the full circular-angular aperture that contains 68.3% of the reflected (or transmitted) flux. This value is valid only for fairly specular materials, since no attempt is made to normalize to the hemispherical reflectance of the sample. For very specular materials which do not scatter appreciably outside the smallest available aperture, the value for  $\sigma$  is estimated based on a linear extrapolation between the smallest measured aperture value and the origin. Caution must be exercised when comparing the PNL values to values obtained by other researchers. The effects of aperture shape and large angle scattering can be significant for many materials.

There are two specific cases where the reported  $\sigma$  values can be applied to engineering calculations without concern: 1) where the material is an isotropic scatterer and specularity is sufficiently high that the 28 mrad aperture contains all hemispherical flux, or 2) when Gaussian statistics are applicable and the flux distribution can be extrapolated for large angles. In cases where the materials are nonisotropic scatterers or Gaussian statistics are not applicable, some judgment must be used in applying the result to general engineering calculations. In either case, the results are useful for comparing similar materials.

A.3 SMEDA, A COMPUTER PROGRAM FOR ANALYZING MEASURED OPTICAL DATA

```

LISTING OF AES38/MATERIAL
06/03/80 12.171

100CDAMES DATA ANALYSIS - MATERIALS
110C
120 COMMON /SPCTRM/ XD(150), XDM(150), SM(150)
130 DIMENSION X(150), YCOR(150), YCV(150)
140 DIMENSION PNAME(2)
150 DATA ISTOP, ITRAN, IREFL/6HSTOP ,6HTRANS ,6HREFLEC/
160 DATA IYES/6HYES /
170C
180C AIR MASS 1.5 SPECTRAL DISTRIBUTION
190C
200 WRITE (6,1007)
210 CALL DSET (KP)
220 WRITE (6,1003) (1,XD(1),XDM(1),SM(1), I=1,KP)
230C
240C READ IN DIGITIZED DATA AND CONVERT TO REAL DATA
250C
260 1 READ (5,1000) IRUNNO, PNAME, ITYPE, ADATE
270 IF (IRUNNO .NE. ISTOP) GO TO 2
280 WRITE (6,1002)
290 STOP
300 2 CONTINUE
310 WRITE (6,1008) IRUNNO, PNAME, ADATE
320 READ (5,1008) NP, NEWCOR
330 DO 3 I = 1, NP
340 READ (5,1005) J, X(I), YCV(I)
350 X(I) = X(I)*2.
360 YCV(I) = YCV(I)/10.
370 3 CONTINUE
380 IF (NEWCOR .NE. IYES) GO TO 5
390 DO 4 I = 1, NP
400 READ (5,1005) J, X(I), YCOR(I)
410 X(I) = X(I)*2.
420 YCOR(I) = YCOR(I)/10.
430 4 CONTINUE
440 5 CONTINUE
450C
460C PRINT OUT REAL DATA
470C
480 WRITE (6,1004)
490 DO 10 I = 1, NP
500 CV = YCV(I)*100.
510 COR = YCOR(I)*100.
520 WRITE (6,1001) I, X(I), CV, COR
530 10 CONTINUE
540C
550 SUMB = 0.
560 SUMXBY = 0.
570 DO 20 I = 1, NP
580 XDIG = X(I)
590 YX = 0.97 + YCV(I) - YCOR(I)
600 CALL BETA (XDIG,KP,B)
610 XBY = B*YX
620 SUMB = SUMB + B
630 SUMXBY = SUMXBY + XBY
640 20 CONTINUE
650C
660 SOLRES = SUMXBY/SUMB
670 IF (ITYPE .EQ. ITRAN) WRITE (6,1010) PNAME, SOLRES
680 IF (ITYPE .EQ. IREFL) WRITE (6,1015) PNAME, SOLRES
690 GO TO 1
700C
710 1000 FORMAT (A6,2X,2A6,2X,A6,2X,A6)
720 1001 FORMAT (7X,13,11X,F6.2,13X,F7.3,11X,F7.3)
730 1002 FORMAT (1H1,35HEND OF INPUT DATA HAS BEEN REACHED.)
740 1003 FORMAT (7X,13,10X,F8.3,10X,F9.5,9X,F11.6)
750 1004 FORMAT (1H0,19X,9HDIGITIZED,12X,5HCURVE,11X,10HCORRECTION,/,
760 1 9X,1HN,10X,8HPOSITION,11X,8HORDINATE,11X,8HORDINATE,/,
770 2 21X,6H(INCH),15X,3H(%),15X,3H(%),/)
780 1005 FORMAT (14,1X,F7.3,4X,F7.3)
790 1006 FORMAT (1H1,5X,13HSAMPLE NO. = ,A6,12X,11HMATERIAL = ,2A6,
800 1 12X,7HDATE = ,A6)
810 1007 FORMAT (1H1,18X,38HAIR MASS 1.5 SPECTRAL DISTRIBUTION,///,
820 1 20X,9HDIGITIZED,12X,4HWAVE,14X,5HSCLAR,/,
830 2 9X,1HN,10X,8HPOSITION,12X,6HLENGTH,11X,10HIRRADIANCE,/,
840 3 21X,6H(INCH),12X,8H(MICRON),10X,9H(W/CM**2),/)
850 1008 FORMAT (14,2X,A6)
860 1010 FORMAT (1H0,/,5X,15HFOR MATERIAL = ,2A6,3H;
870 1 26HTHE SOLAR TRANSMITTANCE IS,F8.4)
880 1015 FORMAT (1H0,/,5X,15HFOR MATERIAL = ,2A6,3H;
890 1 24HTHE SOLAR REFLECTANCE IS,F8.4)
900 END
910C
920C *****

```

APPENDIX B

TENSILE PROPERTIES OF PILOT PLANT KYNAR FILM

Strain rate - 50.8 mm/min (2 in/min)  
 Gauge length - 101.6 mm (4 in)  
 Room temperature except where noted.

Sample	Width		Thickness		Force		Tensile Strength		Elongation at Break, %
	mm	(in)	mm	(in)	N	(lb)	MPa	(ksi)	
Machine	17.8	(0.700)	0.11	(0.0044)	321	(72.2)	161	(23.4)	103
Direction	17.8	(0.700)	0.099	(0.0039)	271	(61.0)	154	(22.3)	87
	17.6	(0.695)	0.094	(0.0037)	245	(55.1)	148	(21.4)	79
	17.7	(0.697)	0.099	(0.0039)	270	(60.7)	154	(22.3)	87
	16.7	(0.657)	0.10	(0.0040)	274	(61.5)	161	(23.4)	94
<hr/>									
Transverse	18.0	(0.709)	0.086	(0.0034)	245	(55.1)	158	(22.9)	78
Direction	17.4	(0.686)	0.084	(0.0033)	242	(54.3)	165	(24.0)	79
	17.6	(0.691)	0.084	(0.0033)	231	(51.9)	157	(22.8)	75
	17.5	(0.688)	0.084	(0.0033)	245	(55.2)	168	(24.3)	80
	17.4	(0.685)	0.086	(0.0034)	226	(50.8)	150	(21.8)	74
<hr/>									

Sample	Tensile Stress		Elongation %	Apparent Set %
	MPa	(ksi)		
1	72.4	(10.5)	20	6.25
2	46.9	(6.8)	10	2.56
3	35.2	(5.1)	4	0
4	40.0	(5.8)	6	0.8
5	68.2	(9.9)	20	6.5
5 repeat	77.9	(11.3)	20	5.25
50°C				
6	77.2	(11.2)	20	5.0
6 repeat	88.2	(12.8)	20	5.0

```

930C
1000C DSET      AIR MASS 1.5 DATA
1010C
1020      SUBROUTINE DSET (KP)
1030      COMMON /SPCTRM/ XD(150), XDM(150), SM(150)
1040      DIMENSION XM(122), SI(122)
1050      DATA XM /0.295,0.305,0.315,0.325,0.335,0.345,0.355,0.365,
1060      1      0.375,0.385,0.395,0.405,0.415,0.425,0.435,0.445,
1070      2      0.455,0.465,0.475,0.485,0.495,0.505,0.515,0.525,
1080      3      0.535,0.545,0.555,0.565,0.575,0.585,0.595,0.605,
1090      4      0.615,0.625,0.635,0.645,0.655,0.665,0.675,0.685,
1100      5      0.695,0.6983,0.70,0.710,0.720,0.7277,0.73,0.740,
1110      6      0.750,0.7621,0.77,0.780,0.790,0.800,0.8059,0.825,
1120      7      0.830,0.835,0.8465,0.86,0.870,0.875,0.8875,0.900,
1130      8      0.9075,0.915,0.925,0.930,0.940,0.950,0.955,0.965,
1140      9      0.975,0.985,1.018,1.082,1.094,1.098,1.101,1.128,
1150      A      1.131,1.137,1.144,1.147,1.178,1.189,1.193,1.222,
1160      B      1.236,1.264,1.276,1.288,1.314,1.335,1.384,1.432,
1170      C      1.457,1.472,1.543,1.572,1.599,1.608,1.626,1.644,
1180      D      1.650,1.676,1.732,1.782,1.862,1.955,2.008,2.014,
1190      E      2.057,2.124,2.156,2.201,2.266,2.320,2.338,2.356,
1200      F      2.388,2.415/
1210C
1220      DATA SI /0., 1.32,20.96,113.48,182.23,234.43,286.01,355.88,
1230      1      386.80,381.78,492.18,751.72,822.45,842.26,890.55,
1240      2      1077.07,1162.43,1180.61,1212.72,1180.43,1253.83,
1250      3      1242.28,1211.01,1244.87,1299.51,1273.47,1276.14,
1260      4      1277.74,1292.51,1284.55,1262.61,1261.79,1256.43,
1270      5      1240.19,1243.79,1233.96,1188.32,1228.40,1210.08,
1280      6      1200.72,1181.24,973.53,1173.31,1152.70,1133.83,
1290      7      974.30,1110.93,1086.44,1070.44,733.08,1038.01,
1300      8      1018.42,1003.58,988.11,860.28,932.74,923.87,914.95,
1310      9      407.11,857.46,843.02,835.10,817.12,807.83,793.87,
1320      A      778.97,217.12,163.72,249.12,231.30,255.61,279.09,
1330      B      529.64,486.64,585.03,486.20,448.74,486.72,500.57,
1340      C      100.86,116.87,108.68,155.44,139.19,374.29,383.37,
1350      D      424.85,382.57,383.81,323.83,344.11,345.69,284.24,
1360      E      175.28,2.42,30.05,67.14,59.89,240.85,226.14,220.46,
1370      F      211.76,211.26,201.85,199.68,180.50,161.59,136.85,
1380      G      2.01,39.43,72.56,80.01,72.57,70.29,64.76,68.29,
1390      H      62.52,57.03,53.57,50.01,31.93,28.10/
1400C
1410C      INITIALIZE DATA
1420C
1430      DS 10 I = 1,150
1440      XD(I) = 0.
1450      XDM(I) = 0.
1460      SM(I) = 0.
1470      10 CONTINUE
1480C
1490      XDM(1) = 0.30
1500      SM(1) = SI(2)*(XDM(1)-XM(1))
1510      K = 2
1520      JSAVE = 0
1530      30 CONTINUE
1540      XD(K) = XD(K-1) + 0.2
1550      XDM(K) = (XD(K)*0.03175006) + 0.3
1560      IF (XDM(K) .GT. 0.70) XDM(K) = (XD(K)*0.12700025)-0.9002
1570      DS 40 I = 1,122
1580      IF (XDM(K) .GE. XM(I)) GO TO 40
1590      J = I-1
1600      GO TO 50
1610      40 CONTINUE
1620      50 CONTINUE
1630      DX1 = XM(J) - XDM(K-1)
1640      IF (DX1 .LT. 0.) DX1 = 0.
1650      DX2 = XDM(K) - XM(J)
1660      IF (J .LE. JSAVE ) DX2 = XDM(K)-XDM(K-1)
1670      SM(K) = DX1*SI(J) + DX2*SI(J+1)
1680      IF (XDM(K) .GE. 2.40) GO TO 60
1690      JSAVE = J
1700      K = K+1
1710      GO TO 30
1720      60 CONTINUE
1730      KP = K
1740      RETURN
1750      END
1760C
1770C *****
1780C
2000C BETA      BETA
2010C
2020      SUBROUTINE BETA (XDIG,KP,B)
2030      COMMON /SPCTRM/ XD(150), XDM(150), SM(150)
2040C
2050      X = XDIG + 1.60
2060      DS 10 I = 1,KP
2070      TEMP = XD(I)
2080      DIFF = X - TEMP
2090      IF (ABS(DIFF) .GT. 1.E-5) GO TO 10
2100      B = SM(I)
2110      RETURN
2120      10 CONTINUE
2130      PRINT 2000
2140      2000 FORMAT (1H1,5X,19HIN SUBROUTINE BETA, ,
2150      1      32HTHERE IS NO MATCH IN X-POSITION,/,
2160      2      16HPROGRAM STOPPED)
2170      STOP
2180      END

```

Appendix B (Continued)  
 TEAR PROPAGATION RESISTANCE OF PILOT PLANT KYNAR FILM (ASTM D 1938)

Sample Number	Transverse Direction					Sample Number	Machine Direction						
	Thickness		Load		Maximum		Thickness		Load		Maximum		
	mm	(in)	Minimum N	(lb)			N	(lb)	mm	(in)		Minimum N	(lb)
1	0.096	(0.0038)	0.418	(0.094)	0.467	(0.105)	1	0.094	(0.0037)	0.467	(0.105)	0.489	(0.110)
			0.422	(0.095)	0.445	(0.100)				0.480	(0.108)	0.556	(0.125)
			0.414	(0.093)	0.445	(0.100)				0.445	(0.100)	0.512	(0.115)
2	0.089	(0.0035)	0.405	(0.091)	0.414	(0.093)	2	0.094	(0.0037)	0.512	(0.115)	0.578	(0.130)
			0.391	(0.088)	0.414	(0.093)				0.520	(0.117)	0.565	(0.127)
			0.405	(0.091)	0.422	(0.095)				0.489	(0.110)	0.556	(0.125)
3	0.084	(0.0033)	0.347	(0.078)	0.356	(0.082)	3	0.094	(0.0037)	0.480	(0.108)	0.534	(0.120)
			0.347	(0.078)	0.369	(0.083)				0.480	(0.108)	0.534	(0.120)
			0.356	(0.080)	0.374	(0.084)				0.503	(0.113)	0.538	(0.121)
4	0.089	(0.0035)	0.369	(0.083)	0.387	(0.087)	4	0.112	(0.0044)	0.609	(0.137)	0.636	(0.143)
			0.365	(0.082)	0.378	(0.085)				0.596	(0.134)	0.640	(0.144)
			0.369	(0.083)	0.378	(0.085)				0.596	(0.134)	0.632	(0.142)
5	0.089	(0.0035)	0.422	(0.095)	0.458	(0.103)	5	0.096	(0.0038)	0.445	(0.100)	0.489	(0.110)
			0.414	(0.093)	0.454	(0.102)				0.440	(0.099)	0.476	(0.107)
			0.418	(0.094)	0.445	(0.100)				0.436	(0.098)	0.480	(0.108)
6	0.091	(0.0036)	0.391	(0.088)	0.431	(0.097)	6	0.094	(0.0037)	0.485	(0.109)	0.534	(0.120)
			0.391	(0.088)	0.436	(0.098)				0.507	(0.114)	0.552	(0.124)
			0.409	(0.092)	0.427	(0.096)				0.503	(0.113)	0.543	(0.122)

Appendix B (Continued)

CREEP PROPERTIES OF PILOT PLANT KYNAR FILM (DIMENSIONLESS STRAIN)

Stress, MPa(ksi)	9.17 (1.33)		17.7 (2.57)		46.0 (6.67)		69.0 (10.0)	69.0 (10.0)	18.4 (2.67)	46.0 (6.67)
Condition	Room Temp. A B		Room Temp. A B		Room Temp. A B		Room Temp.	Weathered 9x10 <sup>5</sup> Langleys	50°C	50°C
TIME										
0 (no load)	1.973	1.980	1.976	1.966	1.963	1.970	1.940	1.967	1.955	1.939
0 (Loaded)	1.976	1.981	1.976	1.966	1.969	1.979	2.090	2.111	1.991	2.093
2 min.	1.976	1.981	1.977	1.968	1.969	1.979	2.193	2.156	2.025	2.148
10 min.	1.977	1.982	1.980	1.969	1.974	1.982	2.206	2.162	2.038	2.156
30 min.	1.978	1.982	1.981	1.972	1.974	1.988	2.215	2.164	2.051	2.177
1 hour	1.978	1.982	1.982	1.975	1.976	1.989	2.220	2.190	2.053	2.181
4 hours	1.978	1.982	1.988	1.983	1.976	1.989	2.243	2.210	2.066	2.224
24 hours	1.978	1.982			1.978	1.991	2.261	2.216	2.071	2.228
48 hours	1.978	1.983			1.978	1.991	2.275	2.237	2.073	2.233
120 hours	1.979	1.983			1.983	1.993	2.278	2.243	2.076	2.249
300 hours	1.979	1.983			1.987	1.998	2.286		2.082	2.264
700 hours					1.988	1.999	2.306		2.082	2.265
1000 hours					1.988	1.999	2.311		2.082	2.266
No load							2.090		2.004	2.050

74

Appendix C

EFFECT OF WEATHERING ON TENSILE PROPERTIES OF POTENTIAL ENCLOSURE MATERIALS

EXPOSURE, 10 <sup>3</sup> LANG- LEYS/CONC OF SUNLIGHT	KYNAR				LLUMAR			
	20% OFFSET YIELD STRENGTH, MPa (psi)	ULTIMATE TENSILE STRENGTH, MPa (psi)	ELONGATION AT BREAK, %		YIELD STRENGTH, MPa (psi)	ULTIMATE TENSILE STRENGTH, MPa (psi)	ELONGATION AT BREAK, %	
NONE	107.6 (15,600)	160.6 (23,300)	87		62.0 (9,000)	179.3 (26,000)	103	
	107.6 (15,600)	160.9 (23,300)	86.5		51.7 (7,500)	202.7 (29,400)	146	
	98.4 <sup>(a)</sup> (14,270)	167.5 <sup>(a)</sup> (24,300)	104 (a)		59.3 <sup>(a)</sup> (8,600)	164.9 <sup>(a)</sup> (23,900)	62.5 (a)	
0.48/1X	106.1 <sup>(a)</sup> (15,400)	157.9 <sup>(a)</sup> (22,900)	95 (a)		82.0 (11,900)	190.6 (26,200)	114	
	106.9 (15,500)	153.8 (22,300)	79		78.6 (11,400)	180.6 (26,200)	110	
	97.9 <sup>(a)</sup> (14,200)	127.5 <sup>(a)</sup> (18,500)	54 (a)		69.0 (10,000)	173.1 (25,100)	105	
	99.3 (14,400)	147.5 (21,400)	96.5		79.3 (11,500)	161.3 (23,400)	90	
0.95/1X	105.8 (15,350)	153.1 (22,200)	89		70.3 (10,200)	130.3 (18,900)	47.5	
	108.2 (15,700)	149.6 (21,700)	77.5		74.5 (10,300)	142.7 (20,700)	62.5	
	103.4 (15,000)	145.5 (21,100)	83.8		71.0 (10,300)	139.2 (20,200)	56	
	100.7 <sup>(a)</sup> (14,600)	127.6 <sup>(a)</sup> (18,500)	51 (a)		63.4 (9,200)	129.6 (18,800)	50.2	
1.3/1X	102.8 (14,909)	162.0 (23,500)	100.5		-- --	-- --	--	
	101.3 <sup>(a)</sup> (14,696)	146.2 <sup>(a)</sup> (21,200)	82 (a)		53.1 (7,700)	95.2 (13,800)	37.5	
	99.5 (14,435)	151.7 (22,000)	92		63.4 (9,200)	94.5 (13,700)	43	
	102.4 (14,859)	160.6 (23,300)	105		61.4 (8,900)	96.8 (14,300)	51.5	
1.3/8X	91.0 (13,200)	140.6 (20,400)	113		58.6 (8,500)	94.5 (13,700)	29	
	84.1 (12,200)	144.8 (21,000)	124		73.8 <sup>(b)</sup> (10,700)	134.4 (19,500)	63	
	89.6 <sup>(a)</sup> (13,000)	128.2 <sup>(a)</sup> (18,600)	85 (a)		65.5 (9,500)	117.2 (17,000)	46	
	-- --	-- --	--		73.8 (10,700)	125.5 (18,200)	47	
1.8/1X	-- --	-- --	--		91.0 (13,200)	131.7 (19,100)	55	
	93.8 (13,600)	135.1 (19,600)	100		66.2 (9,600)	80.0 (11,600)	3.5	
	93.1 <sup>(a)</sup> (13,500)	118.6 <sup>(a)</sup> (17,200)	56 (a)		66.2 (9,600)	97.2 (14,100)	26	
	93.9 <sup>(a)</sup> (13,600)	128.9 <sup>(a)</sup> (18,700)	72.5 (a)		69.6 (10,100)	97.9 (14,200)	15	
2.5/8X	35.1 (13,800)	143.4 (20,800)	112.5		64.1 (9,300)	73.1 (10,600)	14	
	86.9 (12,600)	141.3 (20,500)	125		63.4 (9,200)	91.0 (13,200)	20	
	91.0 (13,200)	140.6 (20,400)	108		68.9 (10,000)	95.8 (13,900)	23.5	
	96.9 (14,050)	147.5 (21,400)	112.5		68.2 (9,900)	100.7 (14,600)	15.5	
3.4/4X	-- --	-- --	--		-- --	-- --	--	
	95.4 (13,843)	124.8 (18,100)	49		72.4 (10,500)	106.2 (15,400)	18	
	90.7 (13,158)	128.2 (18,500)	103		55.8 <sup>(a)</sup> (8,100)	80.7 <sup>(a)</sup> (11,700)	5 (a)	
	89.3 (12,950)	151.7 (22,000)	111.5		69.6 (10,100)	110.3 (16,000)	19	
3.8/8X	36.9 (12,610)	143.4 (20,800)	100		64.8 (9,400)	93.1 (13,500)	12	
	85.5 <sup>(a)</sup> (12,400)	131.0 <sup>(a)</sup> (19,000)	101 (a)		57.9 (8,400)	92.4 (13,400)	5.5	
	98.6 (14,300)	148.9 (21,600)	109		46.2 (6,700)	87.6 (12,700)	7	
	83.4 (12,100)	108.2 (15,700)	52.5		55.2 (8,000)	85.5 (12,400)	5	
5.1/8X	-- --	-- --	--		60.7 (8,800)	88.2 (12,900)	5	
	63.9 (9,257)	144.8 (21,000)	127.5		-- --	-- --	--	
	63.9 (9,253)	150.3 (21,800)	138.5		-- --	-- --	--	
	64.9 (9,414)	144.7 <sup>(a)</sup> (20,900)	119 (a)		-- --	-- --	--	
6.3/8X	68.1 (9,884)	144.8 <sup>(a)</sup> (21,000)	110.5 (a)		-- --	-- --	--	
	35.2 (12,364)	131.0 (19,000)	106		-- --	-- --	--	
	91.7 (11,848)	125.6 (18,800)	114.5		-- --	-- --	--	
	85.3 (12,370)	125.6 (18,800)	102		-- --	-- --	--	
7.6/8X	92.1 (13,352)	139.2 (20,200)	105.5		-- --	-- --	--	
	95.7 (13,875)	134.4 (19,500)	89		-- --	-- --	--	
	91.4 (a) (13,250)	139.2 <sup>(a)</sup> (20,200)	108.5 (a)		-- --	-- --	--	
	26.3 (12,582)	116.5 (16,900)	58.5		-- --	-- --	--	
9.0/8X	95.5 (13,350)	113.3 (16,500)	44		-- --	-- --	--	
	30.3 (a) (13,399)	111.2 <sup>(a)</sup> (16,100)	43 (a)		57.3 (8,400)	36.9 (12,500)	4.5	
	30.2 (13,350)	137.2 (20,300)	123		37.2 (5,300)	33.4 (12,100)	3	
	82.5 (11,964)	124.8 (18,100)	98.5		67.6 (9,800)	91.7 (13,300)	5	
13.1/16X	88.9 (a) (12,890)	136.5 <sup>(a)</sup> (19,800)	111.5 (a)		51.0 (7,400)	75.8 (11,000)	4.5	
	37.7 (12,717)	137.9 (20,000)	106		-- --	-- --	--	
	88.5 (12,838)	137.9 (20,000)	116		-- --	-- --	--	
	90.3 (a) (13,350)	137.9 (a) (20,000)	111.5 (a)		-- --	-- --	--	
13.1/16X	89.3 (a) (12,950)	159.3 (a) (23,100)	125 (a)		-- --	-- --	--	
	(a)	33.8 (a) (4,900)	12.5 (a)		57.2 (8,300)	84.8 (12,300)	5	
	97.9 (14,200)	133.8 (19,400)	60		59.3 (8,600)	81.4 (11,800)	3	
	(a)	77.2 (a) (11,200)	24 (a)		53.1 (7,700)	75.2 (10,900)	4	
(a)	65.5 (a) (9,500)	17.5 (a)		62.7 (9,100)	77.9 (11,300)	3		

(a) Grip failures.  
(b) Specimens were tested using a 1.0 inch gage length

(a) Grip failures  
(b) Specimens were tested using a 1.0 inch gage length

Appendix C

EFFECT OF WEATHERING ON TENSILE PROPERTIES OF POTENTIAL ENCLOSURE MATERIALS (Continued)

EXPOSURE, 10 <sup>3</sup> LANG- LEYS/CONC OF SUNLIGHT	MELINEX OM				
	YIELD STRENGTH MPa	(psi)	ULTIMATE TENSILE STRENGTH, MPa	ELONGATION AT BREAK, %	
NONE	72.4	(10,500)	194.4	(28,200)	144
	72.4	(10,500)	185.5	(26,900)	145
	83.4 (a)	(12,100)	166.3 (a)	(24,200)	75 (a)
	79.3 (a)	(11,500)	161.3 (a)	(23,300)	103 (a)
0.48/1X	62.7	(9,100)	102.0	(14,800)	20
	66.2	(9,600)	91.0	(13,200)	10
	75.2 (a)	(12,100)	77.9 (a)	(11,300)	1.5 (a)
	67.6	(9,800)	81.4	(11,300)	3
0.95/1X	54.4	(7,900)	91.0	(13,200)	6.5
	46.9 (a)	(6,800)	66.2 (a)	(9,600)	3.5 (a)
	59.3 (a)	(8,600)	89.6 (a)	(13,000)	6.0 (a)
	57.9	(8,400)	86.2	(12,500)	7.5
1.3/1X	--	--	--	--	--
1.3/9X	49.6 (a)	(7,200)	87.6 (a)	(12,700)	13.5 (a)
	57.9	(8,400)	86.9	(12,900)	10
	53.1	(7,700)	93.8	(13,600)	10
	58.6 (a)	(8,500)	91.7 (a)	(13,300)	7.5 (a)
1.8/1X	53.1	(7,700)	90.3	(13,100)	6
	62.7	(9,100)	87.6	(12,700)	7
	53.8	(7,800)	83.4	(12,100)	5.5
	48.3	(7,000)	79.6	(11,400)	6
1.9/8X	62.0	(9,000)	97.2	(14,100)	14
	62.0	(9,000)	88.2	(12,800)	6
	55.8	(8,100)	84.8	(12,300)	5
	55.8	(9,100)	86.9	(12,600)	5
2.5/8X	55.5	(9,500)	85.5	(12,400)	4
	57.9	(8,400)	86.2	(12,500)	7.5
	44.1	(6,400)	84.8	(12,300)	5
	54.5	(7,900)	83.4	(12,100)	6
3.4/4X	52.4	(7,600)	83.4	(12,100)	4.5
	60.7	(8,900)	91.7	(13,300)	4.5
	62.7	(9,100)	83.4	(12,100)	4.5
	57.2	(8,300)	78.6	(11,400)	4
3.9/2X	44.1	(6,400)	71.7	(10,400)	3.5
	49.6	(7,200)	71.0	(10,300)	10.5
	--	--	--	--	--
5.1/2X	--	--	--	--	--
6.3/2X	--	--	--	--	--
7.6/8X	--	--	--	--	--
8.8/2X	46.2 (a)	(6,700)	71.0 (a)	(10,300)	5 (a)
	47.6	(6,900)	71.7	(10,400)	4
	44.1	(6,400)	73.8	(10,700)	4
	46.2 (a)	(6,700)	69.0 (a)	(10,000)	4 (a)
9.0/2X	--	--	--	--	--
13.7/15X	40.0	(5,900)	62.1	(9,000)	3.5
	44.8	(6,500)	50.7	(8,200)	3
	44.8	(6,500)	51.3	(8,300)	3
	--	--	--	--	--

(a) Grip failures  
 (b) Specimens were tested using a 1.0 inch gage length.

Appendix D

EFFECT OF WEATHERING ON STRENGTH OF BONDED SAMPLES

Sample Exposure, Langley's $\times 10^{-5}$ /conc. of sunlight	Bond Strength, N/m (lb/in)							
	LLumar, electromagnetically bonded Sample 332		LLumar, Adhesively bonded Sample 321		Kynar, electromagnetically bonded Sample 361		Kynar, Adhesively bonded Sample 372	
None	7900	(45)	10,400	(59.4)	9300	(53)	14,000	(80)
	7350	(42)	10,350	(59.1)	8600	(49)	15,600	(89)
	7350	(42)	10,200	(58.1)	8600	(49)	13,000	(74)
	8600	(49)	9400	(53.8)	9450	(54)	12,600	(72)
	9100	(52)	10,450	(59.6)	8600	(49)		
1.9 / 1X	Failed		8900	(51)	11,550	(66)	16,600	(95)
			8400	(47.9)	11,100	(63.5)	16,300	(93)
			8300	(47.4)	11,400	(65.2)	14,400	(82)
			8200	(46.7)	11,100	(63.5)	14,400	(82)
3.4 / 4X	1650	(9.4)	8050	(46)	11,100	(63.5)	13,600	(77.5)
	2800	(16)	8250	(47.1)	11,850	(67.7)	10,950	(62.5)
	2100	(12)	8250	(47.1)	11,600	(66.1)	12,400	(71)
	3300	(19)	8400	(47.9)	11,500	(65.8)	12,300	(70)
9.0 / 8X	4200	(24)	6800	(39)	10,950	(62.5)	13,100	(75)
	4300	(24.5)	6400	(36.5)	10,600	(60.4)	10,500	(60)
	4050	(23.1)	6750	(38.5)	10,800	(61.9)	10,150	(58)
	4400	(25)	6400	(36.6)	10,650	(60.9)	9650	(55)
13.1 x 16X	--	--	6300	(36)	11,400	(65)	11,800	(67.5)
	--	--	6050	(34.5)	11,600	(66.5)	14,800	(84.5)
	--	--	6300	(36)	10,500	(60)	12,250	(70)
	--	--	4850	(27.7)	12,200	(69.8)	14,700	(84)

Appendix E

FAILURE MODE OF WEATHERED BOND SAMPLES

Spec. No.	Bond Strength		Failure Mode			
	N/m	(lb/in )	At Bond Line	In Bond Interface	In Gage Length	Grip Failure
321-1	8900	(51.0)			x	
	8400	(47.9)			x	
	8300	(47.4)			x	
	8200	(46.7)	x			
361-1	11,550	(66.0)			x	
	11,100	(63.5)			x	
	11,400	(65.2)			x	
	11,100	(63.5)			x	
372-1	16,600	(94.6)	x			
	16,300	(93.2)				x
	14,400	(81.8)		x		
	14,400	(82.3)		x		
321-2	8050	(46.0)		x		
	8250	(47.1)			x	
	8250	(47.1)		x		
	8400	(47.9)			x	
332-2	1650	( 9.4)		x		
	2800	(16.0)		x		
	2100	(12.0)		x		
	3300	(19.0)		x		
361-2	11,100	(63.5)			x	
	11,850	(67.7)			x	
	11,600	(66.1)			x	
	11,500	(65.8)			x	
372-2	13,600	(77.4)			x	
	10,950	(62.5)		x		
	12,400	(70.8)		x		
	12,300	(69.8)		x		

Appendix E

FAILURE MODE OF WEATHERED BOND SAMPLES (Continued)

Spec. No.	Bond Strength		Failure Mode			
	N/m	(lb/in )	At Bond Line	In Bond Interface	In Gage Length	Grip Failure
321-3	6800	(39.0)			x	
	6400	(36.6)			x	
	6750	(38.5)			x	
	6400	(36.6)			x	
332-3	4200	(24.0)			x	
	4300	(24.5)	x			
	4050	(23.1)	x			
	4400	(22.9)	x			
361-3	10,950	(62.5)			x	
	10,600	(60.4)			x	
	10,800	(62.0)			x	
	10,650	(60.9)			x	
372-3	13,100	(75.0)	x			
	10,500	(59.8)	x			
	10,150	(58.3)	x			
	9650	(55.2)	x			
321-4	6300	(36.1)			x	
	6050	(36.0)			x	
	6300	(34.5)			x	
	4850	(27.8)			x	
361-4	11,400	(65.0)			x	
	11,600	(66.5)			x	
	10,500	(60.0)			x	
	12,200	(69.8)			x	
372-4	11,800	(67.6)		x		
	14,800	(84.6)		x		
	12,250	(69.8)		x		
	14,700	(84.0)		x		

SAMPLE	CODE
321	LLumar, bonded with Adcote 76M5
332	LLumar, electromagnetically bonded
361	Kynar, electromagnetically bonded
372	Kynar, bonded with experimental adhesive
-1	Exposed to $1.9 \times 10^5$ Langleys
-2	Exposed to $3.4 \times 10^5$ Langleys
-3	Exposed to $9.0 \times 10^5$ Langleys
-4	Exposed to $13.1 \times 10^5$ Langleys

Appendix F

STRENGTH OF BONDS NOT SELECTED FOR WEATHERING

<u>Bond Type</u>	<u>Bond Strength</u>	
	<u>N/m</u>	<u>(lb/in)</u>
Melinex OW, Electromagnetically Bonded	13,500	(77)
	11,900	(68)
	13,100	(75)
	12,250	(70)
	13,500	(77)
Melinex OW, Ultrasonically Bonded	5400	(31)
	6100	(35)
	5800	(33)
	5600	(32)
	5100	(29)
LLumar, Ultrasonically Bonded	6650	(38)
	6500	(37)
	7700	(44)
	8200	(47)
	8200	(47)
Kynar, RF Bonded	10,850	(62)
	11,000	(63)
	11,000	(63)
	10,700	(61)
	10,700	(61)
LLumar, Adhesively Bonded, Transverse Direction	9450	(54)
	9300	(53)
	8400	(48)
	9800	(56)
	9600	(55)
Kynar, Ultrasonically Bonded	7900	(45)
	5800	(33)
	4900	(28)
	6650	(38)
	9100	(52)
Kynar, Adhesively Bonded, Transverse Direction	15,400	(88)
	16,600	(95)
	15,200	(87)
	5800	(33)
	4900	(28)

UNLIMITED RELEASE

INITIAL DISTRIBUTION

U.S. Department of Energy  
Washington, D. C. 20545  
Attn: M. U. Gutstein  
L. Melamed  
J. E. Rannels

S. D. Elliott  
San Francisco Operations Office  
U.S. Department of Energy  
1333 Broadway  
Oakland, CA 94612

R. N. Schweinberg  
Solar 10-MW Project Office  
SAN/STMPO  
U.S. Department of Energy  
Suite 210  
9550 Flair Drive  
El Monte, CA 91731

Jacques Hull  
Acurex  
485 Clyde Avenue  
Mountain View, CA 94042

Philip de Rienzo  
Aerospace Corporation  
El Segundo Boulevard  
El Segundo, CA 90274

M. A. Lind  
Battelle Pacific Northwest Labs  
P. O. Box 999  
Richland, Washington 99352

Ernie Lam (M/S 50/16)  
Bechtel National, Inc.  
P. O. Box 3965  
San Francisco, CA 94119

Roger Gillette  
Boeing Engineering & Construction  
P. O. Box 3707  
Seattle, WA 98124

C. G. Howard  
Booz, Allen & Hamilton, Inc.  
8801 E. Pleasant Valley Road  
Cleveland, OH 44131

G. Cottingham  
Brookhaven National Laboratory  
Upton, NY 11973

Ken Busche  
Busche Energy Systems  
7288 Murdy Circle  
Huntington Beach, CA 92647

Jill Jankowski  
Dow Corning Corporation  
3901 Saginaw Road  
Midland, MI 48640

John Bigger  
Electric Power Research Institute  
P. O. Box 10412  
Palo Alto, CA 93403

Howard Sund  
Ford Aerospace  
3939 Fabian Way, T33  
Palo Alto, CA 94303

Paul Tremblay  
Foster-Miller Associates  
135 Second Avenue  
Waltham, MA 02154

General Electric Company  
1 River Road  
Schenectady, NY 12345  
Attn: John Garate  
R. N. Griffin  
Richard Horton

R. Hobbs, Room 7310  
General Electric Company  
P. O. Box 8661  
Philadelphia, PA 19101

Jet Propulsion Laboratory  
Building 502-201  
4800 Oak Grove Drive  
Pasadena, CA 91103  
Attn: William Carroll  
Edward Cuddihy

Los Alamos Scientific Laboratory  
P. O. Box 1663  
Los Alamos, NM 87545  
Attn: Stanley W. Moore

Martin Marietta Corporation  
P. O. Box 179  
Denver, CO 80201  
Attn: T. R. Heaton  
Lloyd Oldham

McDonnell Douglas Astronautics Company  
5301 Bolsa Avenue  
Huntington Beach, CA 92647  
Attn: R. L. Gervais  
D. A. Steinmeyer

J. A. Pietsch  
Northrup, Inc.  
302 Nichols Drive  
Hutchins, TX 75141

Floyd Blake  
Blake Laboratory  
Northrup, Inc.  
Suite 306  
7061 S. University Boulevard  
Littleton, CO 80122

Mark Bowman  
Phillips Chemical Co.  
13-D2 Phillips Building  
Bartlesville, OK 74004

John C. Schumacher  
Schumacher & Associates  
2550 Fair Oaks Boulevard, Suite 120  
Sacramento, CA 95825

Solar Energy Research Institute  
1536 Cole Boulevard  
Golden, CO 80401  
Attn: Barry Butler  
Leita Dunham, TID  
R. Ortiz, SEIDB  
Holly Roberts  
John Thornton

B. Baum  
Springborn Laboratories  
Water Street  
Enfield, CT 06082

Van Leer Plastics  
15581 Computer Lane  
Huntington Beach, CA 92649  
Attn: Larry Nelson

Walter Moore  
Veda, Inc.  
400 N. Mobil, Building D  
Camarillo, CA 90310

C. N. Vittitoe, 4231  
G. E. Brandvold, 4710  
T. A. Dellin, 4723  
J. A. Leonard, 4725  
R. G. Kepler, 5810  
L. A. Harrah, 5811  
J. G. Curro, 5813  
F. P. Gerstle, Jr., 5814  
J. N. Sweet, 5824, Attn: R. B. Pettit  
T. B. Cook, 8000, Attn: A. N. Blackwell, 8200  
B. F. Murphey, 8300  
D. M. Schuster, 8310, Attn: W. R. Hover, 8312, for M. D. Skibo  
A. J. West, 8314  
W. R. Even, 8315  
R. L. Rinne, 8320  
C. F. Melius, 8326  
P. L. Mattern, 8342  
L. Gutierrez, 8400, Attn: R. A. Baroody, 8410  
C. S. Selvage, 8420  
D. E. Gregson, 8440  
C. M. Tapp, 8460  
H. R. Sheppard, 8424  
R. C. Wayne, 8450  
T. D. Brumleve, 8451

W. R. Delameter, 8451

P. J. Eicker, 8451 (5)

C. L. Mavis, 8451 (5)

H. F. Norris, Jr., 8451

C. J. Pignolet, 8451

W. S. Rorke, Jr., 8451

S. S. White, 8451

A. C. Skinrood, 8452

W. G. Wilson, 8453

Publications Division, 8265, for TIC (27)

Publications Division, 8265/Technical Library Processes and Systems Division, 3141

Technical Library Processes and Systems Division, 3141 (2)

Education Division, 8214 (3)